การตรวจสอบกลไกการเกิดแผ่นดินไหวและมิติแฟรกทัล
บริเวณชายแดนประเทศไทย-ลาว-พม่า

นางสาวกนกกาญจน์ เวชชกรรม

วิทยานิพนธ์นี้เป็นส่วนหนึ่งของการศึกษาตามหลักสูตรปริญญาวิทยาศาสตรมหาบัณฑิต
สาขาวิชาโลกศาสตร์ ภาควิชาธรณีวิทยา
คณะวิทยาศาสตร์ จุฬาลงกรณ์มหาวิทยาลัย
ปีการศึกษา 2559

INVESTIGATION OF FOCAL MECHANISM AND FRACTAL DIMENSION IN THE THAILAND-LAOS-MYANMAR BORDERS

Miss Kanokkarn Vajchakom

A Thesis Submitted in Partial Fulfillment of the Requirements
for the Degree of Master of Science Program in Earth Sciences
Department of Geology
Faculty of Science
Chulalongkorn University
Academic Year 2016

Thesis Title	INVESTIGATION OF FOCAL MECHANISM AND FRACTAL DIMENSION INTHE THAILAND- LAOS-MYANMAR BORDERS
By	Miss Kanokkarn Vajchakom
Field of Study	Earth Sciences
Thesis Advisor	Associate Professor Santi Pailoplee, Ph.D.

Accepted by the Faculty of Science, Chulalongkorn University in Partial Fulfillment of the Requirements for the Master's Degree

.....Dean of the Faculty of Science
(Associate Professor Polkit Sangvanich, Ph.D.)

THESIS COMMITTEE

.....Chairman
(Assistant Professor Sombat Yumuang, Ph.D.)

.....Thesis Advisor
(Associate Professor Santi Pailoplee, Ph.D.)

.....Examiner
(Professor Montri Choowong, Ph.D.)

.....External Examiner
(Assistant Professor Krit Won-in, Ph.D.)

กนกกาญจน์ เวชชกรรม : การตรวจสอบกลไกการเกิดแผ่นดินไหวและมิติแฟรกทัลบริเวณชายแดนประเทศไทย-ลาว-พม่า (INVESTIGATION OF FOCAL MECHANISM AND FRACTAL DIMENSION INTHE THAILAND-LAOS-MYANMAR BORDERS) อ.ที่ปรึกษาวิทยานิพนธ์หลัก: รศ. ดร. สันติ ภัยหลบลี้, 102 หน้า.

ในการศึกษานี้เป็นการตรวจสอบกลไกการเกิดแผ่นดินไหว (focal mechanism) และรูปแบบการเกิดแผ่นดินไหว (fractal dimension) บริเวณชายแดนประเทศไทย-ลาว-พม่า ในส่วนของการตรวจสอบกลไกการเกิดแผ่นดินไหว ลักษณะการเลื่อนตัวจะเป็นในแนวระดับ โดยมีมุมเอียงเทเฉลี่ยประมาณ 65 องศาและ 85 องศา นอกจากนั้นผู้วิจัยยังได้ศึกษา 8 รอยเลื่อนที่สำคัญ เช่น รอยเลื่อนน้ำมา รอยเลื่อนเม็งซิง และรอยเลื่อนเดียนเบียนฟู เป็นต้น ซึ่งรอยเลื่อนเหล่านี้มีการเลื่อนตัวในแนวระดับ ในส่วนของการศึกษารูปแบบการเกิดแผ่นดินไหวนั้น มีการศึกษาในเชิงพื้นที่และเวลาโดยได้แบ่งข้อมูลเป็น 2 ชุดคือ ก่อนการคัดเลือกข้อมูลกับหลังการคัดเลือกข้อมูล นอกจากนั้นยังได้มีการวิเคราะห์ค่า b โดยเป็นการศึกษาความเครียดในพื้นที่ ผลการศึกษาในเชิงพื้นที่ พบว่าบริเวณตอนเหนือของประเทศไทยกับทางตะวันออกของพม่า มีค่า b ต่ำ ระหว่าง 0.5-0.8 ในขณะที่บริเวณอื่นๆ มีค่า b อยู่ระหว่าง 0.8-1.2 ผลการศึกษาในเชิงเวลานั้น พบว่าค่า b มีการลดลงอย่างต่อเนื่องก่อนที่จะเกิดแผ่นดินไหวแม่ลาว (Mae Lao earthquake) กับแผ่นดินไหวทาเลย์ (Tarlay earthquake) และค่า Dc ก็ลดลงอย่างชัดเจนก่อนเกิดแผ่นดินไหวเช่นกัน นอกจากนั้นความสัมพันธ์ระหว่างค่า Dc กับค่า b บริเวณรอยเลื่อนชายแดนประเทศไทย-ลาว-พม่าเป็นแบบแปรผันตามกัน

ภาควิชา ธรณีวิทยา ลายมือชื่อนิสิต .....

สาขาวิชา โลกศาสตร์ ลายมือชื่อ อ.ที่ปรึกษาหลัก .....

ปีการศึกษา 2559

5672154823 : MAJOR EARTH SCIENCES
KEYWORDS: EARTHQUAKE DECLUSTERING / B VALUE / FRACTAL DIMENSION / FOCAL MECHANISM / THAILAND-MYANMAR BORDERS

KANOKKARN VAJCHAKOM: INVESTIGATION OF FOCAL MECHANISM AND FRACTAL DIMENSION INTHE THAILAND-LAOS-MYANMAR BORDERS. ADVISOR: ASSOC. PROF. SANTI PAILOPLEE, Ph.D., 102 pp.

According to Indo-Australian and Eurasian plate collision, a large number of seismogenic fault zones were dominant as the intraplate earthquake sources in the Mainland Southeast Asia including the Thailand-Laos-Myanmar border (TLMB). In this study, we investigated the mechanism of earthquake faulting and pattern of earthquake occurrence in this region. Based on focal mechanism data reported by the Harvard Moment Centroid, the average fault movement was strike-slip faulting in NE-SW direction. The angle of fault dipping varied between 65 and 85 degree with rake angle revealing left lateral movement. In addition, we investigated 8 significant faults in TLMB such as Nam ma, Mengxing, Dein Bein Fu. The mechanism illustrates differently strike-, oblique- and dip-slips.

In order to clarify the earthquake pattern, fractal dimension (Dc) was calculated with both dataset of before- and after-declustering process. In addition b value of the frequency-magnitude distribution was also analyzed. As a result for spatial investigation, the northern Thailand and eastern Myanmar reveal comparatively low b, between 0.5-0.8. Meanwhile, the other areas are comparatively high with b ranged 0.8-1.2. In temporal investigation, b value decreases continuously before both Mae Lao and Tarlay earthquakes posed and the Dc values are drop down suddenly during these earthquakes were generated. For b-Dc relationships, Mae Lao earthquake indicate the positive relation while Tarlay earthquake express negative relation. This relation, therefore, may accord to the different characteristic or activities of each fault zone.

Department: Geology Student's Signature .....
Field of Study: Earth Sciences Advisor's Signature .....
Academic Year: 2016

ACKNOWLEDGEMENTS

I would like to sincerely and gratefully thank my advisor,Associate Professor Dr. Santi Pailoplee, Department of Geology, Faculty of Science, Chulalongkorn University for his supports,encouragements, tolerant guidance, understanding and everything he gave throughout this thesis. I thank to Mr.Santawat Sukrungsri for his kindly help and suggestion throughout my study at the university.

Furthermore, I would also like to thank "The 90th anniversary of Chulalongkorn University fund (Ratchadaphiseksomphot Endowment Fund)" for scholarship research.

Finally, I must express my gratitude to my parents, Mr. Kheammanat Wedchakam and Mrs. Sudjai ,Wedchakam for their motivation and everything support throughout my life

CONTENTS

Page

Page

Page

LIST OF TABLES

LIST OF FIGURES

CHAPTER I
INTRODUCTION

1.1. Background

There are various kinds of natural disasters; an earthquake is one of the most important devastating disasters. The earthquake causes the massive loss of life and damage to the economy, environment and ecology. Plate boundaries are the most common places on earth where earthquakes are produced. In general, they have occurred along the collision between two of the tectonic plates which marked boundaries known as subduction zones. The earthquakes along these zones can generate large tsunami sometimes as the December 26th, 2004 Sumatra Andaman earthquake. This event had magnitude (Mw) 9.1 at 07:58 a.m. local time (00:58 UTC) generated one of the worst notable historical tsunami. The wave run-up heights of more than 30 meters were observed along the west coast of Sumatra. It's one of the deadliest disasters on record that 108,100 people were killed, 127,700 are missing and 426,800 were displaced for Aceh and Sumatera Utara provinces only. The other countries around the epicenter also got severe damage, such as Thailand, Myanmar, Malaysia and India. The Tohoku, Japan earthquake occurred on March 11th, 2011 with Mw 9.0 at 02:46 p.m. (05:46 UTC). The earthquake caused the nuclear accident; the cooling core was melted, then released the radioactive through the environment. After the earthquake, 15,729 people had died, 5,719 had injured and 4,539 were missing. It savagely damaged to 125,000 buildings and 4.4 million houses. The economic impact of this situation estimated USD309,000. However, the earthquakes can occur into the intraplate, for example, the Mw 6.0 South Napa earthquake on August 24, 2014 occurred at 03:20 a.m. (10:20:44.03) near Napa, California (Figure 1.2a, b). It was the largest hit in northern California since the Loma Prieta earthquake in 1989. There were 80 aftershocks of Mw ≥ 1.8 in the first month after the main shock (USGS, 2014). The San Francisco earthquake occurred at 05:12 a.m. local time on April 18th, 1906, which ruptured on the northernmost 477 km of San Andreas Fault with magnitude 7.9. It is one of the

greatest and most destructive earthquakes of all time. More than 3,000 people were killed and 28,000 buildings were terribly destroyed.

Furthermore, the Mw 6.8 Tarlay earthquake occurred along the westernmost section of the Nam Ma fault, Eastern Myanmar at 13:55 (UTC) on March 24th, 2011 with 10 km-depth. The total length of surface rupture is approximately 30 km. The epicenter was located at 20.71^{o}N and 99.95^{o}E (Phodee et al., 2014); Wang et al., 2014). That killed over 150 people, destroyed 9 government buildings and the toll was less than USD100 million. The next event that directly and strongly affected Thailand is the Mae Lao earthquake on May 5th, 2014 with Mw 6.0, occurred at 18:08:43 local time (11:08:43 UTC). The epicenter was at Southwest Chiang Rai, Northern Thailand, located on the Phayao Fault Zone (Figure 1.2d) (Noisagool et al., 2016). It is harmful directly to people, killed a person and damaged more than 1,400 buildings in Chiang Rai province. All of the intraplate earthquakes mentioned above caused by the plate tectonic collisions.

Figure 1. 1. a) The damage of reinforced concrete structure (Soralump et al.,2014). b) The damage of a pagoda in Chiang Saen District (Ruangrassamee et al., 2012).

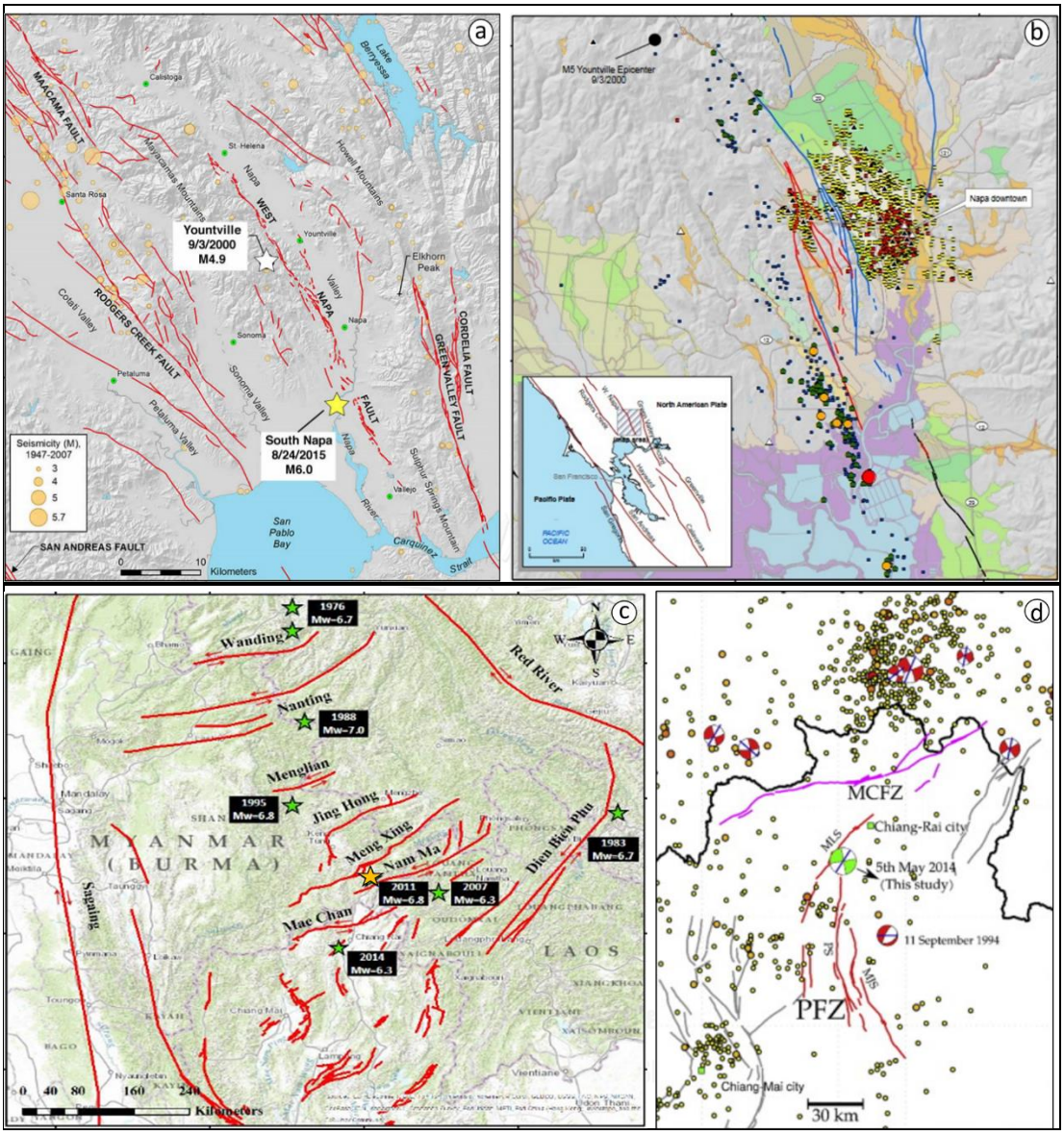

Figure 1. 2. a) Map showing faults and earthquake with Mw ≥ 3.0 of the South Napa earthquake on August 24th, 2014 as the yellow star. The white star showing the Mw 4.9 earthquake in 2000. b) Napa Valley area showing as red and yellow squares. The locations of the main shock, aftershocks and surface ruptures indicate consequently as the red circle, other circles and red lines. c) Map of faults in Shan fault system (red lines). The green stars indicate the epicenters of Mw > 6.3 since 1976. The yellow star presents the epicenter of the Tarlay earthquake. d) Background seismicity in neighboring and focal mechanisms of large earthquakes. The focal mechanism of the main event

from ISC catalog is shown in green, whereas, the red diagrams imply the Mw 5.2 earthquake which occurred on September 11th, 1994.

It has been supported that the Mae Lao and Tarlay earthquake are the strongest seismic events on Southeast Asia peninsular. They are the consequence of the collision between the Indo-Australian and Eurasian plates (Figure 1.3) and the more distant Philippine and West Pacific plates as well. This area is surrounded by convergent margins, including the Andaman thrust and Sunda arc to the west and south, respectively. Nowadays, Australia is moving northward (along a vector of 010° and 020°) towards the Southeast Asia at the convergence rate of 65-70 mm/yr (McCaffrey, 1996). In addition, the Southeast Asia may also be moving towards Eurasia at the rate around 10 mm/yr. From the mentioned, the tectonic plate activity generates the distributed deformation of these plates and across the fault. The deformation within the Eurasian plate is illustrated by the number of seismic faults in this region (Molnar and Deng, 1984).

Currently, the regional tectonic setting of Thailand has accumulated stress, related to the opening of north-south oriented basin, right-lateral and left-lateral slip on northwest-striking faults and northeast-striking faults (Polachan et al., 1991; Packham, 1993). The Cenozoic tectonics of Thailand are consequences of the continuous northward subduction of the Indian plate beneath the Eurasian plate ((Fenton et al., 2003); (Pailoplee et al., 2009)). Despite the fact that the high level of seismic activity is produced by the collision between Indo-Australian and Eurasian plates, the seismic activity does not only occur along the Sumatra-Andaman subduction zone. It is also caused by a widespread intraplate activity where the inland seismogenic faults are dominant (Pailoplee et al., 2009), such as intraplate activity in Thailand (Figure 1.4). Thus, Northern Thailand is dominated by a large number of active fault zones, for instance, Mae Chan, Pua, Phrae, Mae Tha and Mae Kuang and Lampang-Thoen fault zones which have revealed tectonic activity (Pailoplee et al., 2009) (Figure 1.4).

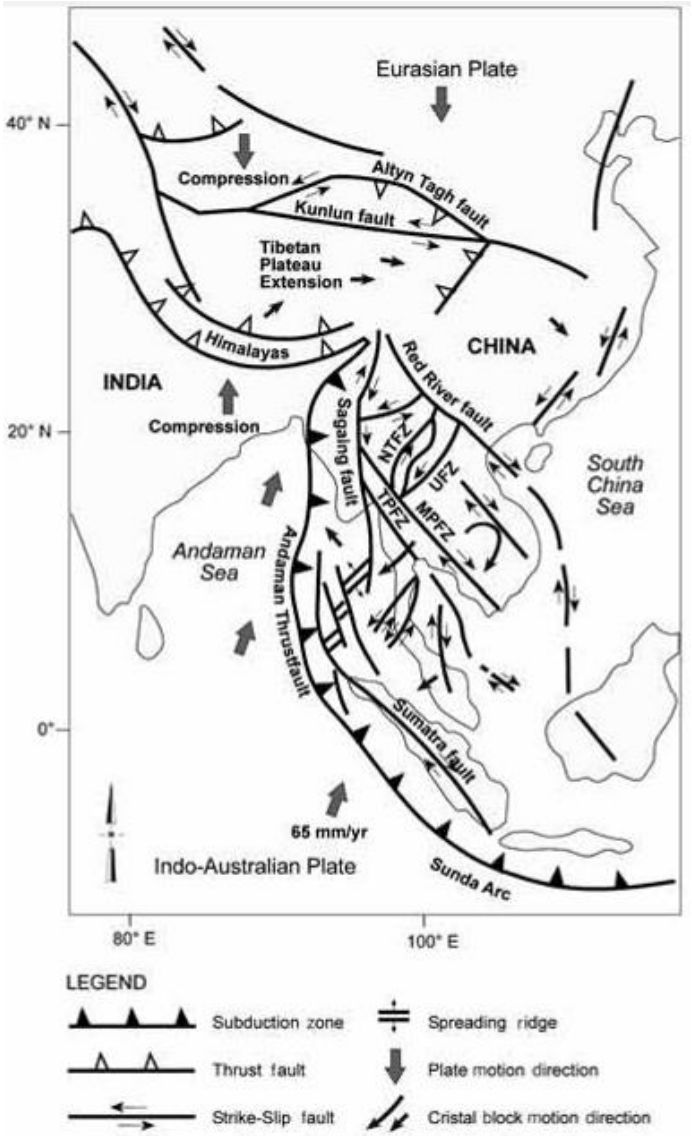

Figure 1. 3. Major tectonic elements in Southeast Asia and Southern China. Arrows show relative directions of motion of crustal blocks during the Late Cenozoic. MPFZ- Mae Ping Fault Zone; NTFZ- Northern Thailand Fault Zone; TPFZ- Three Pagodas Fault Zone; UFZ- Uttaradit Fault Zone. Modified from Polachan et al. (1991).

1.2. Previous work

The seismologists have tried to determine the characteristics, behaviors of the tectonic setting and the prediction for the upcoming earthquakes in Thailand-Lao-Myanmar

borders region. We reviewed the relevant literatures to realize what concepts, theories and methods have been applied to the topic in the study area.

Firstly, Pailoplee et al. (2009) investigated the seismic hazard in Thailand and adjacent areas. They identified 55 active fault zones by using remote sensing data of earthquake source parameters derived from both active fault data and earthquake catalogues. They found the high-risk seismic hazard areas which are Thailand's neighboring countries, namely Myanmar, Laos, Vietnam, Indonesia (Sumatra Island), and northern, western, and southern Thailand that were dominated by active fault zones (Figure 1.4).

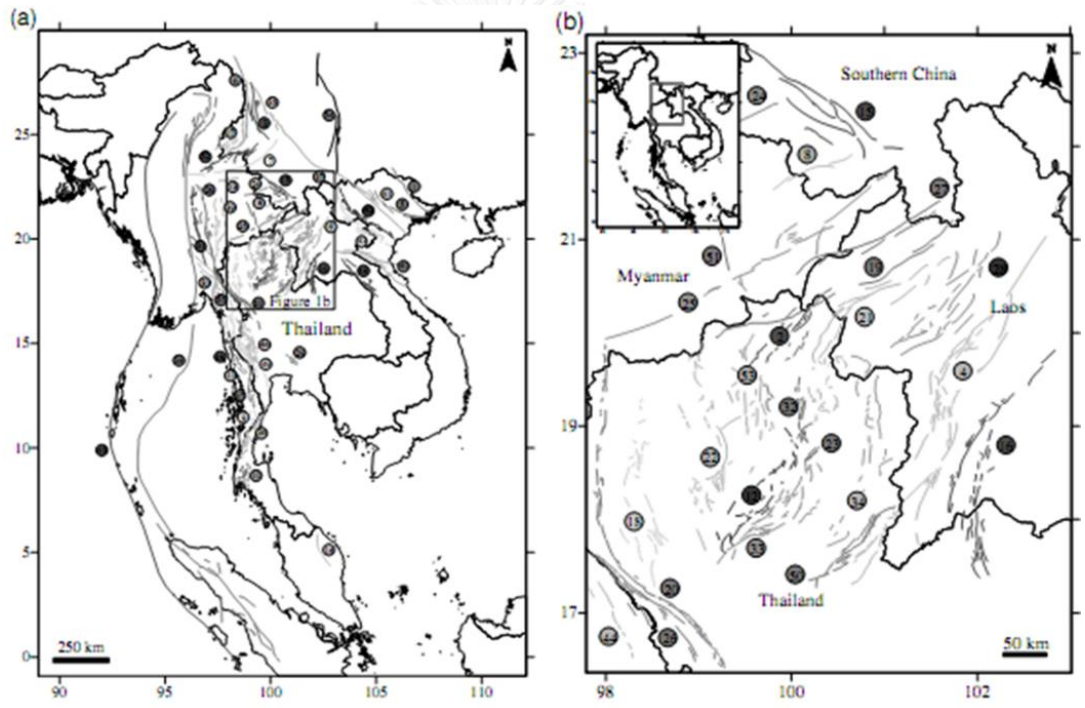

Figure 1. 4. a) Active faults in Thailand and adjacent areas interpreted from remote sensing data. b) Map showing active faults interpreted in northern Thailand and surrounding areas. The individual fault zones are distinguished by color and numbers. (Pailoplee et al., 2009)

The next work is studying Mainland Southeast Asia (MSEA) which is different tectonic systems area. Pailoplee et al. (2013) applied the frequency magnitude

distribution to estimate the seismic hazard parameters for individual earthquake source zones within MSEA. They divided the area into 13 earthquake source zones (Figure 1.5), based on the lately geological, tectonic and seismic data during 1964 to 2010. Moreover, they found the probability of magnitude ≤ 6.0 being triggered in the next 25 years in all of seismic source zones for 100%. The probable maximum magnitude and the average return period depended on the seismic source zones, such as the Sumatra Andaman Interplate (zone A) have a tendency to occur magnitude 9.0 in every 50 years. (Pailoplee et al., 2013)

As reported by Pailoplee et al. (2014), the fractal dimensions (D_c) and the frequency magnitude distribution (b value) were investigated in the 13 seismic source zones to examine the earthquake characteristic in region. The b and D_c values were calculated by the completeness dataset to imply seismotectonic stress. The relationship between b and D_c values indicated the level of seismic hazard. For example, the J seismic source zone which is Northern Thailand-Dein Bein Phu provided the b value of 0.732 ± 0.09 and Dc value of 1.86 ± 0.04 (Table 1.1). Additionally, the Thailand-Laos-Myanmar borders (TLMB) were researched on the maximum possible magnitude, return periods and earthquake prediction. They were analyzed from the completeness of dataset by instrumental records along the region. The possible largest earthquake magnitude is located on the northeastern part of Mong Pan, Pak Beng dam and Luang Prabang dam which is around Mb 4.0 - 5.0 in a years and up to Mb 7.0 in 50 years as shown in Figure 1.6.

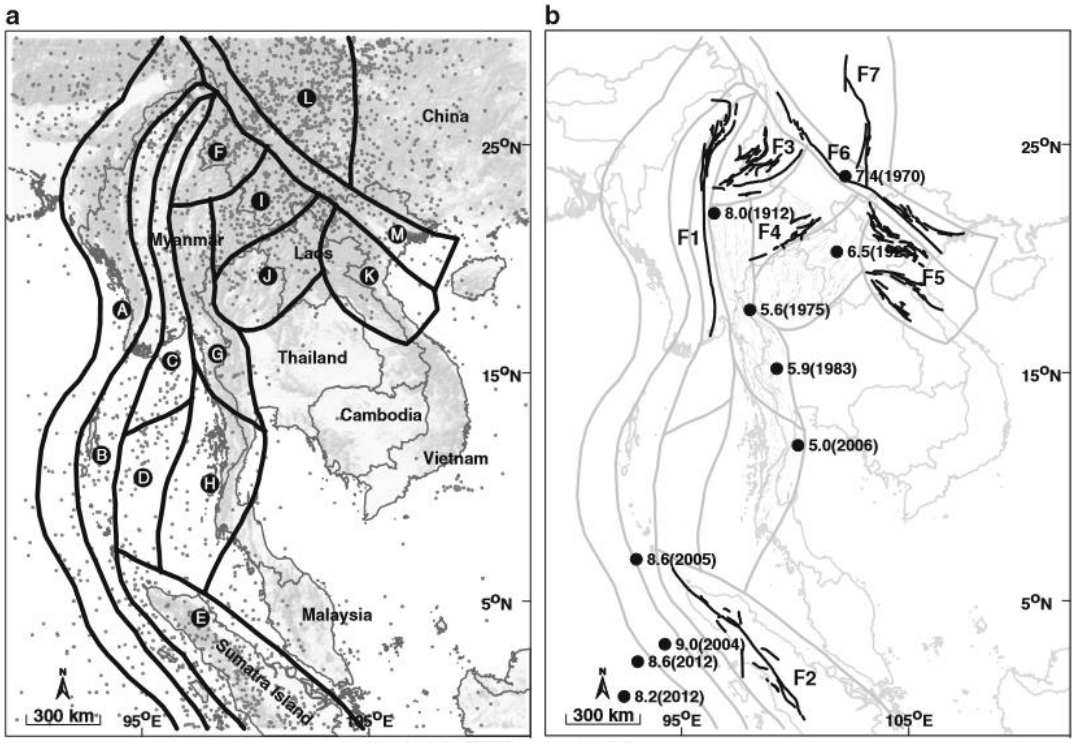

Figure 1. 5. Map showing the Mainland Southeast Asia region. a) The 13 seismic source zones. The grey circles are the epicenters recorded from 1964 to 2010. b) The important fault zones indicated by the black lines. The black circles are the earthquake events.

Table 1. 1. FMD coefficients (a and b values) and fractal dimension (Dc) of 13 seismic source zones recognized in MSEA.

name	EQ no.	Mc	a	b	Dc
A: Sumatra-Andaman Interplate	414	4.7	5.98	0.768±0.05	1.91±0.01
B: Sumatra-Andaman Intraslab	560	4.7	6.58	0.877±0.05	2.03±0.02
C: Sagaing Fault Zone	101	4.7	5.80	0.864±0.10	1.61±0.02
D: Andaman Basin	87	4.3	4.51	0.611±0.05	2.17±0.03
E: Sumatra Fault Zone	139	4.8	4.75	0.606±0.06	1.96±0.01
F: Hsenwi-Nanting Fault Zones	48	4.8	6.02	1.010±0.30	1.48±0.01
G: Western Thailand	22	4.4	3.98	0.668±0.20	-
H: Southern Thailand	9	-	-	-	-
I: Jinghong-Mengxing Fault Zones	84	4.2	4.87	0.712±0.08	1.85±0.01

J: Northern Thailand-Dein Bein Phu	62	4.0	4.72	0.732±0.09	1.86±0.04
K: Song Da-Song Ma Fault Zones	10	-	-	-	-
L: Xianshuihe Fault Zone	197	4.5	6.14	0.915±0.09	1.80±0.02
M: Red River Fault Zone	49	4.4	5.99	1.030±0.10	1.48±0.03

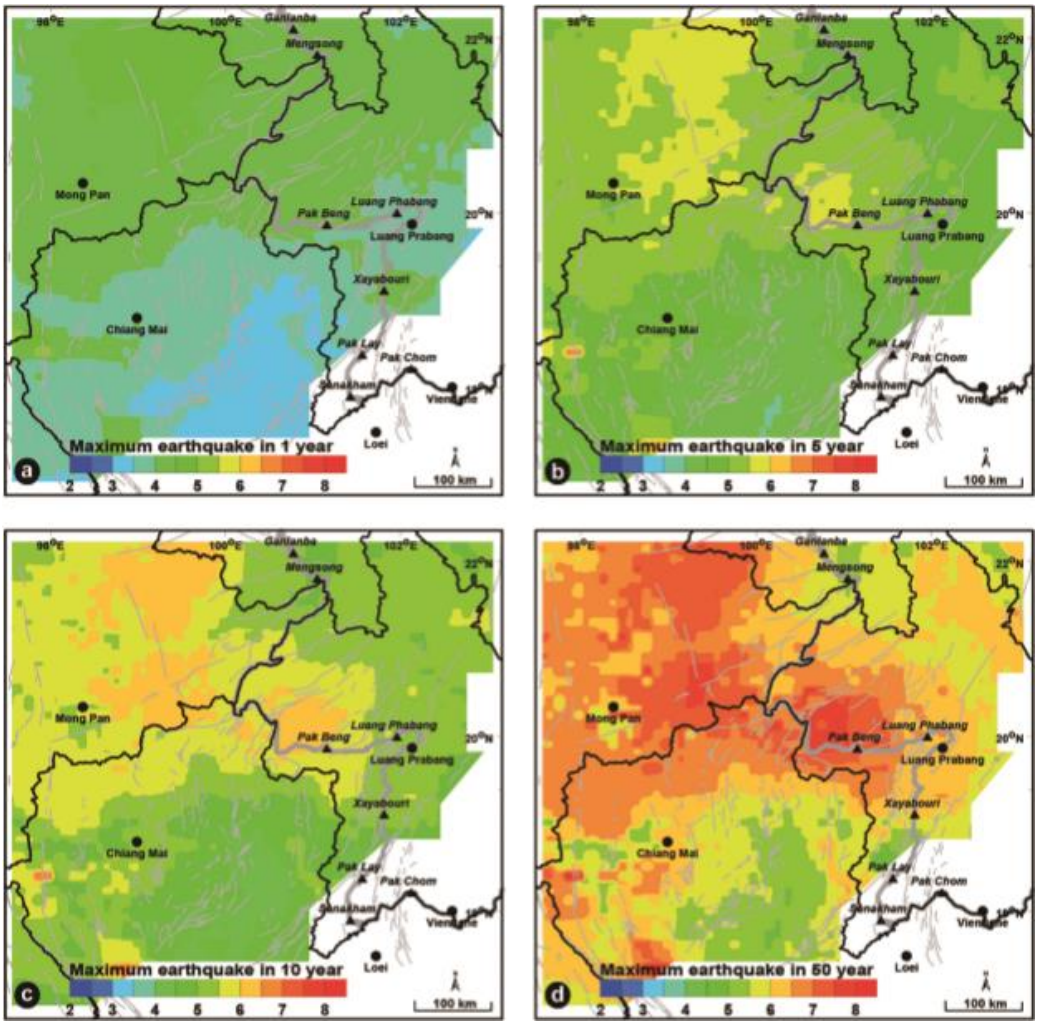

Figure 1. 6. The possibility of large earthquake to be generated in the individual of time as a) 1 year b) 5 years c) 10 years and d) 50 years.

According to Figure 1.7, the northern parts of the Thailand-Laos-Myanmar border region have a significant potentiality to generate the Mb of 4.0, 5.0, 6.0 and 7.0 within 1, 5, 50 and 500 years as the return periods, respectively. However, in the eastern part of Chiang Mai, the Mb of 4.0 -7.0 earthquake can be generate in the average time intervals of 5-5000

years. Finally, the earthquake prediction was analyzed from b value which the low b value represents the high stress in the region. The result has been suggest the possibility that the earthquake may occur at the northern part of Mong Pan, Pak Beng dam and Luang Prabang dam as shown in Figure 1.8 (Pailoplee et al., 2013) .

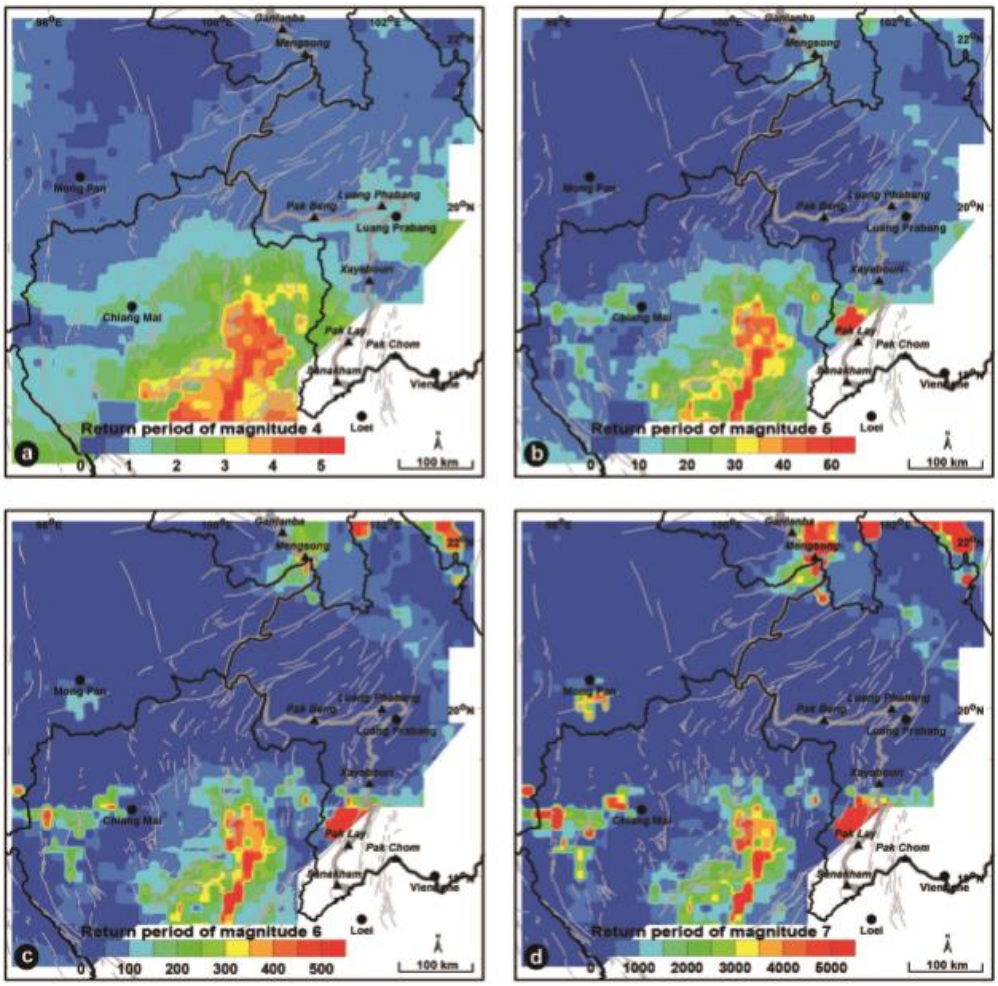

Figure 1. 7. The return period of earthquake magnitude level of a) 4.0, b) 5.0, c) 6.0 and d) 7.

Furthermore, not only the characteristics but also the probabilistic seismic hazard was studied in the northern Thailand. It can be described that Chiang Mai, Lamphun and Lampang provinces have 70-90% chance of the Mw 5.0 and 20-40% of the Mw 6.0 in the next 50 years for earthquake activity. In case of Mw 7.0, the

probability is less than 10%. While, Phayao, Phrae and Uttaradit provinces have 40–70% chance. Almost all of the study areas showed 70–90% of a Mw 5.0 earthquake in the next 50 years. In contrast, there is merely 2-10% for probability of hazard. Therefore, Pailoplee and Charusiri (2015) can assume that the Chiang Mai province showed the high-risk earthquake activities but low hazard.

From the previous works, in spite the fact that the northern Thailand-eastern Myanmar-northern Laos regions are not located on the subduction zone, they could be affected from the neighboring seismic activity like the continuous northward subduction of the Indian plate beneath the Eurasian plate. These reasons have supported that they can generate powerful earthquakes and definitely affect to Thailand. Consequently, we interested in studying the mechanism, pattern of earthquake distribution and characteristics in Thailand-Laos-Myanmar borders.

As we mentioned, Thailand is not located on the subduction zone, but it could be impacted from the nearby earthquake activity. Thailand has many active faults as well. In view of this, Thailand is the risk area. Hence, we should conduct a study more about tectonic activity, faults, earthquake and effect from the shaking of the earth's crust. The aims are to protect and minimize loss of life and damage in all cases.

1.3. Study Area and Scope of Study

The study area of morphological features which indicates seismogenic fault and distribution of earthquake is Thailand-Laos-Myanmar border region, located on 16.77°N – 22.35°N latitude and 97.88°E– 103.16°E longitude, covered northern Thailand, northern and western Laos and eastern Myanmar (Figure 1.9).

The Thailand-Laos-Myanmar border is dominated by a large number of earthquake distributions, such as the earthquake occurred on June 24th, 1983 at latitude of 21.36°N and longitude of 102.58°E with Mw 6.9, occurred at 09:07 local time. (Table 1.2)

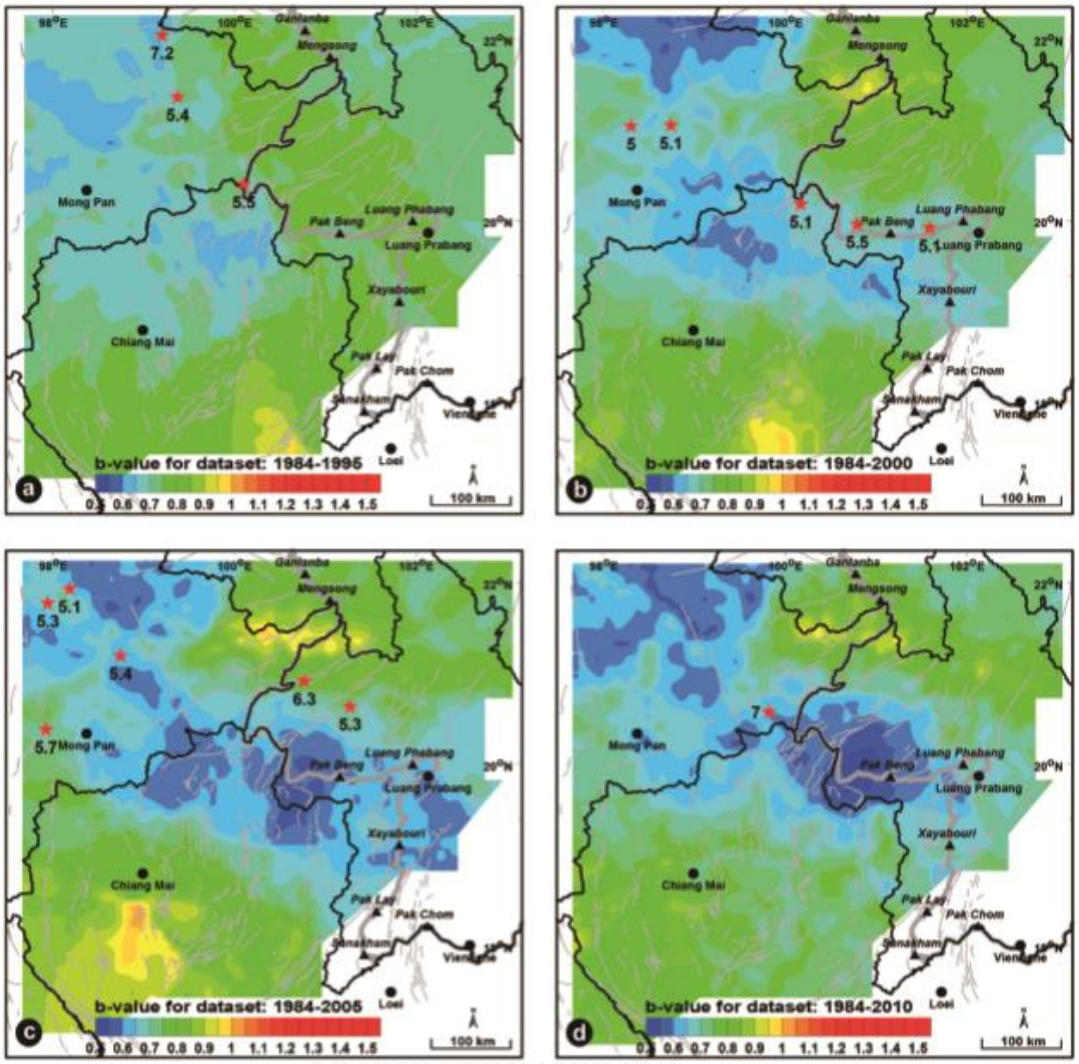

Figure 1. 8. Spatial b-value distributions, as derived using the seismicity data recorded during a) 1984 - 1995, b) 1984 - 2000, c) 1984 - 2005, and d) 1984 - 2010.

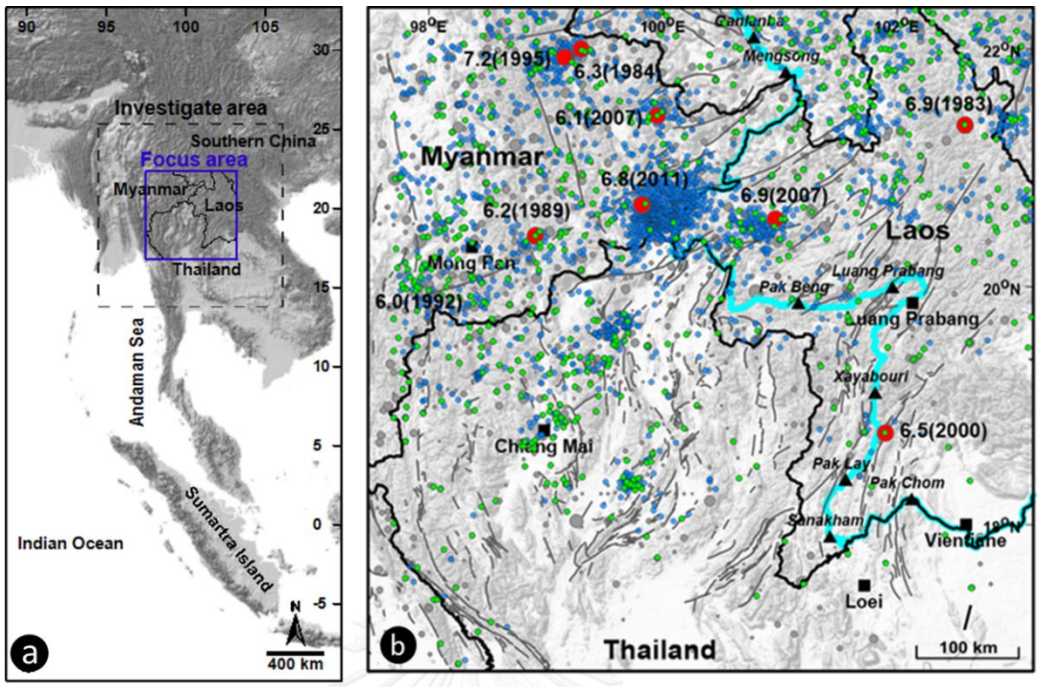

Figure 1. 9. a) Map showing the MSEA, the Sumatra-Andaman zone (thick grey line) and seismogenic faults as compiled by Pailoplee et al. (2009) (thin black line). The study area focuses in the TLMB bounded by the square. b) Map of study area showing the earthquake with Mw ≥ 6.0 (red circles). The fault lines, hydro power dam, major cities are shown with thin blue lines, black triangles and black squares, respectively. The blue and green dots are the earthquake dataset occurred during 1965 to 2016 that before and after declustering process, respectively.

1.4. Objectives

The main goal of the study is to determine the characteristics, mechanisms, understanding the stress and strain regime, including defining the seismic patterns of the earthquake that occurred in the study area. In order to reach these objectives, two different methods were used to analyze the data. The detailed purposes show consecutively as these following.

1. To investigate the mechanism of fault in Thailand-Laos-Myanmar borders by the focal mechanism.

2. To evaluate the seismic pattern in Thailand-Laos-Myanmar border by the fractal dimension.

Table 1. 2. List of earthquakes with a moment magnitude (Mw) ≥ 6.0 posed in the Thailand-Laos-Myanmar border during 1982-2014.

No.	Lon	Lat	Date	Time	Depth (km.)	Magnitude (Mw)
1	102.58	21.36	24/06/1983	09:07	49.0	6.9
2	99.62	21.79	23/04/1984	22:30	17.0	6.3
3	99.06	20.32	28/09/1989	21:52	15.0	6.2
4	99.22	21.89	11/07/1995	21:46	15.0	6.8
5	101.90	18.77	07/06/2000	21:48	33.0	6.5
6	100.89	20.52	16/05/2007	08:56	12.6	6.3
7	100.00	21.49	23/06/2007	08:17	16.1	6.1
8	100.02	20.62	24/03/2011	13:55	13.2	6.8
9	99.68	19.72	05/05/2014	11:08	12.0	6.2

CHAPTER II
THEORY AND METHODOLOGY

The Earth's crust is clearly extremely complex and it is generally accepted that earthquakes are a chaotic phenomenon. Thus, as in the case of weather forecasting and earthquake studying must be considered on a statistical basis. The statistical properties of seismicity patterns can be used to investigation future earthquakes. Basic types of statistical seismicity precursors include foreshock, quiescence, swarms, activation and doughnuts (Nanjo et al., 2006). At present, the method of the earthquake prediction is developed and divided into 3 types which are short term (day-month), intermediate term (month-year) and long term (year) (Shebalin et al., 2006) (Table 2.1). Most of the methods inform the location, time or size of earthquake that may occur in the future. From all of the methods, the intermediate term is the most acceptable prediction and understanding tectonic mechanism because a sample results from statistical analysis.

Table 2. 1. Different kinds of the earthquake forecasting (Shebain et al., 2006 and Pailoplee 2009)

Method	Examples
A. Long-term (years)	
A1. Paleo-seismological study	McCalpin (1996); Pailoplee et al. (2009a)
A2. Historical study	McCue (2004); Stirling and Petersen (2006)
A3. Seismic hazard analysis	Kramer (1996); Pailoplee et al. (2009b)
A4. Global positioning system	Yagi et al. (2001); Fu and Sun (2006)
B. Intermediate-term (months-year)	
B1. b-value anomaly	Nuannin et al. (2005)
B2. Fractal dimension	Maryanto and Mulyana (2008)
B3. Artificial neural network	Bodri (2001); Alves (2006)

B4. Coulomb stress failure	Du and Sykes (2001); Bufe (2006)
B5. Pattern Informatics	Nanjo et al. (2006)
C. Short-term (days-month)	
C1. Animal perception	Kirschvink (2000)
C2. Cloud Precursor	Menshikov et al. (2012)
C3. Ground water fluctuation	Oki and Hiraga (1988)

2.1. The Focal Mechanism

2.1.1. The theory of the focal mechanism

The focal mechanisms are geometrical representations of faulting during earthquake occurrence and refer to the direction of slip in that earthquake. Seismologists use database from seismograms to compute the focal mechanism and indicate it on the maps by beach ball symbol. The focal mechanism beach ball can be obtained from observing the first motion of P-wave, which was the first arriving to each seismograph station. They are divided into 3 types as up motion, down motion and no apparent signal (see also Figure 2.1).

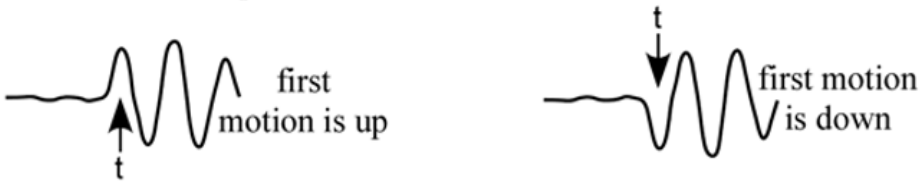

Figure 2. 1. The three types of the P-wave first motion.

The data are ready to plot on a lower-hemisphere stereographic projection. If the first motion of P-wave is down, it presents a circle. If the first motion is up, it signifies a black dot. And if it is no signal, a cross is shown. The schematic diagram is plotted by 3 steps (Figure 2.2). The first is plotting symbols of P-wave first motion into circle. The next is identifying the circle symbol and black dots. The last, beach ball

represents the type and orientation of the fault that produced earthquake. The compression first-motions should lie only in the quadrant containing the tension axis (T), and the dilatation first-motions should lie only in the quadrant containing the pressure axis (P) as shown in the dark quadrants and the white quadrants, respectively (Figure 2.2). The focal mechanism beach ball represents fault and motion of slip as shown in schematic diagram (Figure 2.3).

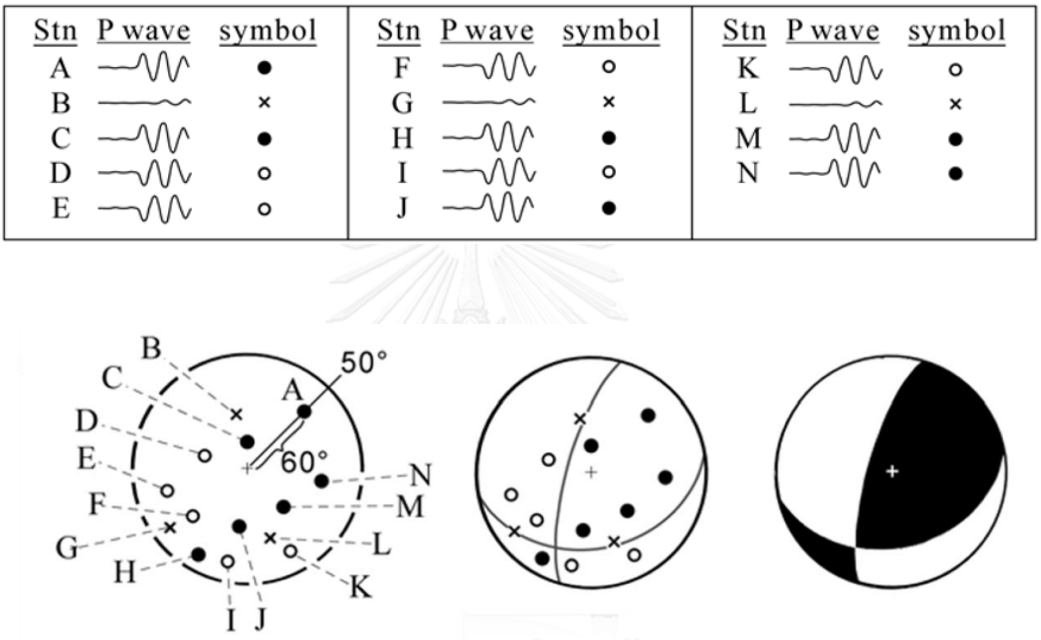

Figure 2. 2. The table shows the P-wave and symbols were recorded by 14 seismograph stations (A-N). The three circles show 3 steps to plot and make beach ball.

From the schematic diagram, we found the consist of relative motion of two blocks of Earth called hanging wall and foot wall. The description of rupture is related to three angles as the strike. dip, rake angles (Figure 2.4):

- Strike is the direction of a line created by the intersection of a fault plane and a horizontal surface, 0° to 360°.

- Dip is the angle between fault and a horizontal plane. The dip of a vertical fault is 90°. The dip of a horizontal fault is 0°.

- Rake is the moving direction during rupture; it is measured relative to fault strike, ±180°.

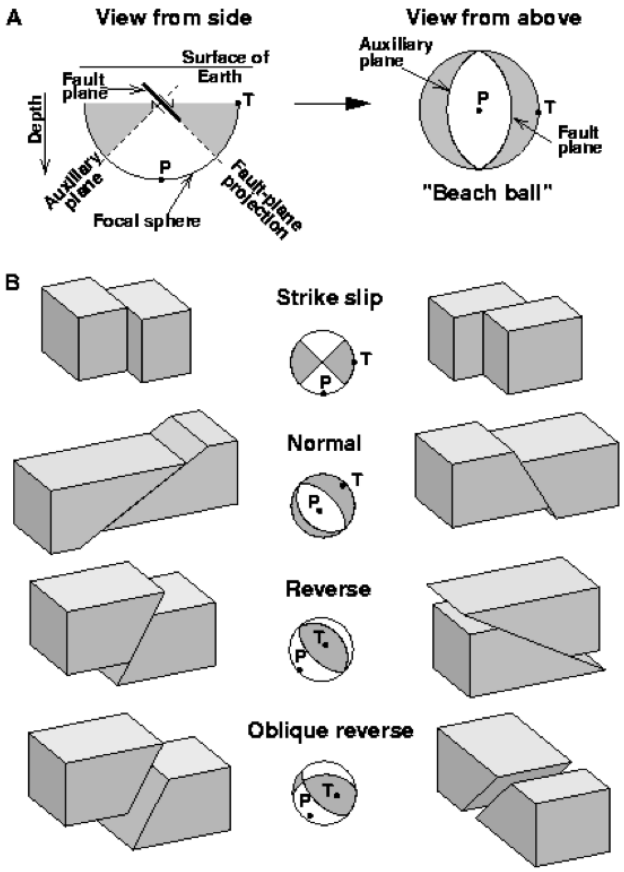

Figure 2. 3. Schematic diagram of a focal mechanism (USGS, 1996)

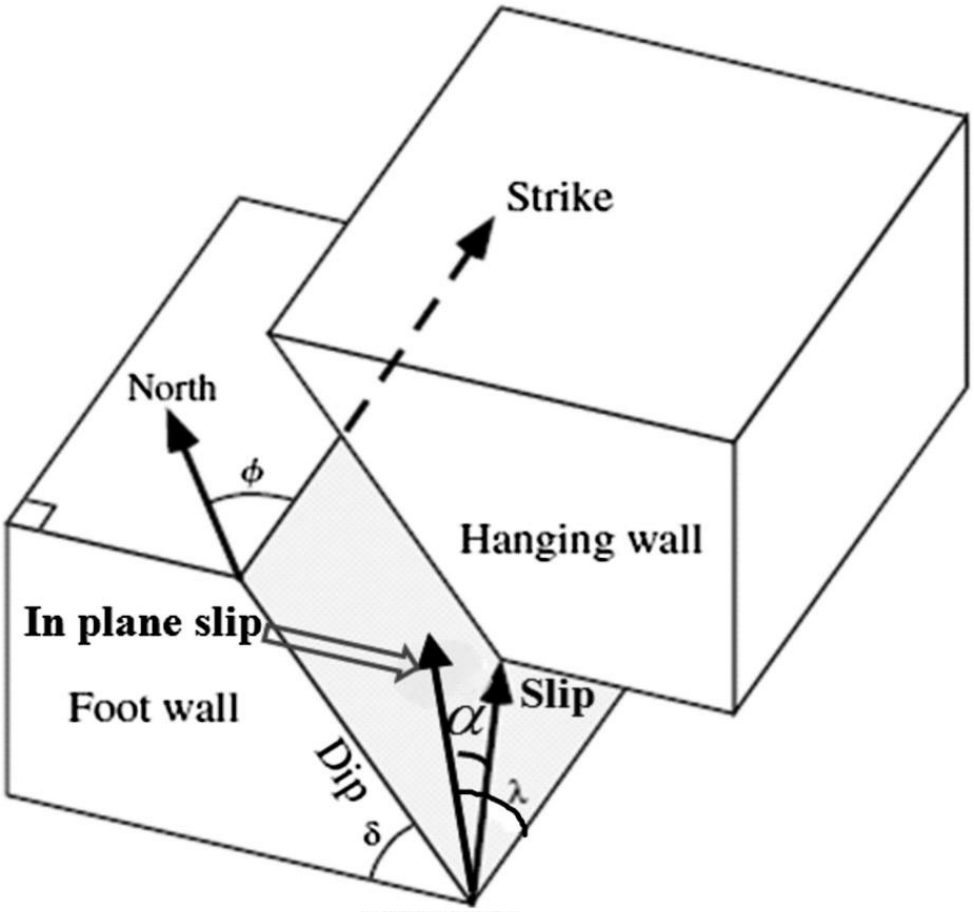

Figure 2. 4. Strike, dip and rake of focal mechanism.

2.1.2. Application of the focal mechanism

In a research article by Shanker et al.(2011), they tried to explain about seisnotectonic of Nepal Himalaya and vicinity. The study area was divided into 4 regions as A, B, C and D based on the spatial distribution of the events from 1803-2006 as illustrated in Figure 2.5. The Central Himalaya comprising Nepal and its adjoining region in which different types of faulting patterns exist have signatures of a great earthquake in 1934 and a number of large events thereafter, advocate serious seismic hazard in the region. (Shanker et al., 2011)

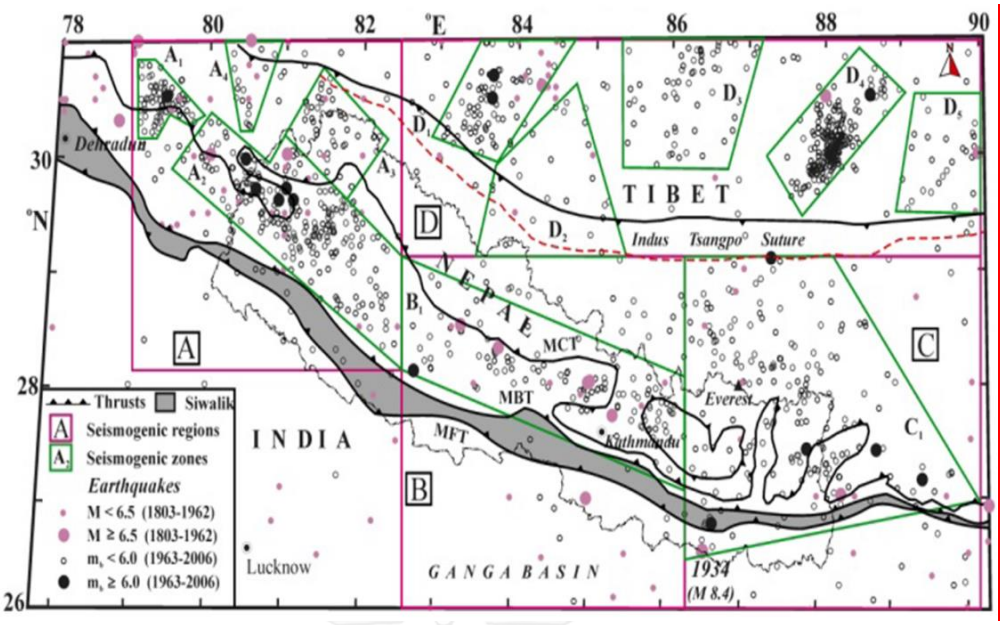

Figure 2. 5. Map of Nepal and adjoin region in the Central Himalaya was divided into 4 zones, using the seismic data from 1803 to 2006. The Main Central Thrust (MCT), Main Boundary Thrust (MBT), Main Frontal Thrust (MFT) and Indus-Tsangpo Suture (ITS) are the major tectonic features in the region.

Morewood and Roberts (2001) studied the focal mechanism and surface slip data in the eastern Gulf of Corinth, Greece. The Gulf of Alkyonides is bounded on its southern shores by the major E- W- striking, north- dipping South Alkyonides fault segment (SAFS). The overall area, almost focal mechanism is normal faults (Figure 2.7). Dominant fault trends in the area are E-W, N-S, NNE-SSW and NE-SW. (Morewood and Roberts, 2001)

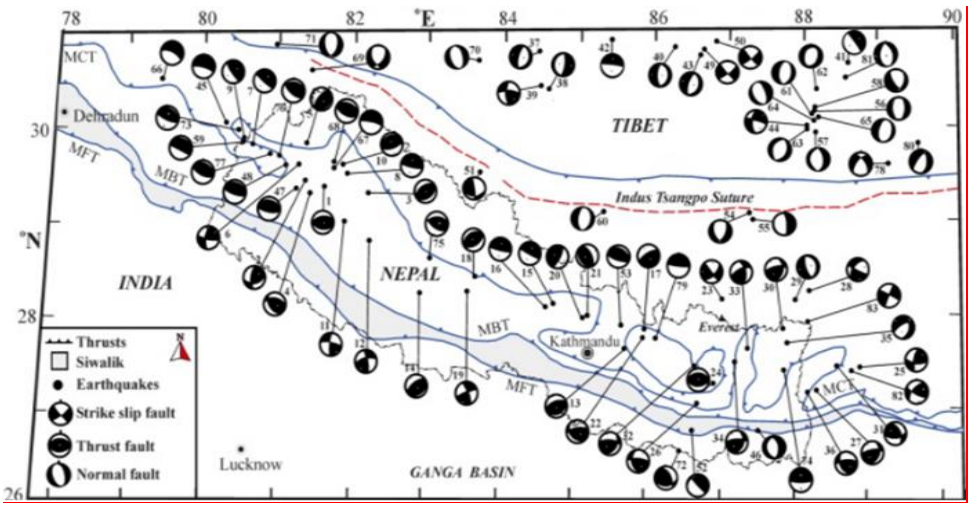

Figure 2. 6. A simplified tectonic map of the Central Himalaya and its adjoining region showing major faults (after Dasgupta et al., 1987).

The fault plane solutions for the 1981 aftershocks (King et al., 1985) were plotted on the fault map of the Porto Germano/Psatha Bay area shown in Figure 2.8. The result suggested that the 1981 aftershocks occurred on fault planes that are oblique and normal motion. For example, aftershock no.19 occurred on a N-S-striking normal fault at a depth of 7.09 ± 2 km. While aftershock no.26 occurred on a NE-SW-striking normal fault plane at a depth of 8.34 ± 2 km.

2.2. The Fractal Dimension

2.2.1. The theory of the fractal dimension

Though major surface traces of the faults are generally well mapped, a significant fraction of regional seismicity occurs in secondary and sometimes on hidden structures (Hanksson 1990; Jones et al., 1990). The fractal dimension provides a measure of the degree of fractal clustering of point in the space. Tosi (1998) implied that the possible value of fractal dimension (Dc) is bounded to range between 0 and 2, which is dependent on the dimension of the embedding space. Interpretation of such limit values is that a set with Dc = 0 has all events clustered into one point. At the other end of the scale, Dc = 2 indicates that the events are random or

homogeneously distributes over a 2D embedding space. Aki (1981) separated the characteristics of a fault by value of Dc close to 3 signifies that a volume of the crust, a value close to 2 signifies that a plane and a value close to 1 means line sources.

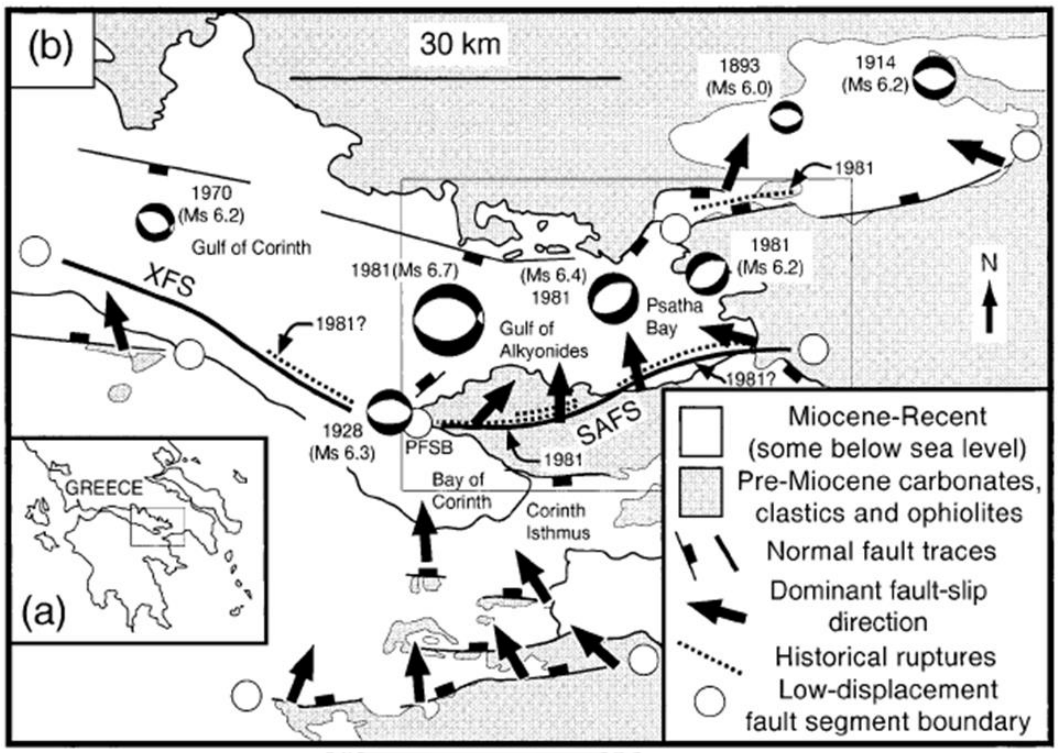

Figure 2. 7. a) Location map of Greece. b) Map showing the segmented normal fault system at the eastern end of the Gulf of Corinth which indicates by strike in Figure 2. 8. These sets of faults exhibit a mutually cross- cutting relationship, for example, N-S faults cut E-W faults and vice versa. Mean fault dips for each locality vary from 51° to 84°.

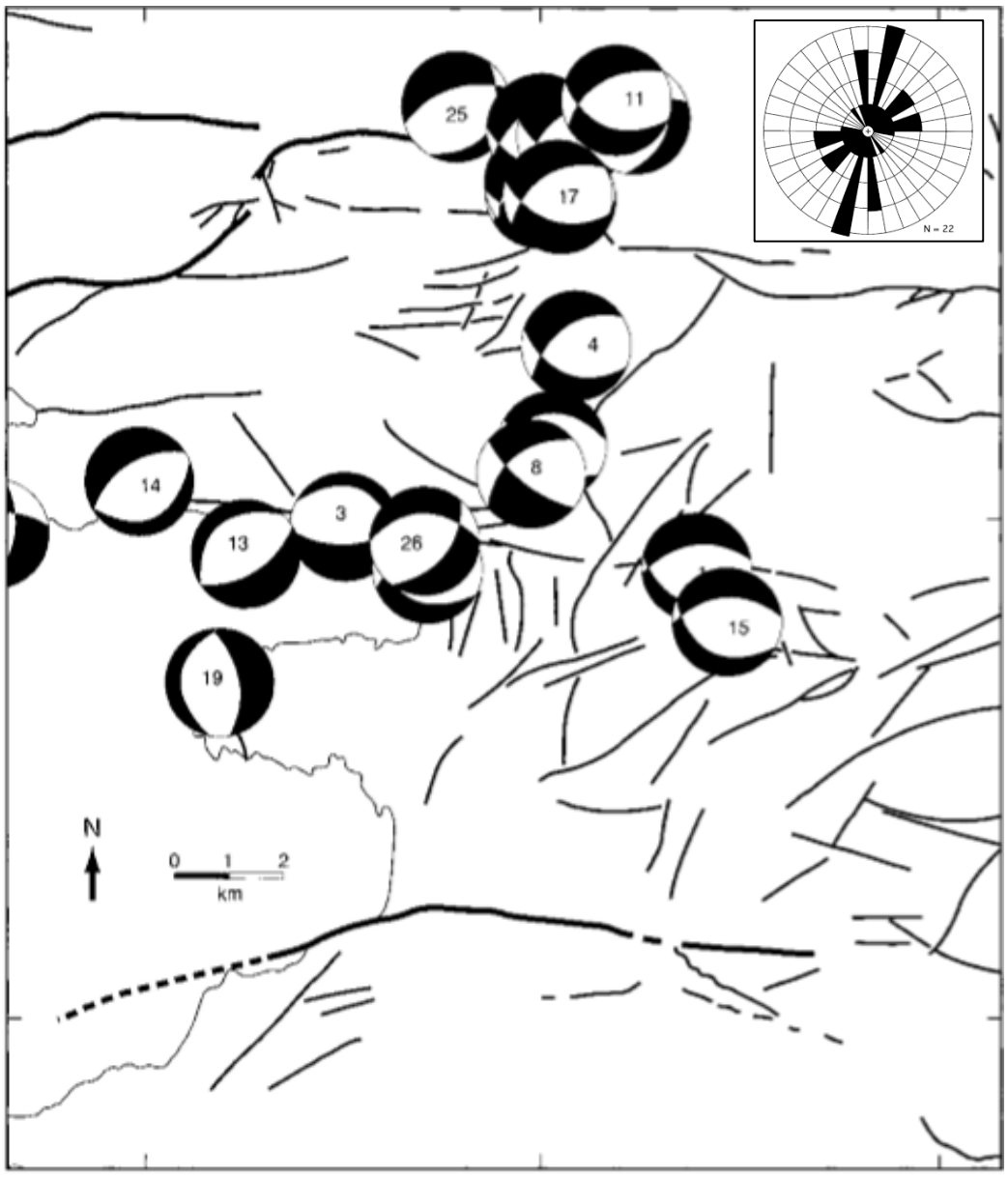

Figure 2. 8. Map of the Porto Germano/Psatha Bay area with focal mechanisms of the 1981 aftershocks. The rose diagram showing the strikes of fault planes.

The fractal dimension is estimated by using the correlation integral method of Kagan and Knopoff (1980) which measures the Dc. (Kagan and Knopoff, 1980) The correlation integral method is widely applied in seismology, especially to spatial distributions of earthquake epicenters. This technique is preferred to the box-counting method because of its greater reliability and sensitivity to small changes in cluster

properties (Kagan and Knopoff, 1980; Hirata, 1989). The correlation integral is given by Grassberger and Procaccia (1983), expressed as

$$C_r = \frac{2}{N(N-1)} N_{(R<r)} \tag{2.1}$$

Where N is the number of earthquakes analyzed, and $N_{(R<r)}$ is the number of event pairs separated by a distance R < r. The correlation integral is related to the standard correlation function as given by Kagan and Knopoff (1980).

$$C_r \approx r^{D_C} \tag{2.2}$$

Where Dc is a fractal dimension, more strictly, the correlation dimension. Grassberger and Procaccia (1983) introduced a practical algorithm for the measure of the correlation dimension, commonly referred to the Grassberger-Procaccia algorithm, GPA. By plotting C against r on a double logarithmic coordinate, we can practically obtain the fractal dimension Dc form slope of the graph. The distance r between two events, (θ_1, ϕ_1) and (θ_2, ϕ_2) is calculated by using a spherical triangle as is given by Hirata (1989). (Hirata, 1989)

$$r = \cos^{-1}[\cos\theta_1 \cos\theta_2 + \sin\theta_1 \sin\theta_2 \cos(\phi_1 - \phi_2) \tag{2.3}$$

Where θ_1 and θ_2 are the latitudes and ϕ_1 and ϕ_2 are the longitudes of the event 1 and 2, respectively.

The fractal dimension may be used as a quantitative measure of the degree of heterogeneity of seismic activity in fault systems of a region, and it is controlled by the heterogeneity of the stress field and the pre-existing geological, mechanical or structural heterogeneity. If the earthquakes become progressively more clustered, the value of Dc decreases. The b and Dc value change from the region to region because the applied stress level is different in the regions.

2.2.2. Application of the fractal dimension

Bayrak and Bayrak (2012) used the instrumental database recorded between 1900 and 2001, and divided the area of Western Anatolia into 15 seismogenic segments. There were divided based on tectonic and seismotectonic regions. Then, they investigated the regional variation of the Gutenberg-Richter parameter (a and b) and Dc. They got the Dc values varying between 1.91 and 2.21 (Figure 2.9). The Dc values were assumed that faults are spatially distribution in the area. (Bayrak and Bayrak, 2012)

An earthquake with Mw 7.6 took place in central Taiwan on September 21th, 1999. Chen et al. (2006) used a large number of aftershocks of the 1999 Chi-Chi, Taiwan, earthquake (Ml=7.3). The earthquakes were reported in the area around the epicenter over the span of 6 months after the main shock. The seismicity is characterized by the b value of the Gutenberg-Richter relation and fractal dimension Dc. Those large aftershock looks like enveloping the region with Dc ≥ 2.2 in the eastern part of the study area (Figure 2.10). (Chen et al., 2006)

According to Pailoplee and Choowong (2014), the instrumental recorded earthquake data within MSEA were analyzed in terms of b value and Dc value for 13 seismic source zones. The result revealed that regional variations in both of the b and Dc values could imply local tectonic stress and hazard levels. The Dc values varied between 1.48 and 2.17 which appeared on the seismic source zones, viz., A, E, I, L and J as illustrated in the yellow zone. The Dc value ranged from 1.8 to 2, the earthquakes distributed along the fault plane (Figure 2.11). (Pailoplee and Choowong, 2014)

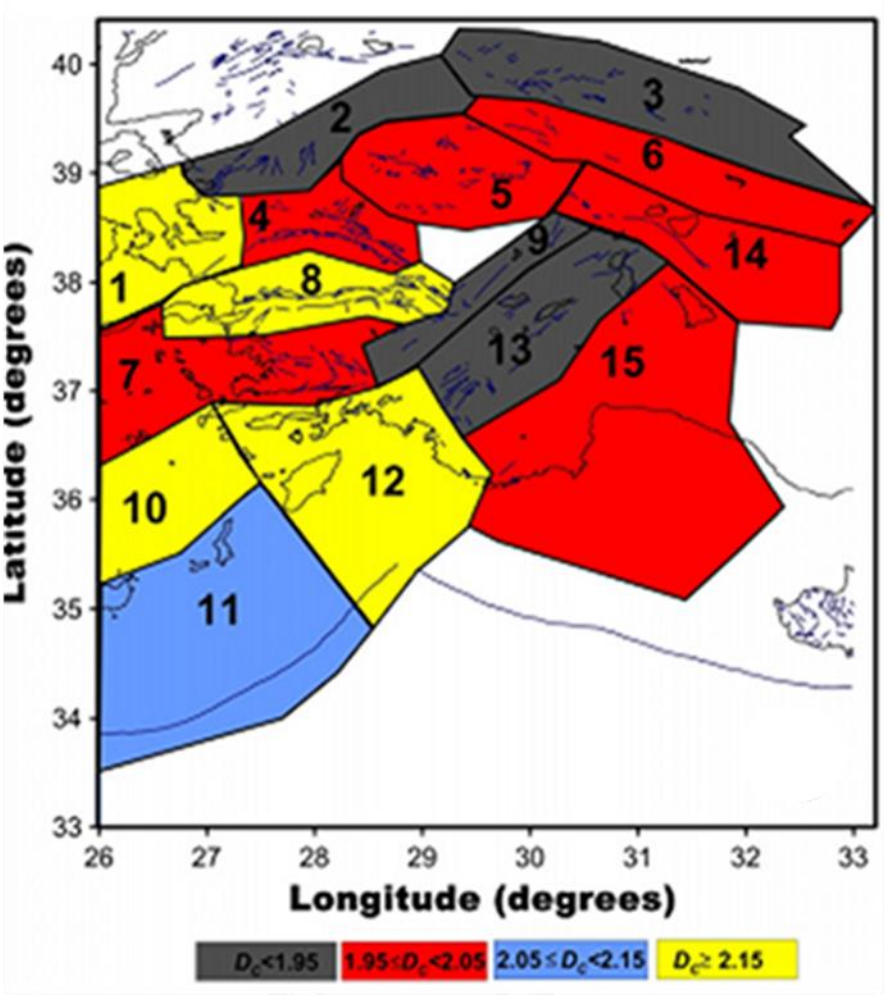

Figure 2. 9. Map of the Dc value. The computed Dc for 15 different seismogenic zones in Western Anatolia(Bayrak and Bayrak, 2012).

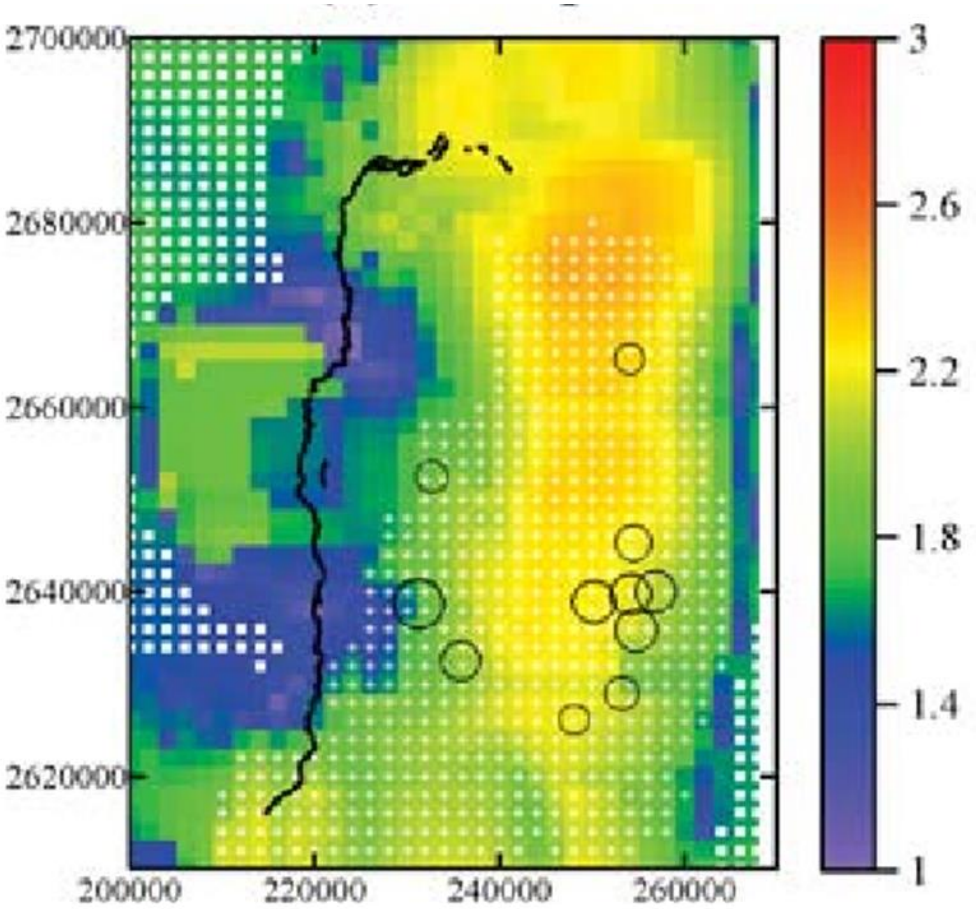

Figure 2. 10. The Dc value from the aftershock sequence occurred within 6 months after the Chi-Chi main shock. The circles denote the main shock and large aftershocks with Ml ≥ 6. The thick black line denotes the Chelungpu thrust fault. Grid points marked by solid squares represent the areas with less than 100 earthquakes, and crosses for the areas with the b-Dc relationship ≥ 2.5 (Chen et al., 2006).

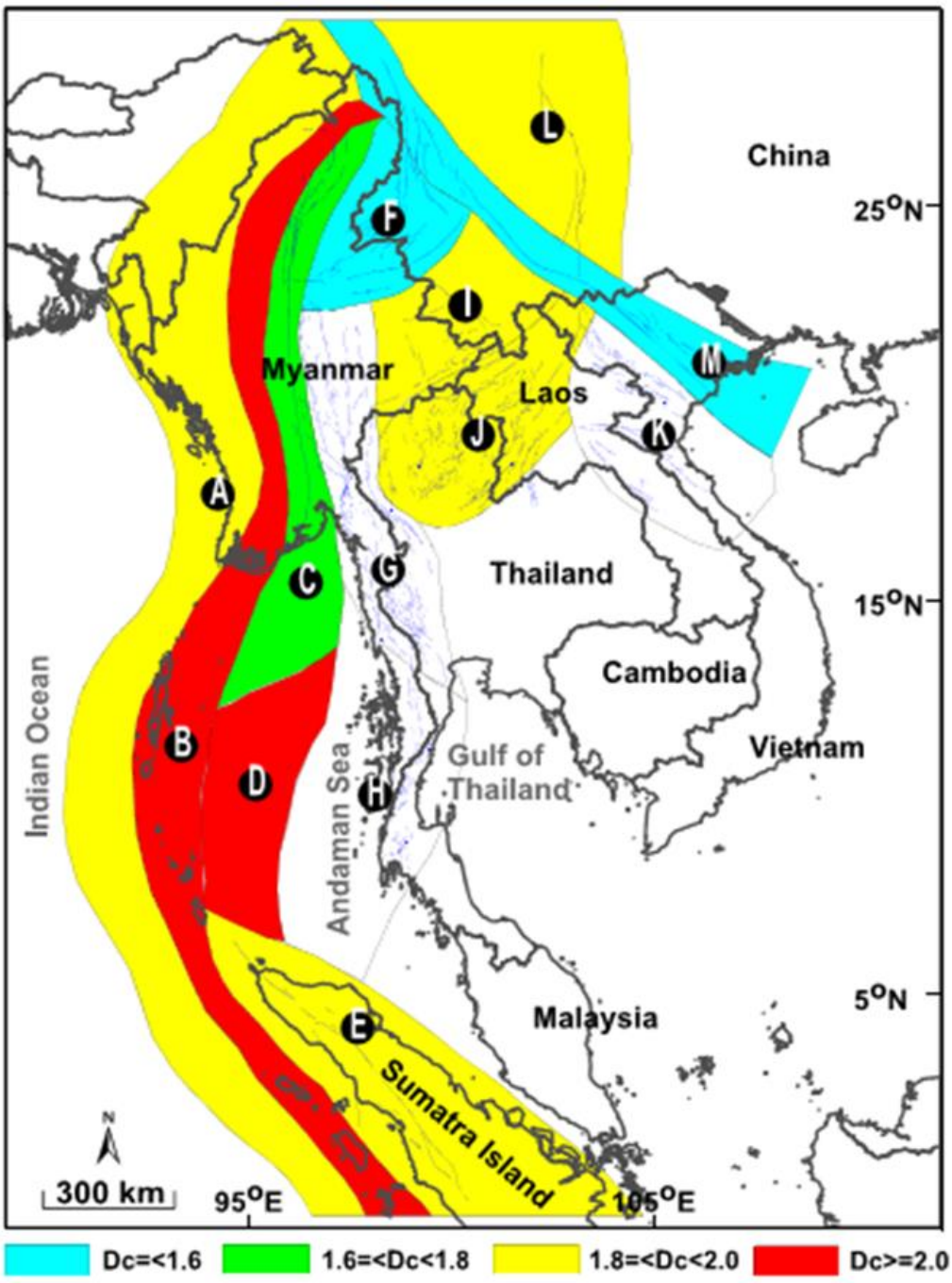

Figure 2. 11. Map showing distributions of estimated Dc for zones A to M in MSEA. (Pailoplee and Choowong, 2014)

The changing in pattern of epicenter distribution before the Tkachi-oki earthquake, Hokkaido, Northern Japan in 2003 with magnitude 8 (Figure 2.12). The Dc values were investigated by temporal variation analysis. In the study, the Dc value has decreased

in 1998 and got the nadir before the main shock occurrence for one year (Figure 2.13). The characteristic result elucidated that decreasing in Dc signified a precursor of the Tkachi-oki earthquake because earthquake activation and quiescence essentially cancel out each other in the number of earthquakes.

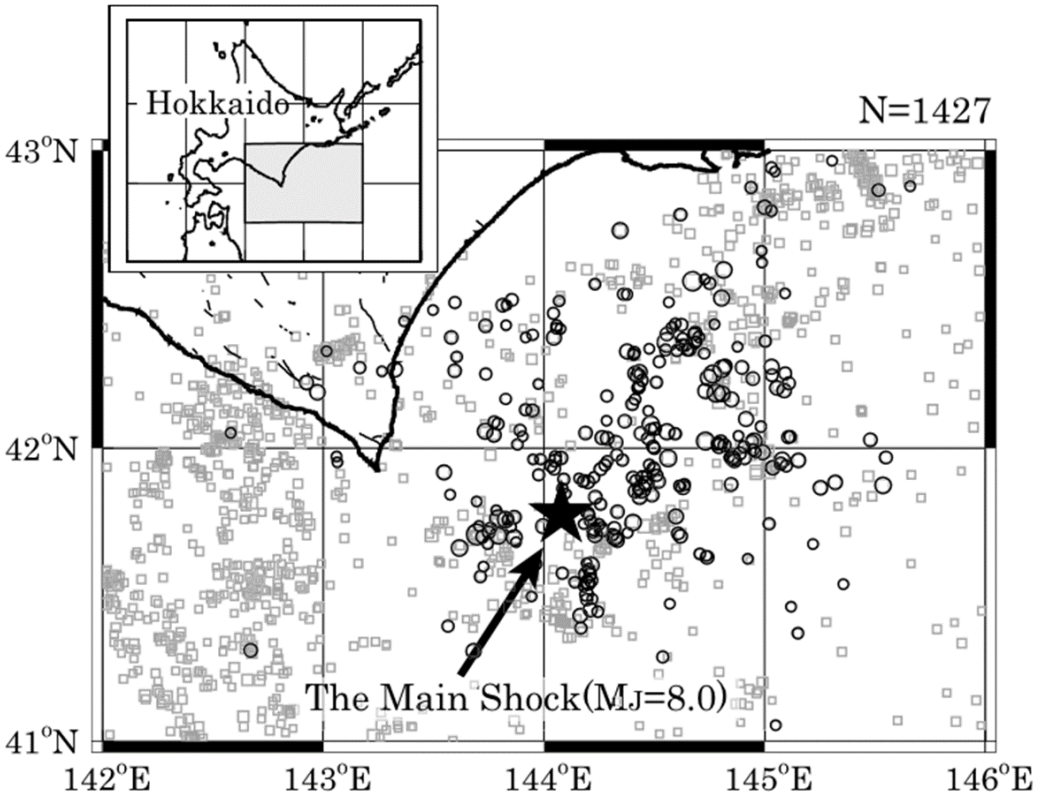

Figure 2. 12. Epicenter distribution with Mj ≥ 3.4 earthquakes in study area. The star is main shock and circles are aftershocks. Squares are earthquakes occurred before the main shock. (Murase, 2004)

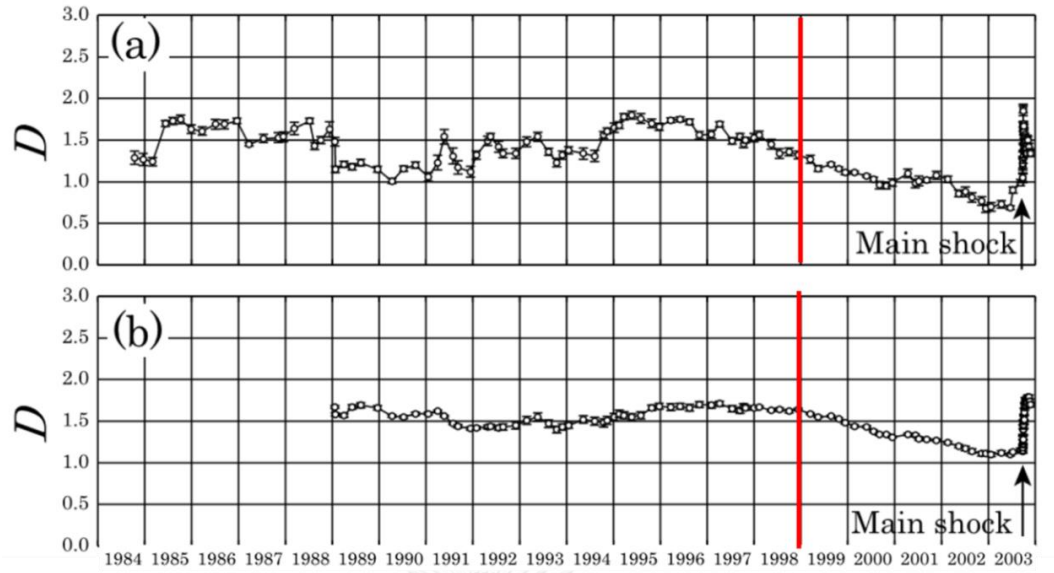

Figure 2. 13. Temporal changes in the Dc value, a) Dc changes with 100 events time-windows. b) Dc changes with 300 events time-windows. *(Murase, 2004)*

2.3 Frequency Magnitude Distribution (b-value)

2.3.1 The theory of the frequency magnitude distribution

According to Gutenberg and Richter (1944), the FMD power law can be expressed as shown in Equation (2.4) (Gutenberg and Richter, 1944).

$$LogN = a - bM \tag{2.4}$$

Where N is the cumulative number of earthquakes with a magnitude ≥ M. The a and b are coefficient value in any specific time and space window. Seismotectonically, the a value indicates the entire seismicity level, and the b value relates to tectonic stress (Mogi, 1967); (Scholz, 1968). Lower b value relates to high levels of accumulated stress (Manakou and Tsapanos, 2000; (Pailoplee and Choowong, 2014))

2.3.2 Application of the Frequency Magnitude Distribution

Bayrak and Bayrak (2012) obtained b values between 0.71-1.02 as shown in Figure 2.14, they found the relation between these parameters for different regions in

Western Anatolia. They observed negative correlation between Dc and b value by Dc = 2.60 – 0.64b, whereas, the positive correlation between Dc and a/b values for difference regions have Dc = 1.17 + 0.14(a/b) (Figure 2.15). The Dc/b values are high may be used as an indicator of the earthquake hazard level of the difference seismogenic zone and can be used for seismicity, earthquake risk and hazard study as well.

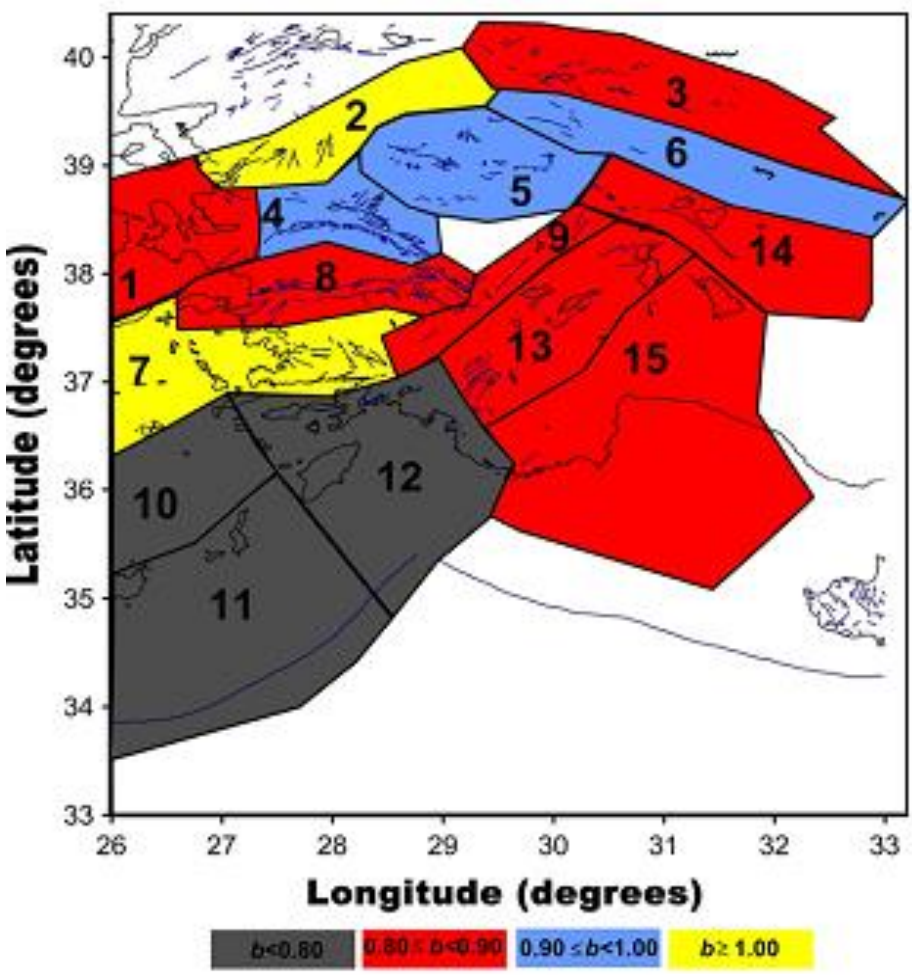

Figure 2. 14. The computed b-values for 15 different seismogenic zones in Western Anatolia. *(Bayrak and Bayrak, 2012)*

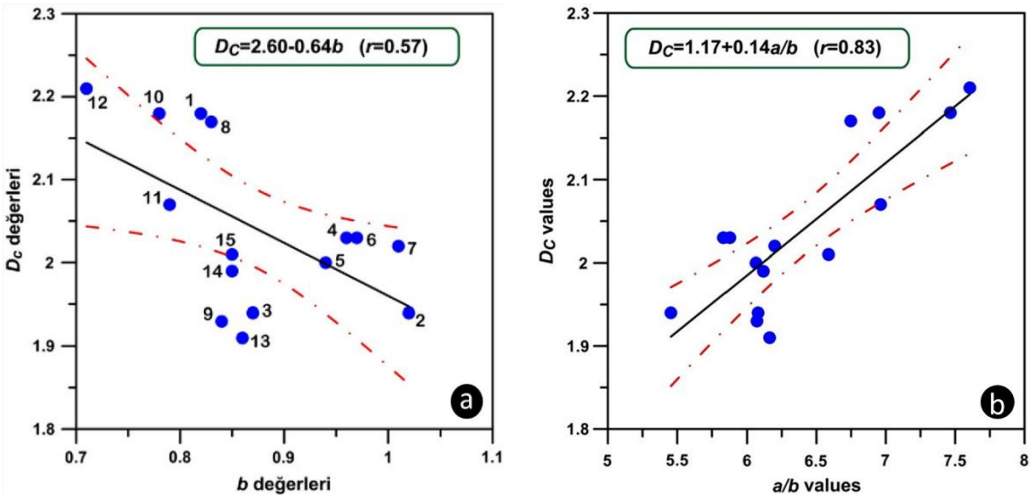

Figure 2. 15. Map showing a) the relationship between b and Dc values. b) the relationship between a/b ratio and Dc values for 15 seismogenic zones in Western Anatolia. Straight line is the linear regression. Dashed lines are 95% confidence limits and r is the correlation coefficient.

Chen et al. (2006) examined a large number of aftershock events from the 1999 Chi-Chi, Taiwan. The area strong suggests the anomalous low b value when the event occurred (Figure 2.16). The result in this research supported the hypothesis that a large aftershock produced a few secondary aftershocks with moderate sizes, therefore, lower the b value. They found the positive correlations between b and Dc from the aftershock sequence. There are D=3b and D=2b, 65% of point lying in between D=2b (Figure 2.17).

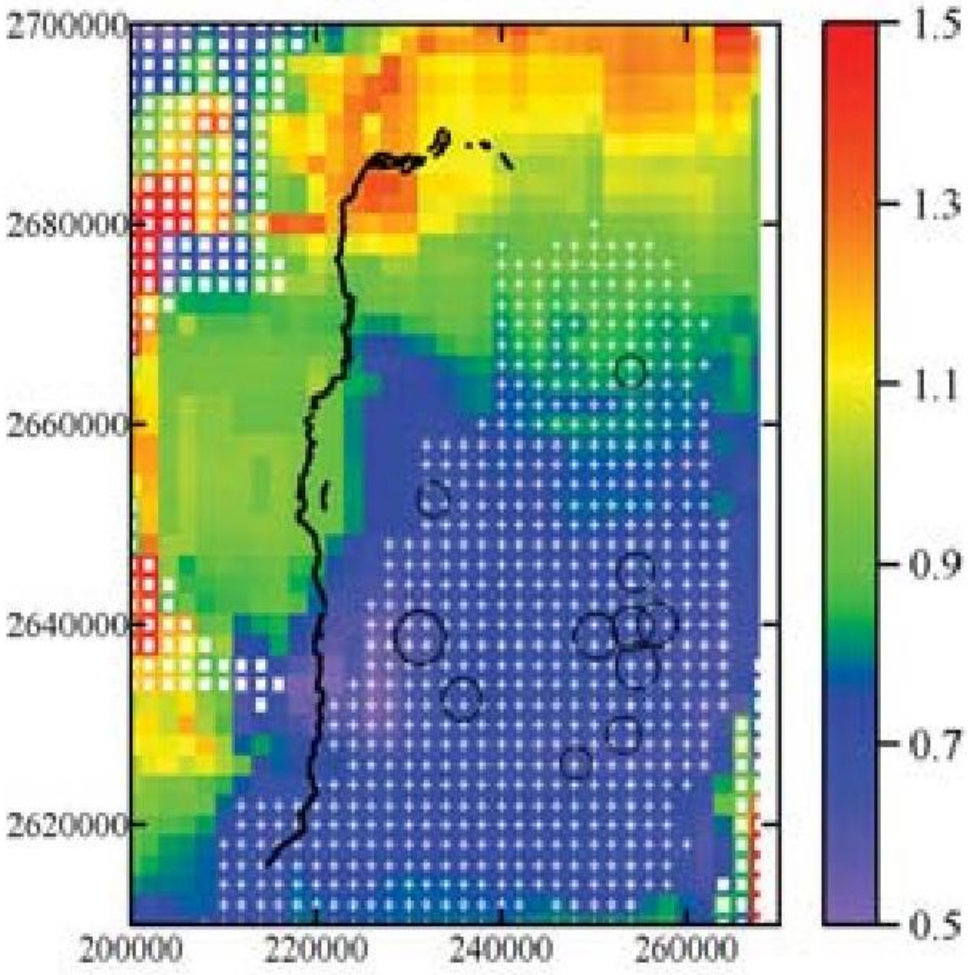

Figure 2. 16. The fractal correlation dimension Dc from the aftershock sequence occurred within 6 months after the Chi-Chi main shock. The circles denote the main shock and large aftershock with Ml ≥ 6. The thick black line denotes the Chelungpu thrust fault. Grid points marked by solid squares represent the areas with less than 100 earthquakes, and crosses for the areas with the B and Dc relationship ≥ 2.5(Chen et al., 2006).

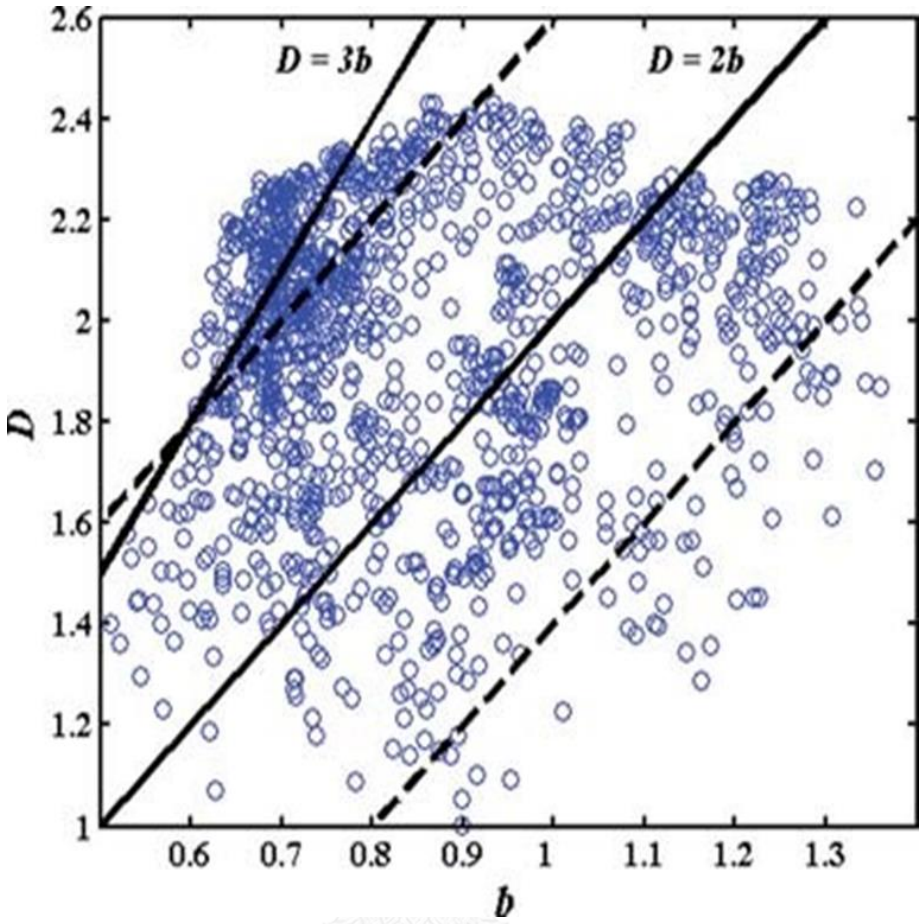

Figure 2. 17. The graph demonstrates the b value and the Dc from the aftershock sequence. Two straight lines show the Dc as D=2b and D=3b.

Pailoplee and Choowong (2014) studied the relationship between b and Dc (Figure 2.19a) and relationship between a/b ratio and Dc (Figure 2.19b) for the MSEA. They got Dc = 2.80 – 1.22b in the relation between b value and Dc, and Dc = 0.27(a/b) – 0.01 in the relation between a/b ratio and Dc. The results reportedly have low b and high Dc values in some zones and some are conversely presented. As stated previously, the anomalous low b zones accumulate high levels of tectonic stress as shown in the blue zones, obtained the b value less than 0.7 (Figure 2.18).

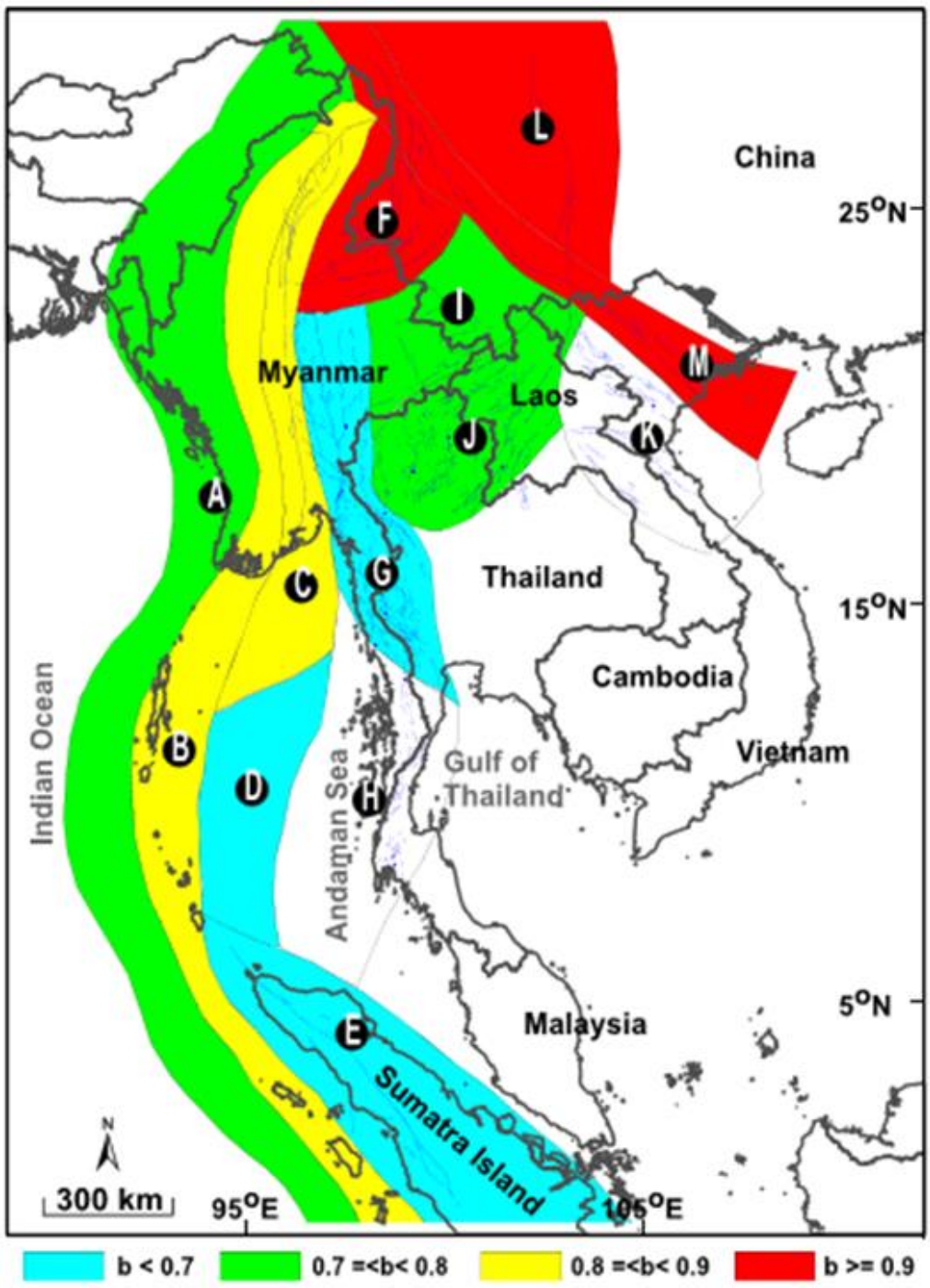

Figure 2. 18. Map showing distributions of estimated b values for zones A to M proposed in MSEA.

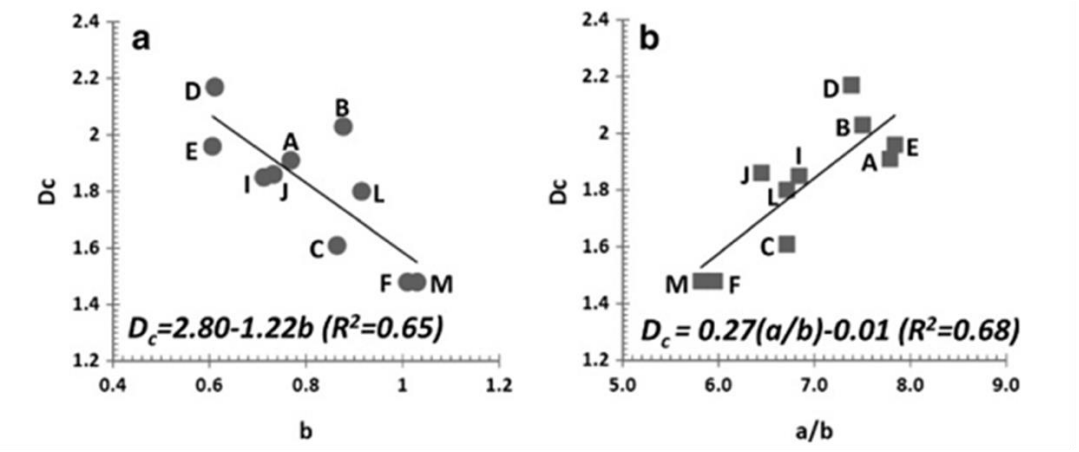

Figure 2. 19. The relationships between a) the b and Dc values and b) the a/b ratios and Dc values for the 13 seismic source zones (A to M). The straight lines represent the linear regressions fitted to the observed data.

CHAPTER III
SEISMICITY DATA AND COMPLETENESS

The seismic data was recorded from history to the present day. It can classify by time record and completeness of data into 3 types which are (i) geological record (ii) historical record and (iii) instrumental record. The geological record and the historical record are a retrospective record called paleo-seismological which record data of earthquake in long time ago (around 10,000-100,000 years ago). Although the seismologists understand the process of previous large earthquake by paleo-seismological. The disadvantage is non-standard measurement. The records are the ambiguous descriptions or depicts which noted by personal experience. Thus, the epicenter, magnitude and occurrence time are all down to individual interpretation. Therefore, the paleo-seismological data have a limitation as dependability and accuracy. On the other hand, the instrumental record could last for much shorter time period of record than others. The process comprises numerical data analysis from mathematics and science. The data consist of latitude and longitude of epicenter, time occurrence (year, month, day, hour, minute and second) and magnitude of the earthquake. The data from the instrumental record called earthquake catalogue which is recording from several seismic network registers worldwide, for instance, (i) International Seismological Center (ISC), (ii) National Earthquake Information (NEIC), (iii) Global CMT Catalogue (CMT) and (iv) The Thai Methodological Department (TMD).

However, the diversity of the earthquake data sources lead to several magnitude scales that created for a specific type of seismic waves measurement. The well-known of earthquake magnitude measurements, i.e., local magnitude (Ml) (Richter, 1935), surface-wave magnitude (Ms) (Gutenberg, 1945), body-wave magnitude (Mb) (Gutenberg and Ritchter, 1956) and moment magnitude (Mw or M) (Hanks and Kanamori, 1979; Kanamori, 1977). A variety of different magnitude scales can definitely influence accuracy and precision in analysis. Thus, we must complete data for statistical analysis.

In this chapter, the seismicity data, i.e., the earthquake catalogue in this study area are clarified in order to improve the completeness of data for both focal mechanism and fractal dimension investigation in the next chapter.

3.1. Focal Mechanism Data

From the instrument recording station, we used the focal mechanism data which covered the study area. The recorded data contain location (longitude and latitude) and mechanism of fault rupture (strike, dip and rake) (Table 3.1.). From the data collecting result, there are 26 earthquake events as presented in Table 3.1. We can analyze the focal mechanism diagram (beach ball) by Faultkin program and examined strike, dip and rake by Grapher program.

Table 3. 1. Examples of focal mechanism data.

long	lat	str1	dip1	rake1	str2	dip2	rake2	sc	iexp	name
98.65	24.39	323	80	-172	232	82	-10	1.22	26	052976A
98.58	24.29	242	88	0	152	90	178	11.2	25	052976B
98.60	24.26	342	72	-169	249	80	-18	1.63	25	053176A
96.24	3.18	338	28	99	147	62	85	3.55	26	062076A
98.57	24.74	338	88	-178	248	88	-2	1.98	25	072176A
99.50	1.08	92	46	132	220	58	56	8.73	24	011277A
100.04	0.50	312	80	179	42	89	10	1.85	25	030877D
92.77	21.60	216	72	3	125	87	162	9.91	24	051277C
98.43	0.70	332	11	112	130	80	86	2.3	24	052377B
95.58	4.26	78	19	-140	310	78	-76	4.15	25	052577B

3.2. Seismicity Data

3.2.1. Earthquake catalogue combination

The earthquake catalogue from instrumental earthquake record is recorded difference data of each database. The collecting seismicity data from several earthquake data sources may provide more useful catalogues which can deploy in seismology (Woessner et al., 2010). This work attempted to collect seismicity data in

the Thailand-Laos-Myanmar border (16.76° – 22.30°N and 97.48° – 103.16°E) as much as possible. The result indicates the main earthquake data sources available in this area from the (i) ISC, (ii) NEIC, (iii) GCMT, (iv) TMD and (v) IDC (International Data Center) (Figure 3.1). The earthquake data includes location (longitude, latitude and depth) and time (year, month, day, hour and minute). The various kinds of magnitude forms are reported in these catalogues including Mb, Ms, Mw and some Ml (Table 3.1).

Table 3. 2. Examples of earthquake catalogue.

Long	Lat	Year	Month	Day	Depth	Hour	Min	Sec	Mw	Mb	Ms	Ml
100.13	-3.57	2007	10	12	15	0	31	32	5.8	-	-	-
100.37	-3.38	2007	10	12	31	0	31	31	5.4	5.5	-	5.8
100.509	-3.28	2007	10	12	15	0	31	29	5.6	5.6	5.5	-
100.509	-3.28	2007	10	12	15	0	31	29	5.6	5.6	5.5	-
100.56	-4.31	2007	10	11	30	20	38	37	5.4	-	-	-
100.978	-3.9	2007	10	11	35	20	38	35	5.4	5.3	5.3	-
100.978	-3.9	2007	10	11	35	20	38	35	5.3	5.3	5.3	-
100.56	-4.31	2007	10	11	30	20	38	35	5.4	-	-	-
100.68	-4.1	2007	10	11	30	20	38	33	5.2	6.1	-	5.8
100.32	-2.96	2007	10	10	15	16	4	21	4.5	5.8	-	4.6

Considering in each of data sources, the reported time and magnitude is different, such as the NEIC and ISC catalogue. Also, both of network store their lowest magnitude of earthquake in a different value which NEIC has the lowest magnitude of 3, whereas, ISC detected at 0. However, both of them recorded earthquake data since 1960. The TMD records a widely magnitude range and constant. Nevertheless, TMD detected seismicity data between 1980 and 2009 only. Despite of the fact that the GCMT have the least seismicity data, they provide the high- quality, accurate and precise earthquake data as they recalculated all data for making the best possible seismicity catalogues. Therefore, we need to improve the quantity and quality of seismicity data which are merged by using the assumption from Suckale and Grünthal

(2009), for avoiding double-counting earthquake events (Figure 3.1). Hence, the composite earthquake catalogue contains total 12,133 numbers of data, ranges in Mw from 0.1 to 7.7 during the 52 year period from 1964–2016 in the study area.

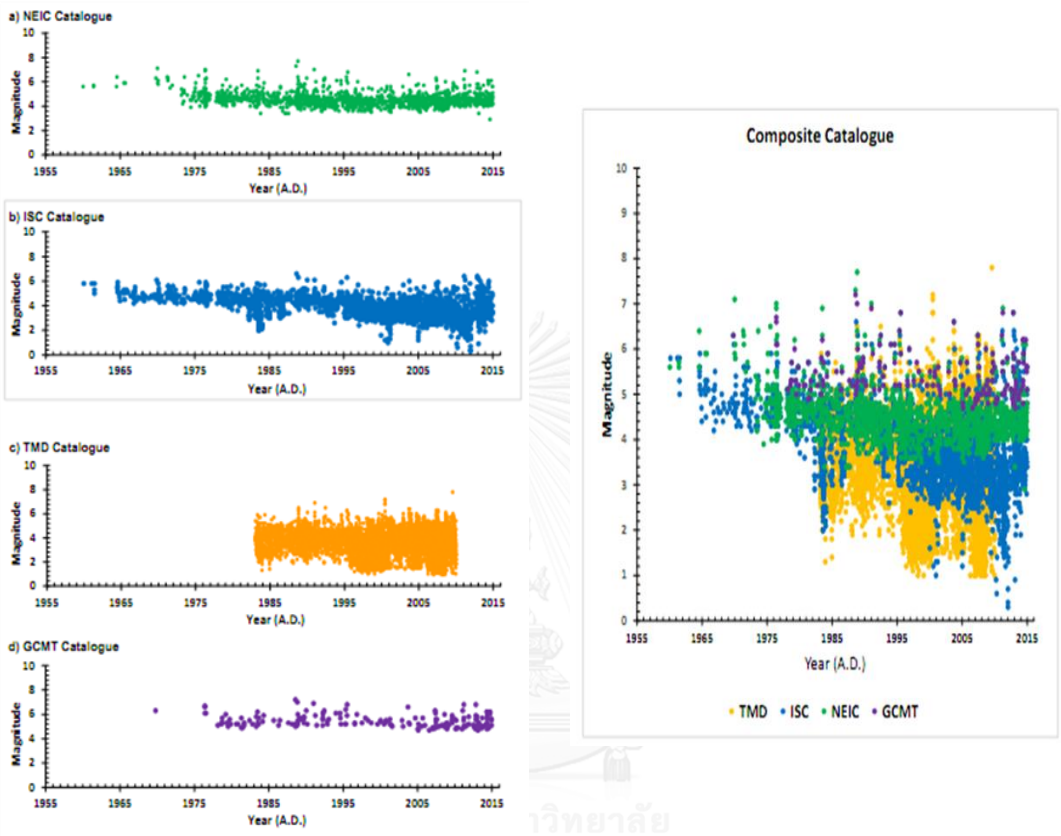

Figure 3. 1. Showing relationships between the magnitude and date of earthquakes record, a) NEIC, b) ISC, c) TMD, d) GCMT and composite catalogue.

3.2.2. Earthquake magnitude conversion

The variety of earthquake catalogues provides the different types of magnitude reported by these agencies. For example, the TMD detects for local seismicity which is recording in Ml. The accuracy is increased with the shaking event that less than 650 km and reduced with the far seismicity source. While, the ISC, NEIC and GCMT can record the global seismicity which is recording in Mb, Ms, and Mw. They recorded in global scale of great distance or the medium and large earthquake. The Mb analysis is obtained from the first arrival P-wave from a seismogram. The Ms and Ml are detected

from the S-wave. The Mw is developed to avoid the error of saturation in other magnitude scale while the large earthquakes occurred which does not depend on an instrument record that make it be the most suitable magnitude scales (Hanks and Kanamori, 1979; Kanamori, 1977) (Figure 3.2).

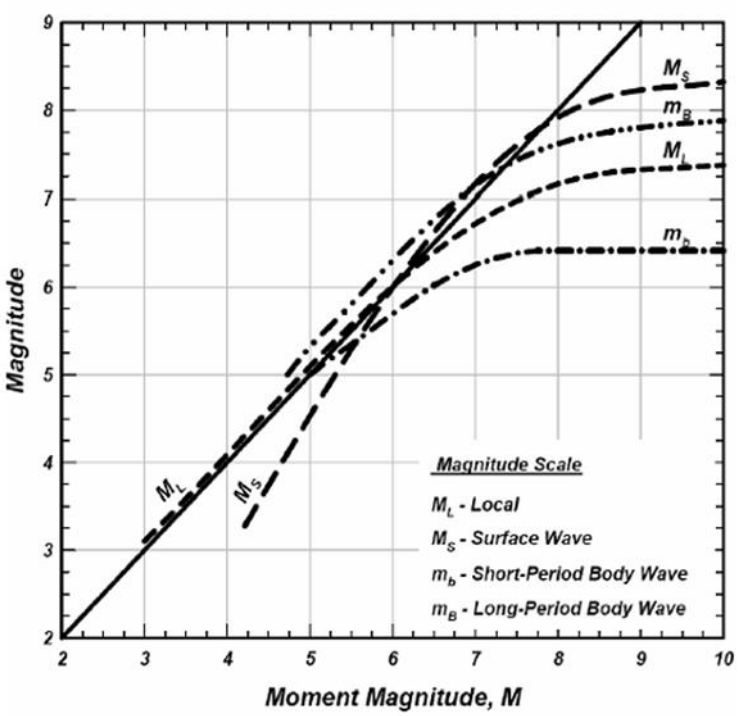

Figure 3. 2. The graph shows the saturation of the various magnitude scales by Kagan and Knopoff (1980b). (Kagan and Knopoff, 1980)

The seismicity data recorded in Thailand-Laos-Myanmar border have reported the different magnitude scales (Mb, Ms and Ml). In this study, we directly converted the different magnitude scales to Mw. In exception for Ml, that must be converted to Mb before converting Mb to Mw later. The conversion can analyze by using the equations from calibrates the empirical relationships between these different scales (Figure 3.3).

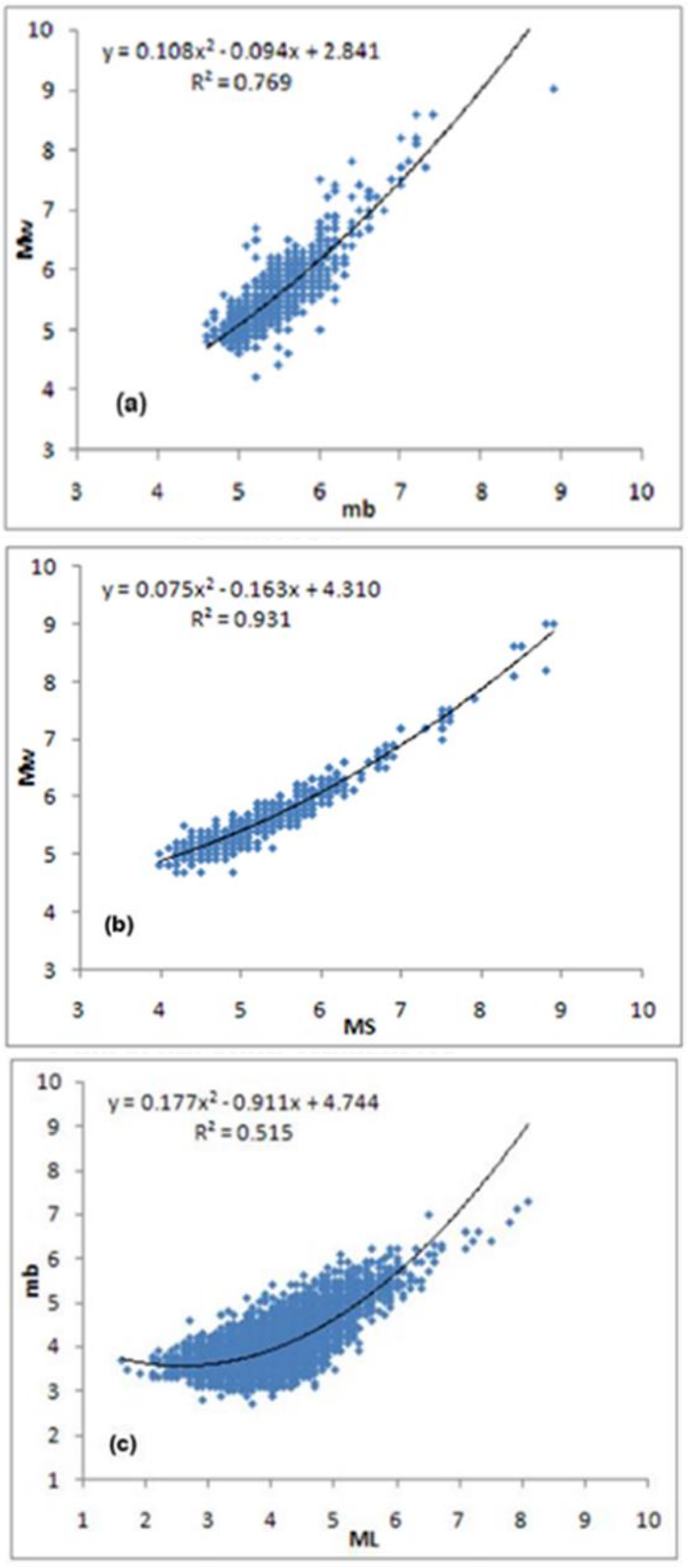

Figure 3. 3. Empirical relationships between (a) Mb - Mw, (b) Ms - Mw and (c) Ml -Mb.

3.3.3. Earthquake declustering

In general, the global and local earthquake catalogue from each data source can be divided the process and classified temporally into 3 types are (i) foreshock (ii) main shock and (iii) aftershock. The main shock generated by stress directly from process of tectonic activity in area. The foreshock is an earthquake which is occurs before the largest earthquake event in the same or nearby time and space. The aftershock is a smaller than mainshock which is generated by strain from energy transplant of fault area. Therefore, the analysis of seismic data must be removed foreshock and aftershock for obtain a complete independent earthquake (Figure 3.4).

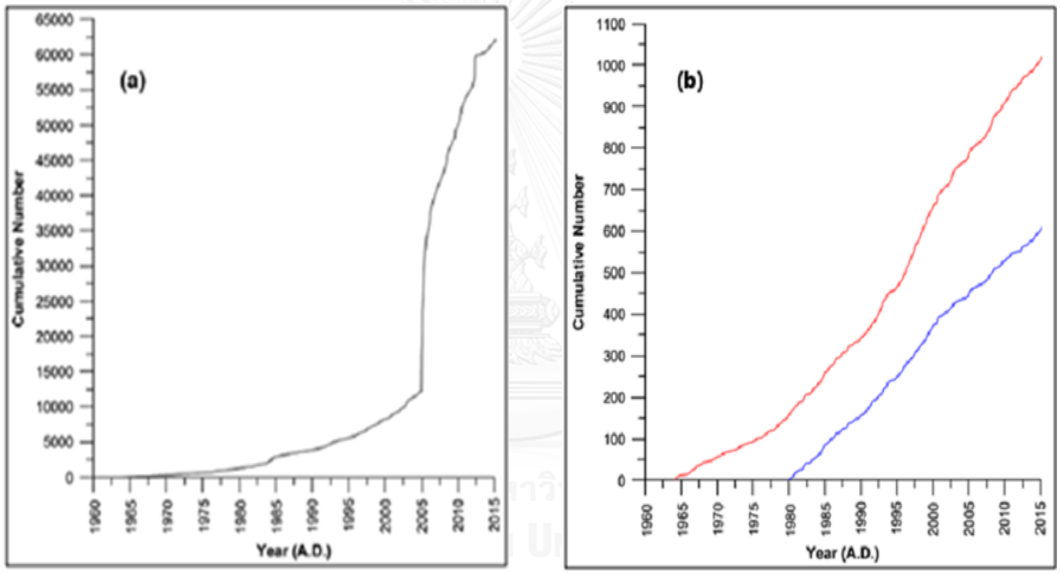

Figure 3. 4. Cumulative number of earthquakes as a function of time for a) Non-declustered catalog. b) Declustered catalogue, the red and blue lines indicate the incompleteness and completeness of the catalogue, respectively.

The seismic data showed that it is repeatedly recorded or called “Identical earthquake”. The model by Gardner and Knopoff (1974) can eliminate the identical earthquake. The extension in time and space of the window is determined by the magnitudes of the earthquake. The window is widely opened for stronger predecessor events (above red lines in Figure 3.5).

After merged of data in this study, a result of earthquake catalogue contains total 12,133 events. The declustering process removes foreshocks and aftershocks. After the declustering, the earthquake data remains 2,195 events, which are used to analyze in the next step. However, in this research, we testified 2 groups of dataset for analysis which are non-declustering and after declustering (Figure 3.6 and 3.7).

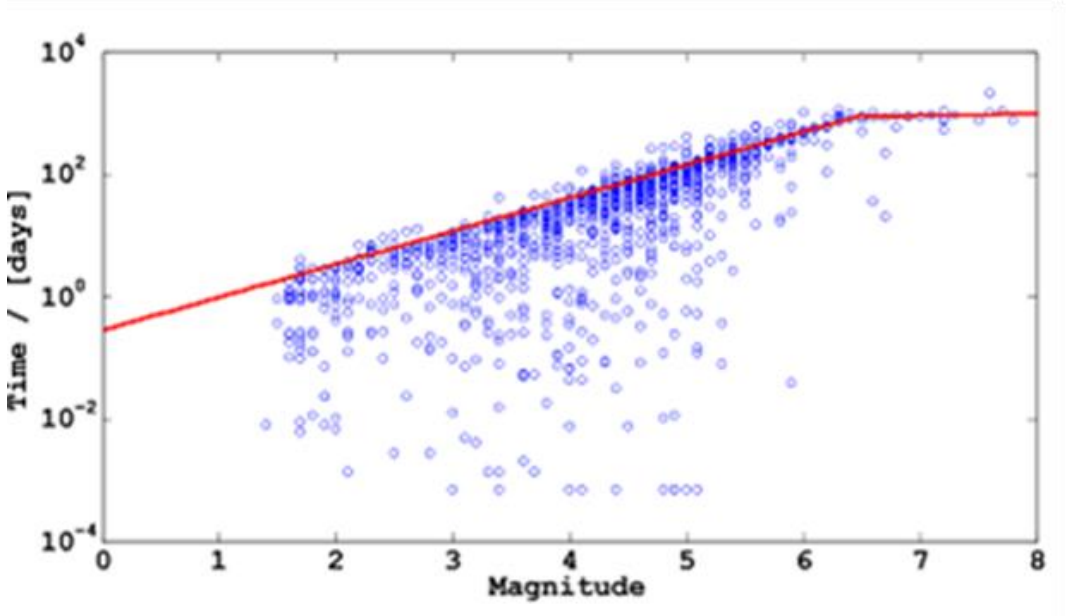

Figure 3. 5.The cumulative numbers of earthquakes as a function of time for a) Non-declustered catalogue b) Declustered catalogue, the red and blue lines indicate the incompleteness and completeness of the catalogue, respectively.

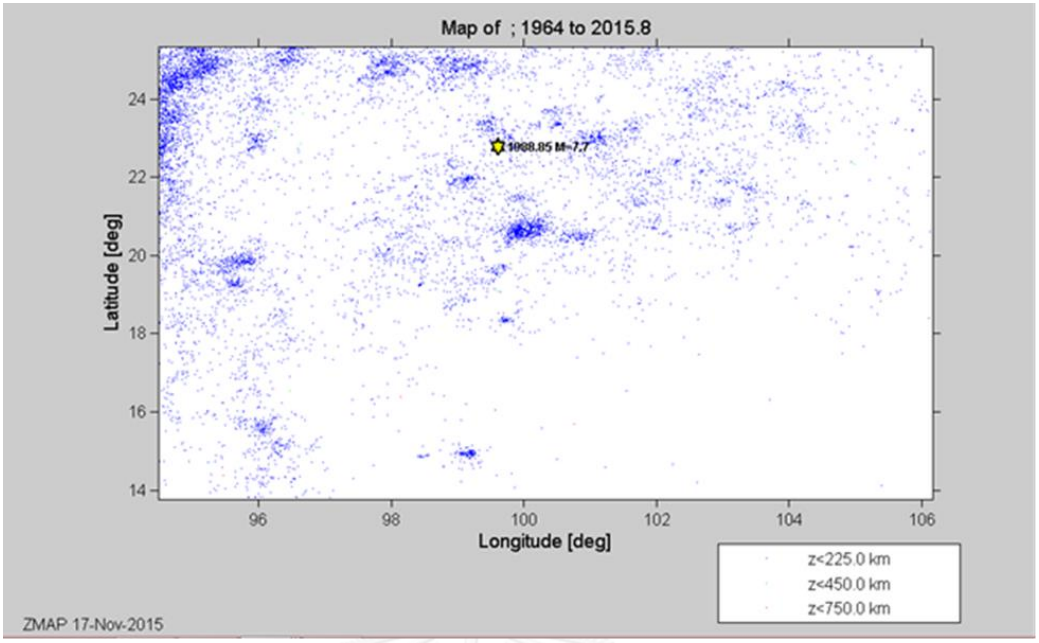

Figure 3. 6. Map of non-declustering earthquake data in the TLMB region.

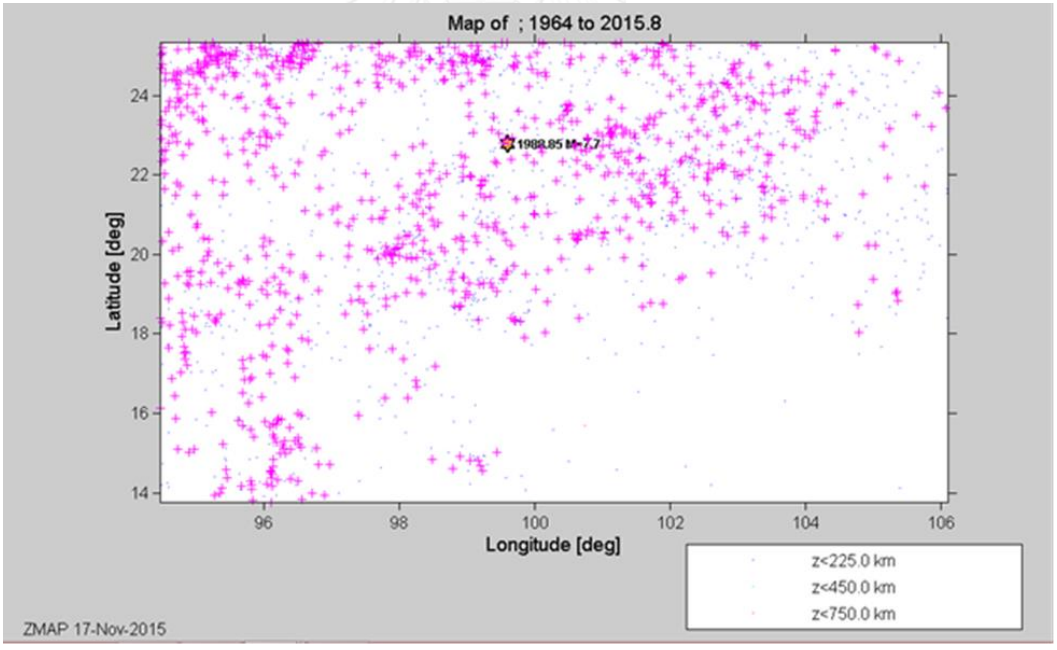

Figure 3. 7. Map of after declustering with the algorithm according to Gardner and Knopoff (1974). (Gardner and Knopoff, 1974)

CHAPTER IV
FOCAL MECHANISM

4.1. Significant of Focal Mechanism

The collision of the two plates can lead to the stress accumulation in interplate and intraplate zone. For that cause a sudden release of energy along the fault, resulting in the large earthquake. The change in stress of main shock occurrence may be great enough to trigger aftershocks. As stated by Omari (1894), the main shock does not release all the stress which that continued release of stress is known as aftershock(Omori, 1894). The frequency of aftershocks decreases roughly with the reciprocal of time after the main shock and the difference in magnitude between a main shock. Its largest aftershock is approximately constant, independent of the main shock magnitude, typically 1.1–1.2 on the moment magnitude scale (Båth, 1965). For example, the earthquake occurred with magnitude 8.7, the possible largest aftershock will be 7.5 that can generate the high damage in the area. We can find changing in stress from Coulomb stress change as a result of calculation from strike, dip and rake angles. We can find these angles from the focal mechanism analysis. In this study, we got the data collection for the focal mechanism that reported by the Global Centroid Moment Tensor (CMT) database, formerly known as the Harvard CMT catalog. The database starts to run on January, 1976 to about 6 months before the present. The database from the CMT reports the longitude, latitude, strike, dip and rake angle as shown in Table 4.1 which demonstrates all of the data for the focal mechanism investigation. There are 26 case studies in the study area. As we considered, the severe earthquake events can cause more vulnerable to damage. We selected the data information of focal mechanism from the event magnitude larger than MW 5.

According to the data analysis, the 26 focal mechanism diagrams were illustrated as beach ball symbols in Thailand-Laos-Myanmar border. Most beach balls present the coherence of the strike-slip faulting. However, the one in Northern Thailand indicates normal slip movement. This implies the existence of a structural boundary trending in NE-SW and NW-SE directions (Figure 4.1).

Table 4. 1. The data of focal mechanism in the study area.

No.	Lon	Lat	Str1	Dip1	Rake1	Str2	Dip2	Rake2
1	100.51	20.26	148	84	177	239	87	6
2	99.71	21.12	77	60	13	341	79	150
3	102.36	21.97	49	66	-3	141	87	-156
4	99.62	21.79	84	69	13	349	78	159
5	99.54	22.15	167	75	-177	76	87	-15
6	98.3	21.61	73	79	9	341	82	169
7	102.61	20.61	25	65	-9	119	82	-154
8	99.06	20.32	76	72	-1	167	89	-162
9	99.23	20.26	85	78	-168	352	78	-13
10	99.91	19.41	64	27	-55	206	68	-107
11	99.28	21.92	64	66	3	333	88	156
12	99.22	21.89	60	85	1	330	89	175
13	101.33	19.92	64	80	4	333	86	170
14	98.3	22.04	92	71	-1	182	89	-161
15	100.89	20.52	324	81	179	54	89	9
16	100	21.49	61	81	8	330	82	171
17	99.93	21.46	334	60	-167	237	79	-31
18	99.99	21.47	234	63	-19	332	74	-152
19	100.02	20.62	339	79	175	70	85	11
20	99.9	20.61	347	72	168	80	79	18
21	99.95	20.6	8	63	166	104	78	28
22	100.29	20.68	236	79	2	146	88	168
23	99.68	19.72	67	81	0	337	90	171
24	99.6	19.64	249	83	4	158	86	173
25	99.71	19.73	160	88	180	250	90	2
26	99.57	19.63	240	66	-24	340	68	-154

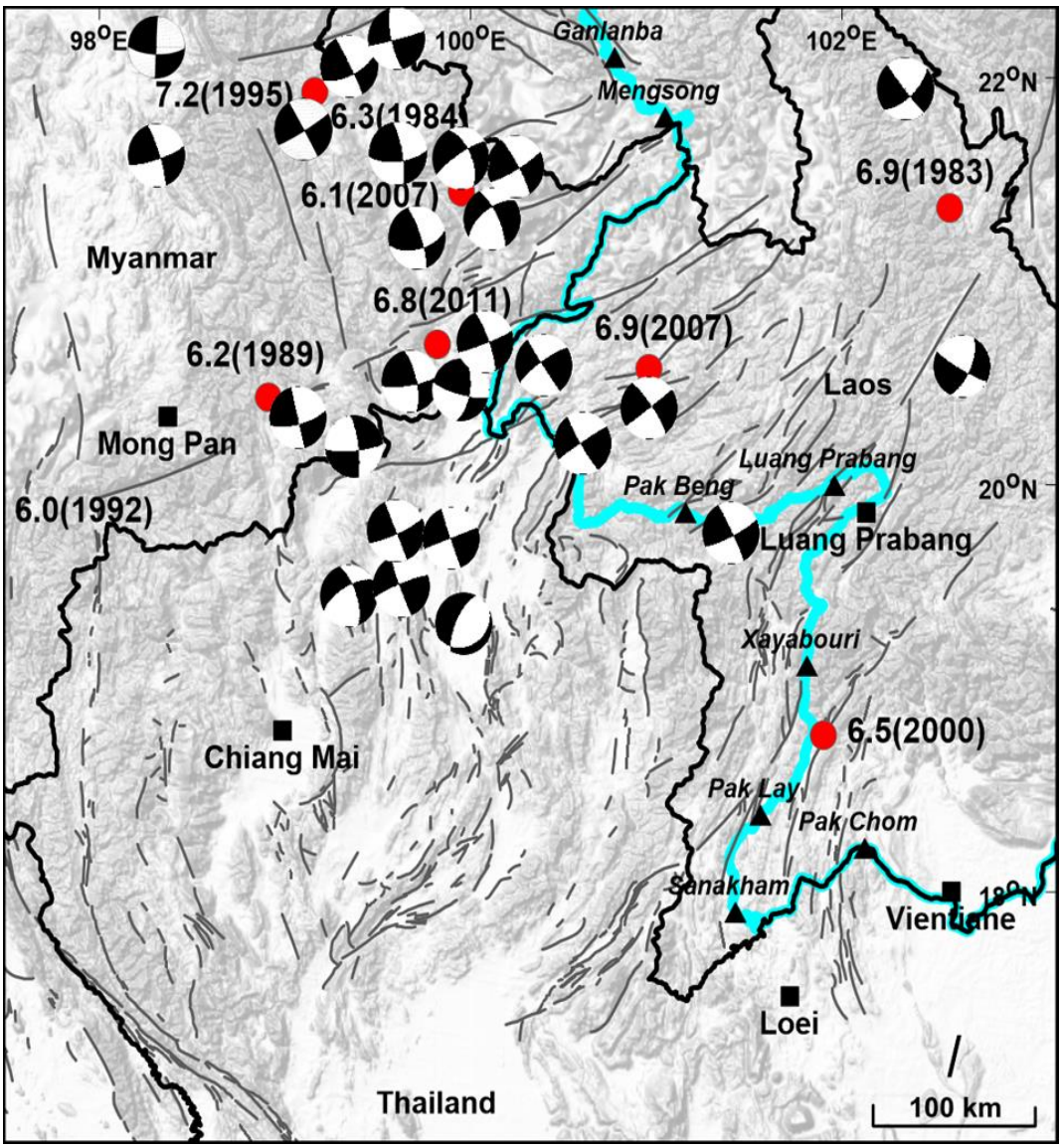

Figure 4. 1. Map showing 26 beach balls of the study area. The earthquakes occurred with magnitude greater than 6 (red dots) within Thailand-Laos-Myanmar border. The fault lines, hydropower dams, major cities are represented as thin grey lines, black triangles and black squares, respectively.

4.2. Total of Focal Mechanism in Thailand-Laos-Myanmar Border Region

In order to compute the average of direction and fault movement, we had to analyze the overall data of 26 events as shown in table 4.1. The diagram implies that the total of study area is strike-slip movement lying on NE-SW and NW-SE directions.

The result of fault mechanism can be described in two sets of strike, dip and rake. The first, it obviously suggests that the strike 1 lies on NW-SE with 65 degrees, dip 1 of this rupture varies between 65 and 85 degrees from the horizontal plane and rake 1 is 0 degree. We assigned fault movement pattern depend on the angle of rake as 0 degree meaning left-lateral strike-slip fault, 180 degrees meaning right–lateral strike-slip fault, 90 degrees meaning reverse dip-slip fault and 270 degrees meaning normal dip-slip fault. Thus, rake 1 can be assumed to be left-lateral strike-slip movement. While the second set is reported that strikes 2 lies on NW direction, whereas, dip 2 is estimated from 85 to 90 degrees. The rake 2 is between 175 and 185 degrees indicating right-lateral strike-slip, as shown in Figure 4.2 to Figure 4.5.

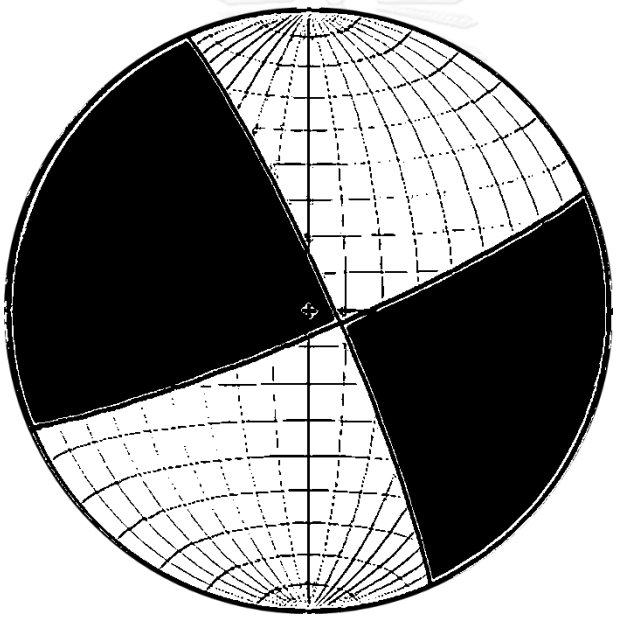

Figure 4. 2. The focal mechanism schematic diagram (beach ball) of TLMB region.

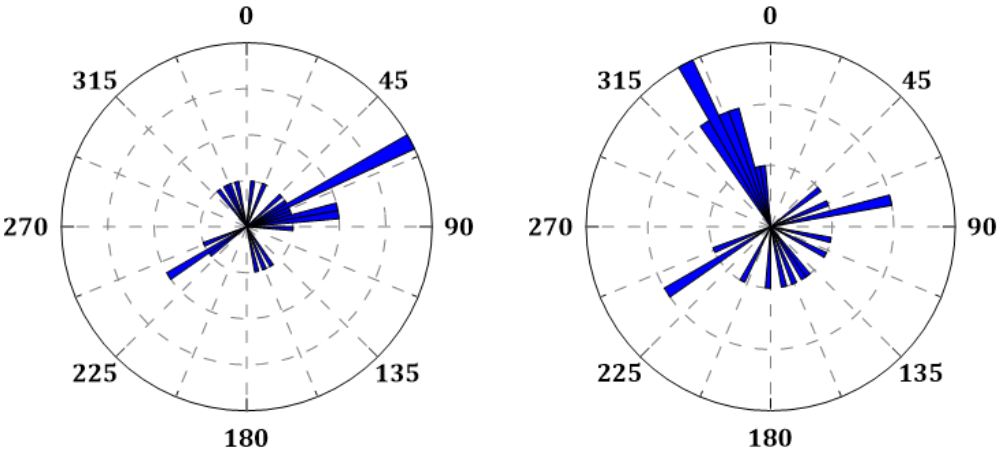

Figure 4. 3. The rose diagram represents the total strike of TLMB region.

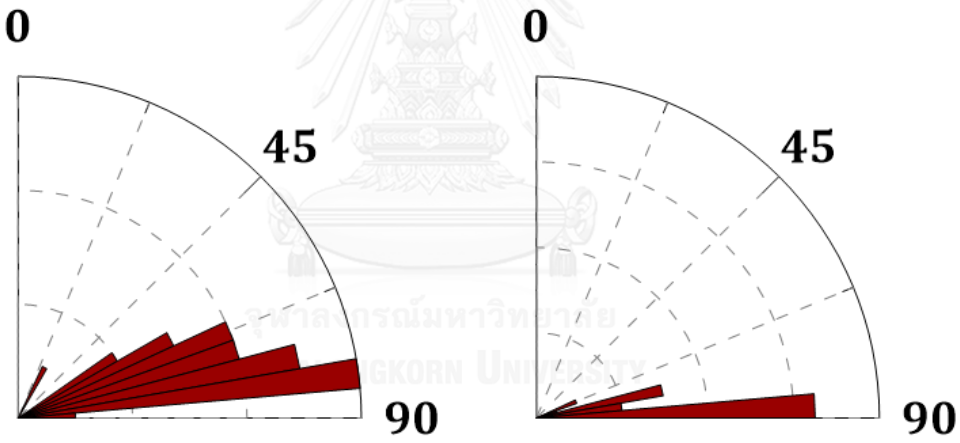

Figure 4. 4. The rose diagram represents the total dip of TLMB region.

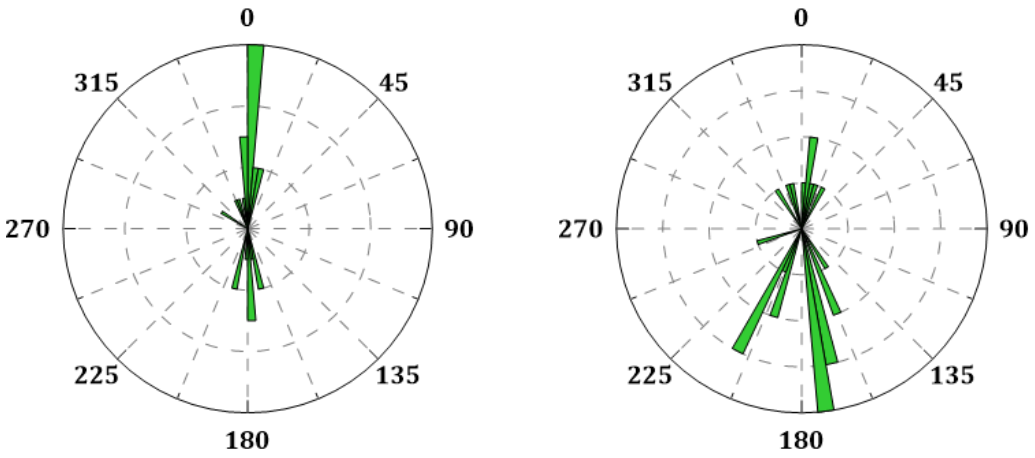

Figure 4. 5. The rose diagram represents the total rake of TLMB region.

In addition, we divided 26 beach balls into 8 groups following the active intraplate fault zones in Northern Thailand. As reported by Pailoplee et al (2009), there are Menglian, Jinhong, Nam Ma, Mengxing, Mae Chan, Mae Ing, Dein Bein Phu and Wang Nua faults, are consequently shown as no. 1 to no. 8 in Figure 4. 6. The map gives the conclusion that they present strike-slip faulting in Menglian, Jinhong, Nam Ma fault zones. While Mengxing and Wang Nua fault zones indicates oblique faulting. The Mae Chan and Mae Ing fault zones are dip-slip faulting. Each fault zone has difference in fault mechanism.

The first is Menglian fault zone which located at Eastern Myanmar. The aggregate of focal mechanisms is shown in Figure 4. 7a which presents strike-slip fault lying on NE-SW and NW-SE orientations. As illustrated in Figure 4. 8, the strike 1 is approximately 70 and 170 degrees. The dip 1 is between 70 and 85 degrees. The Rake 1 is about 0 degree which can be assumed that it is the left-lateral strike slip fault. While the second set presents 80 and 330 degrees of strike 2, 90 degrees of dip 2 and 160, 170 and 340 degrees of rake 2.

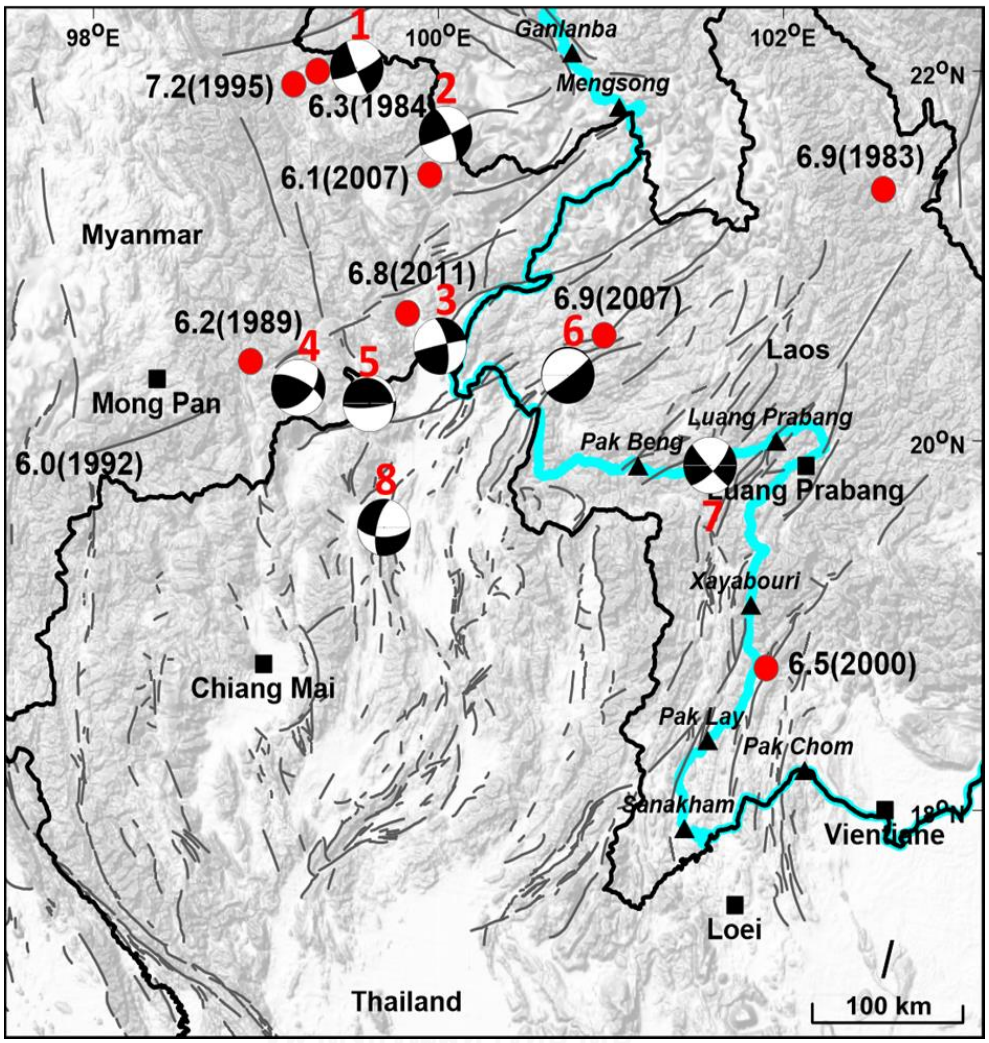

Figure 4. 6. The focal mechanisms of 8 fault zones. Earthquakes occurred with magnitude grate than 6 (red dots) within Thailand- Laos- Myanmar borders. The fault lines, hydro power dam, major cities are shown with thin grey lines, black triangles and black squares, respectively.

According to Figure 4. 7b, the Jinhong fault zone lies on SE direction. The rose diagrams result in the strike-slip movement and NE-SW and NW-SE orientations. The strike 1 ranges from 65 to 80 degrees. Dip 1 are more than 55 degrees. Rake 1 is 10 degrees which can be described to be left-lateral strike-slip and reverse dip-slip fault. While the strike 2 varies between 315 and 360 degrees. Dip 2 is 90 degrees. Rake 2

presents 150 to 170 degrees. That indicates reverse dip-slip, almost to be right-lateral strike-slip fault (Figure 4.9).

From Figure 4.7c, the schematic diagram of total focal mechanic represents the possibility of fault direction as S-E and NE-SW in Nam Ma fault zone which is strike-slip faulting. The result shows strike 1 are 10, 235, 340 and 350 degrees which most lie on NW direction. The strike 2 are 70, 80 100, 145 degrees lying on NE and SE. Both of Dip angles represent about 80 degrees. Rake 1 is 160 degrees, assuming oblique movement (Mixed from right-lateral strike-slip and reverse dip-slip). Rake 2 varies between 10 and 30 degrees, indicating oblique movement as well (Mixed from left-lateral strike-slip and reverse dip-slip), shown in Figure 4.10.

The next is Mengxing fault zone lying on NW-SE and NE-SW direction as shown in Figure 4.7d. The diagram implies that strike 1 is 80 degrees meaning the fault lying close to NE, whereas, strike 2 is about 170 degree lying on SE. Dip 1 and dip 2 are 75 and 90 degrees, respectively. Rake 1 is 0 degree meaning left-lateral strike-slip movement. While rake 2 is around 200 degrees meaning oblique movement.

As illustrated in Figure 4.8e, Mae Chan fault lies on the E-W direction. The strike 1 and strike 2 are approximately 80 and 350 degrees, respectively. The result shows the same dip angle for two set that is 70 degrees. Likewise, they are both indicating oblique fault with different rake angle as 190 and 340 degrees.

The Mae Ing fault zone lies on the NE-SW direction shown in Figure 4.7f. It can be reported that the strike 1 are around 320 and 145 degrees, whereas, the strike 2 are about 50 and 240 degrees. Dip 1 and dip 2 are 80 and 90 degrees, respectively. Rake 1 and rake 2 are 90 and 5 degrees which consequently indicate normal dip-slip and left-lateral strike-slip movement.

The Dein Bein Phu fault zone lying on NE-SW or NW-SE direction shows the beach ball in Figure 4.7g. The rose petals indicate strike-slip movement which implies 23 and 60 degrees of strike 1, 55 and 70 degrees of dip 1 and 0 and 355 degrees of rake 1. The conclusion can be assumed to be left-lateral strike-slip fault. However, the second set indicates 120 and 355 degrees of strike 2, 80-90 degrees of dip 2 and 170 and 210 degrees of rake 2. This can be interpreted to reverse dip-slip, almost to be right-lateral strike slip fault (Figure 4.14).

Ultimately, Wang Nue fault zone have two fault directions which are N-S and E-W. In Figure 4.7h, it reports the strike-slip movement. Most of angles of strike 1 refer faults on NE-SW with 65 and 80 degrees. Dip 1 are more than 80 degrees. Rake 1 is 0 degree which can be described to be left-lateral strike-slip fault. While the strike 2 are 340 degrees. Dip 2 is 90 degrees. Rake 2 presents 175 degrees. That can be characterized to be right-lateral strike-slip fault (Figure 4.15).

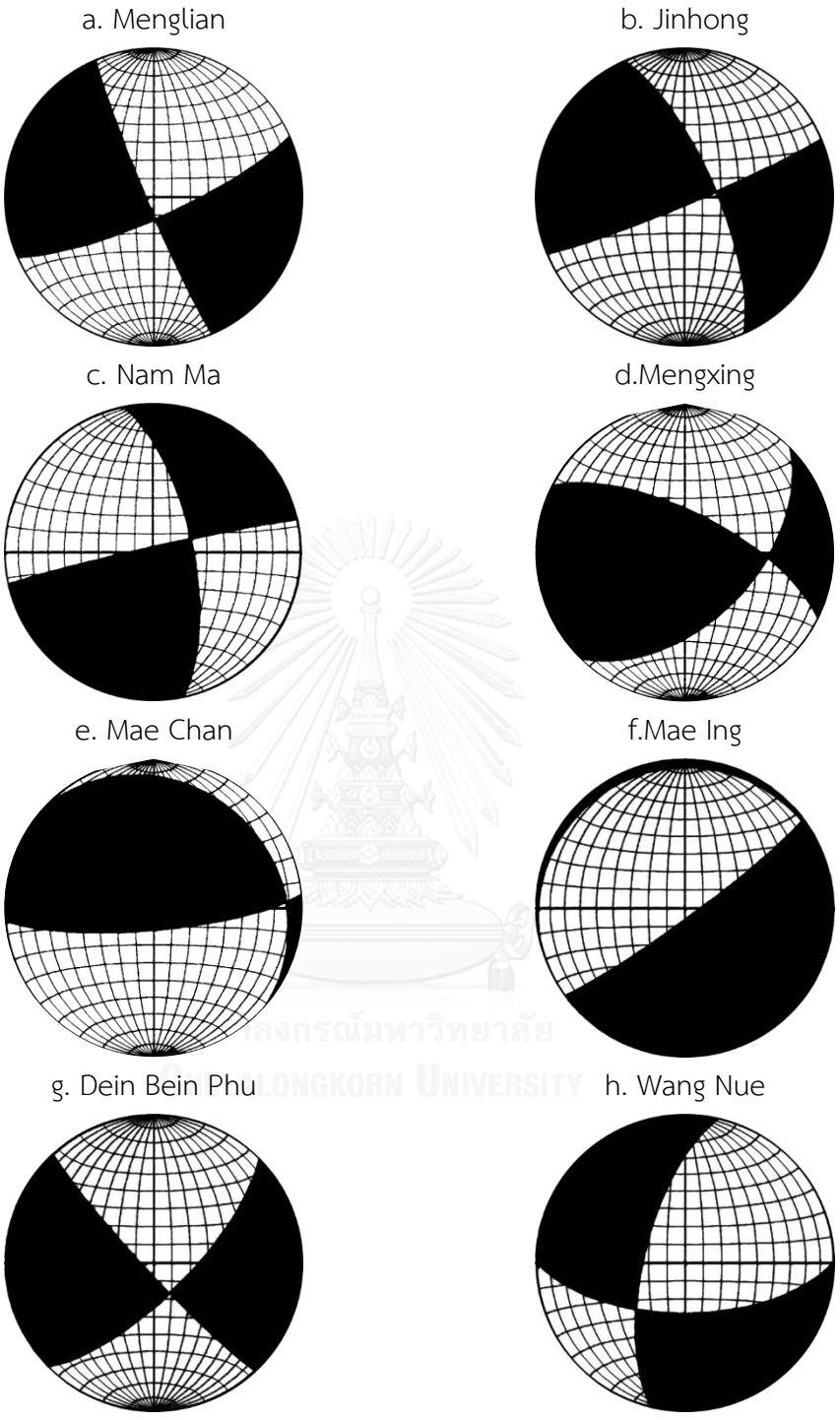

Figure 4. 7. The focal mechanism schematic diagrams (beach balls) of the 8 fault zones.

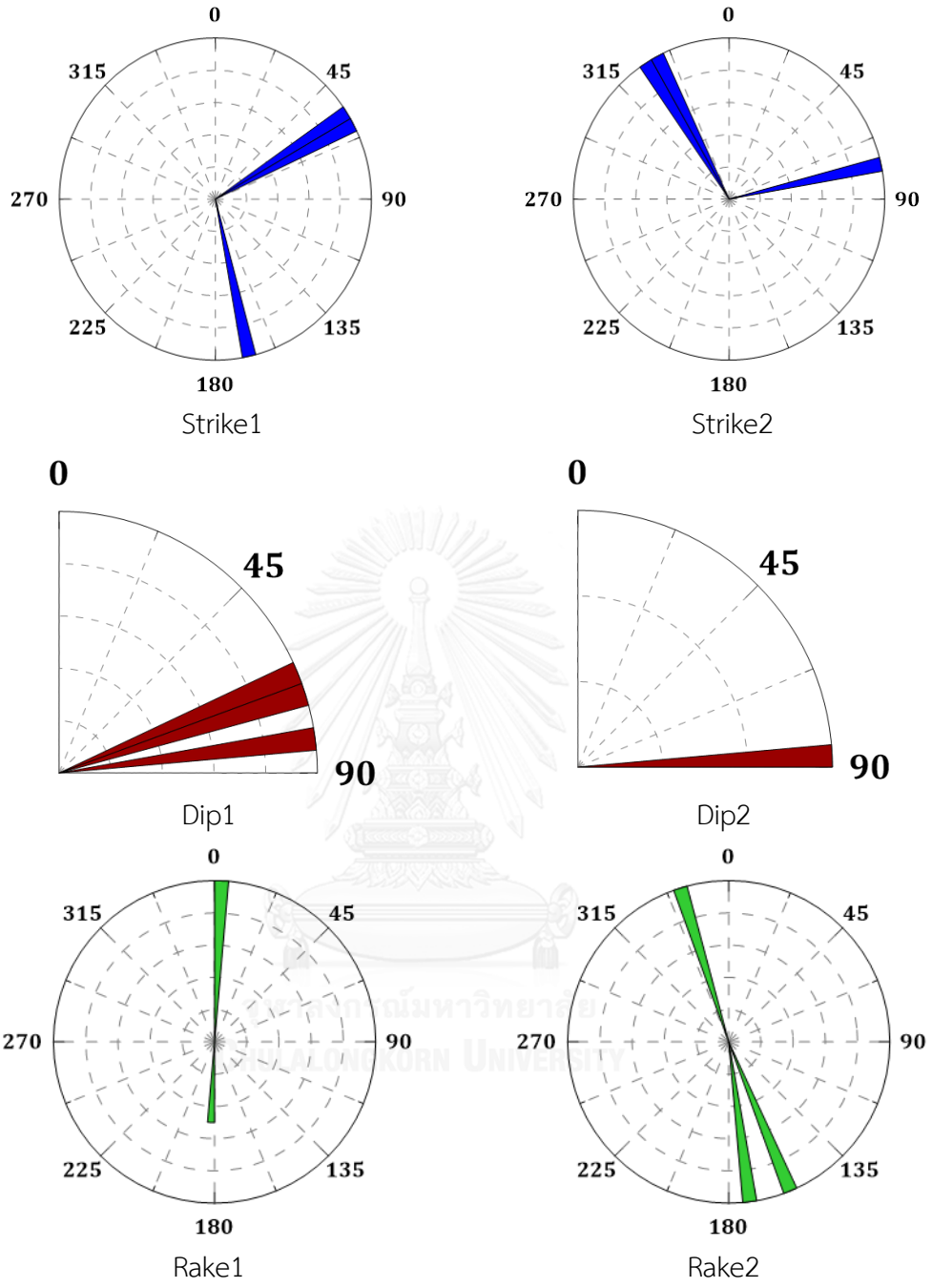

Figure 4. 8. The rose diagrams showing fault mechanism in Menglian fault zone.

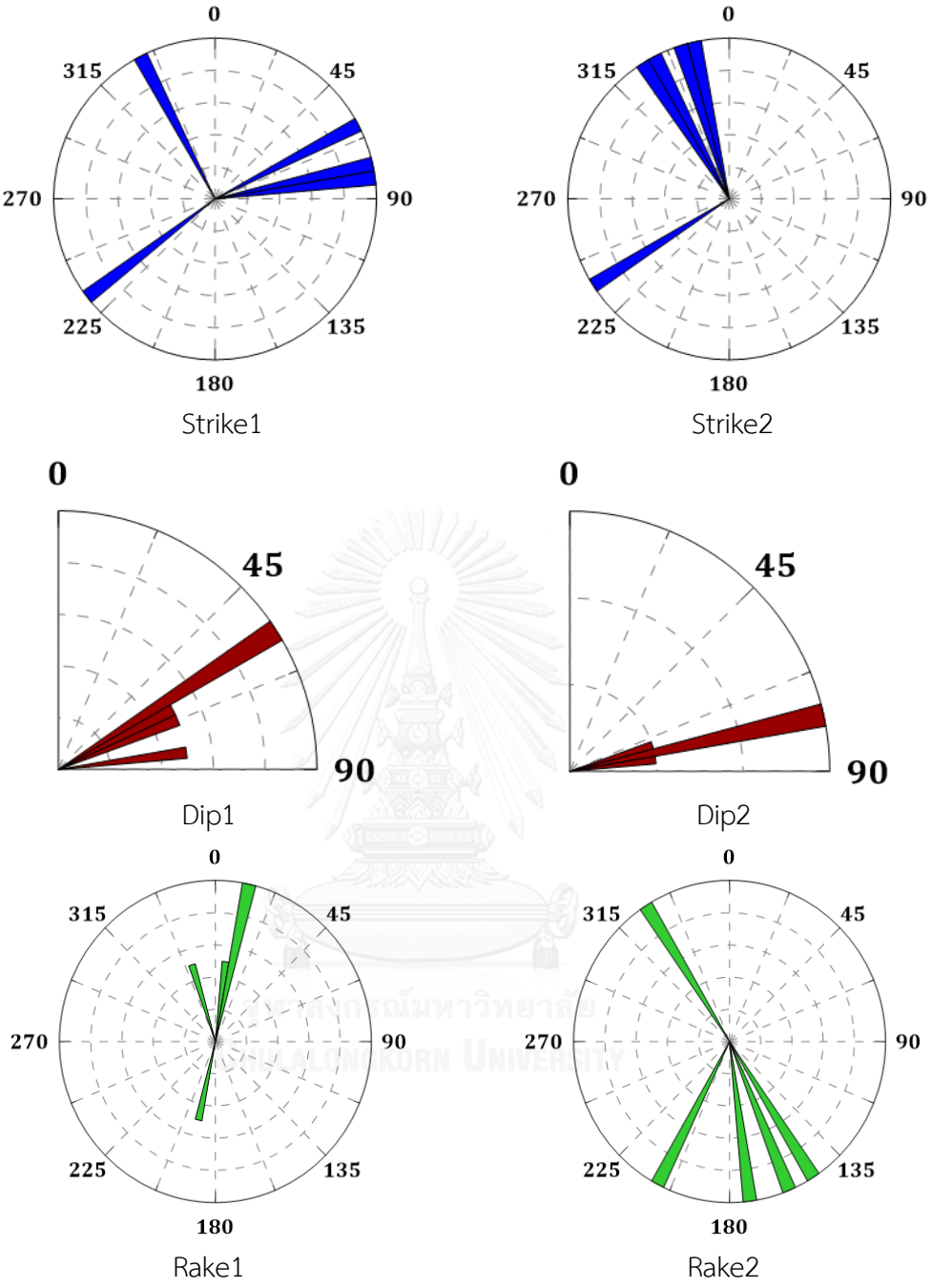

Figure 4. 9. The rose diagrams showing fault mechanism in Jinhong fault zone.

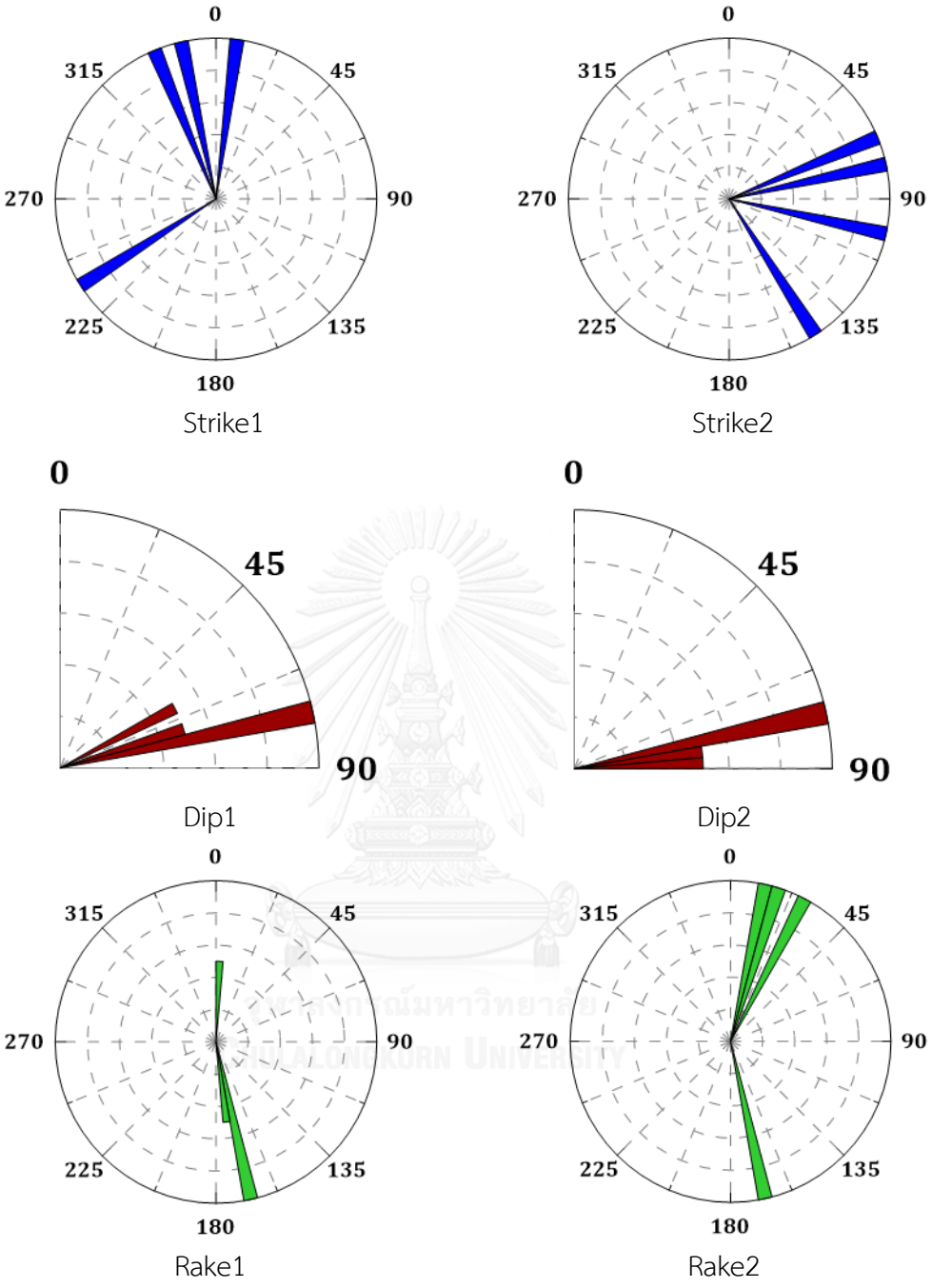

Figure 4. 10. The rose diagrams showing fault mechanism in Nam Ma fault zone.

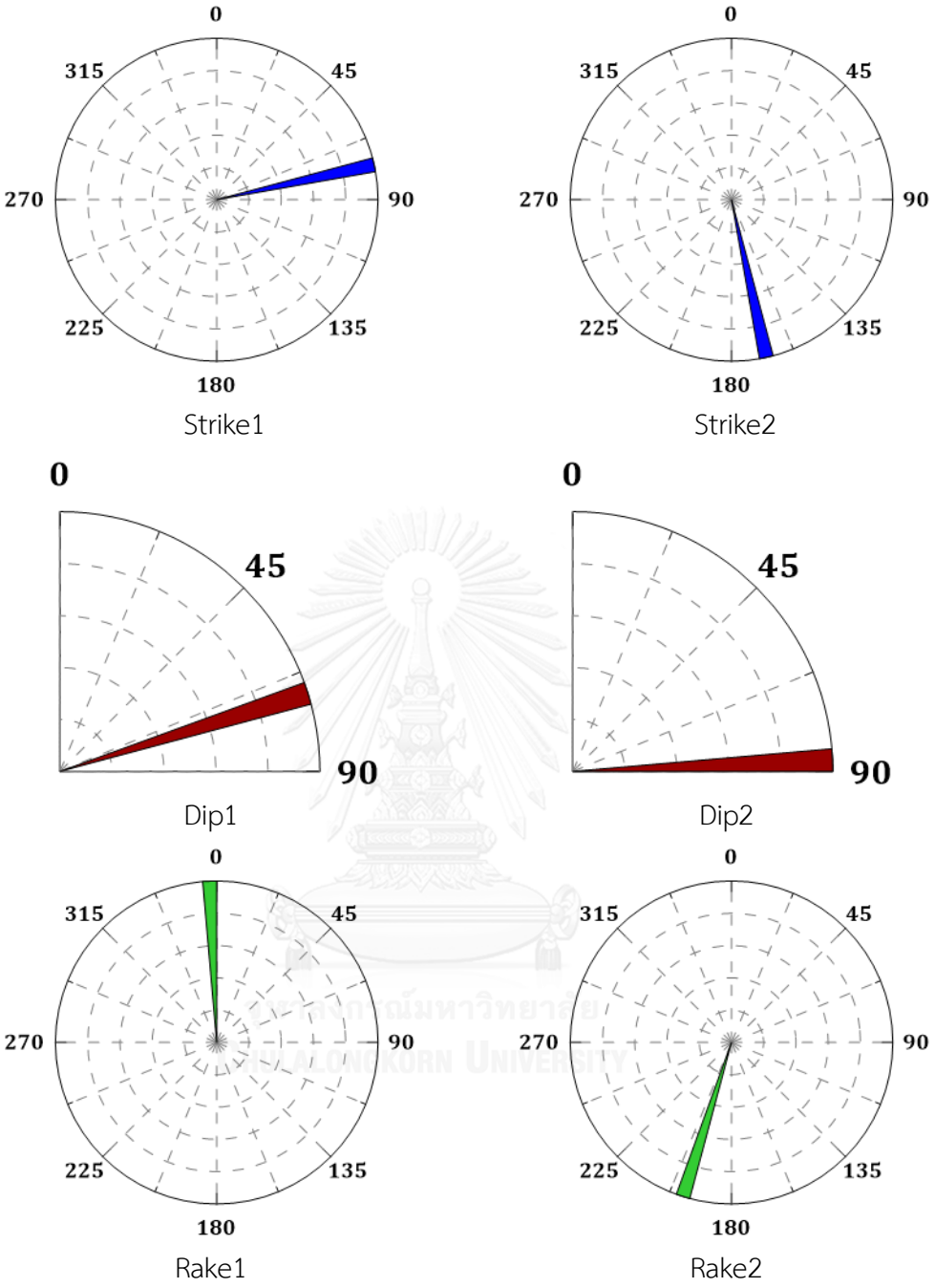

Figure 4. 11. The rose diagrams showing fault mechanism in Mengxing fault zone.

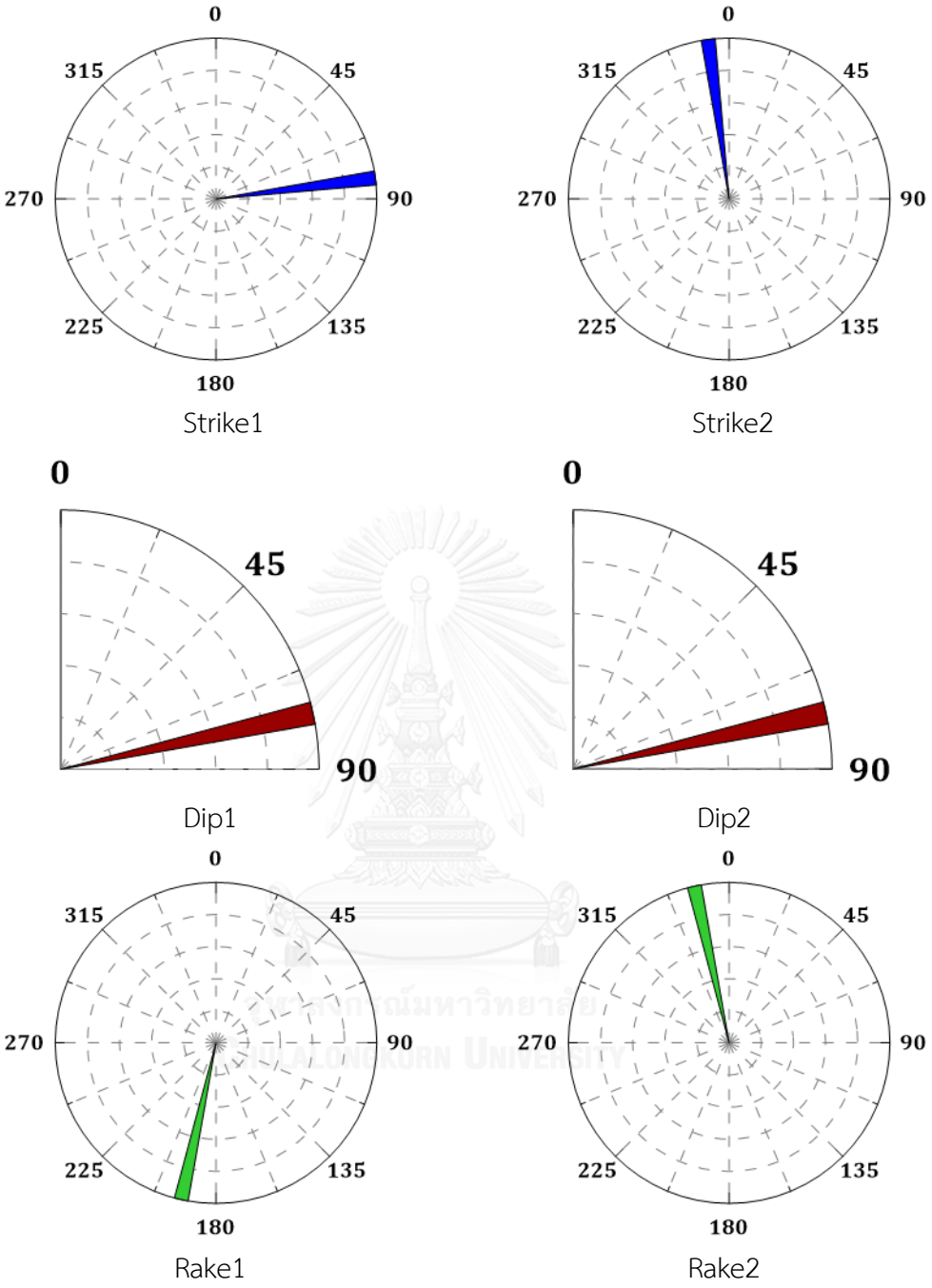

Figure 4. 12. The rose diagrams showing fault mechanism in Mae Chan fault zone.

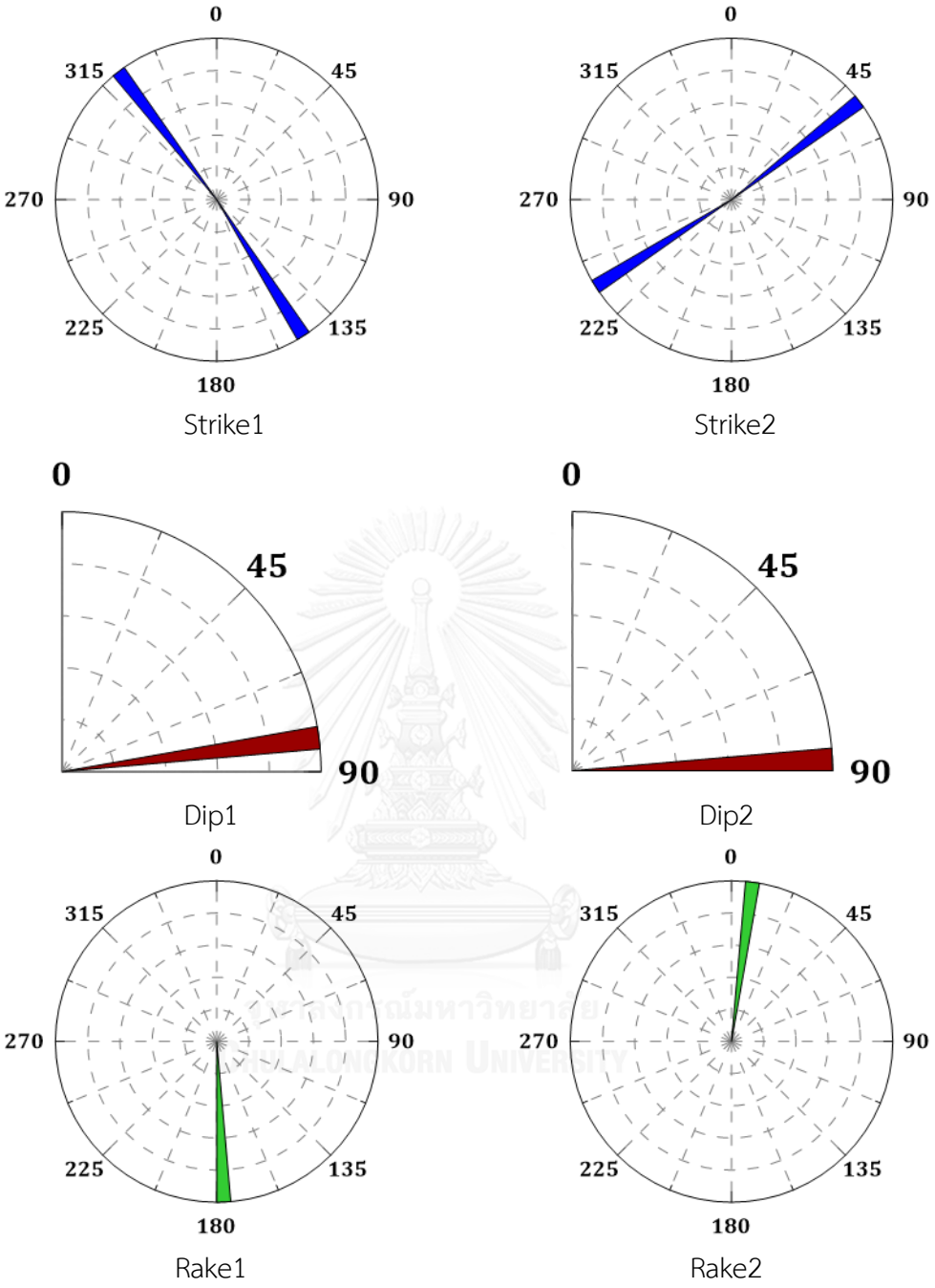

Figure 4. 13. The rose diagrams showing fault mechanism in Mae Ing fault zone.

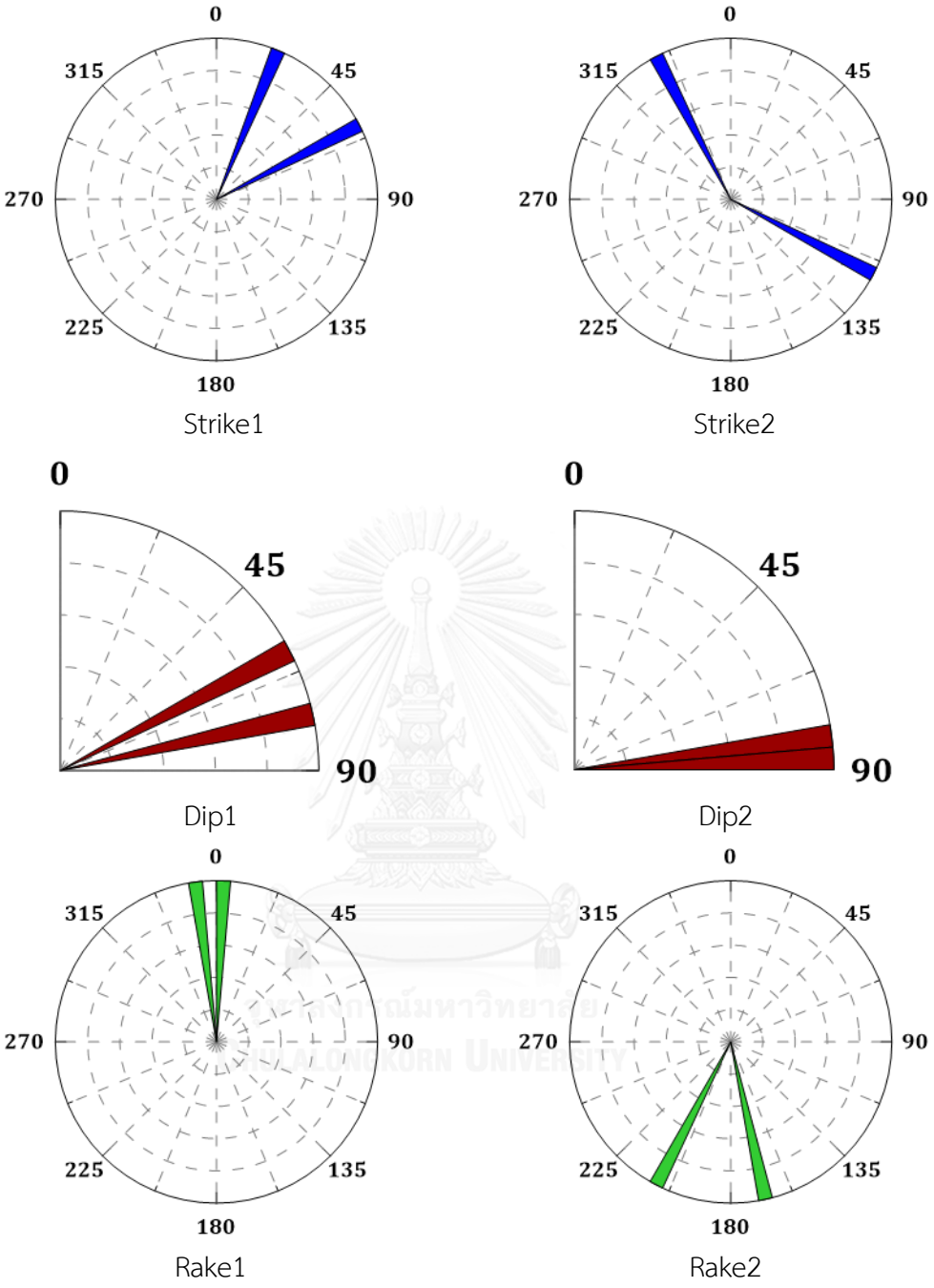

Figure 4. 14. The rose diagrams showing fault mechanism in Dein Bein Phu fault zone.

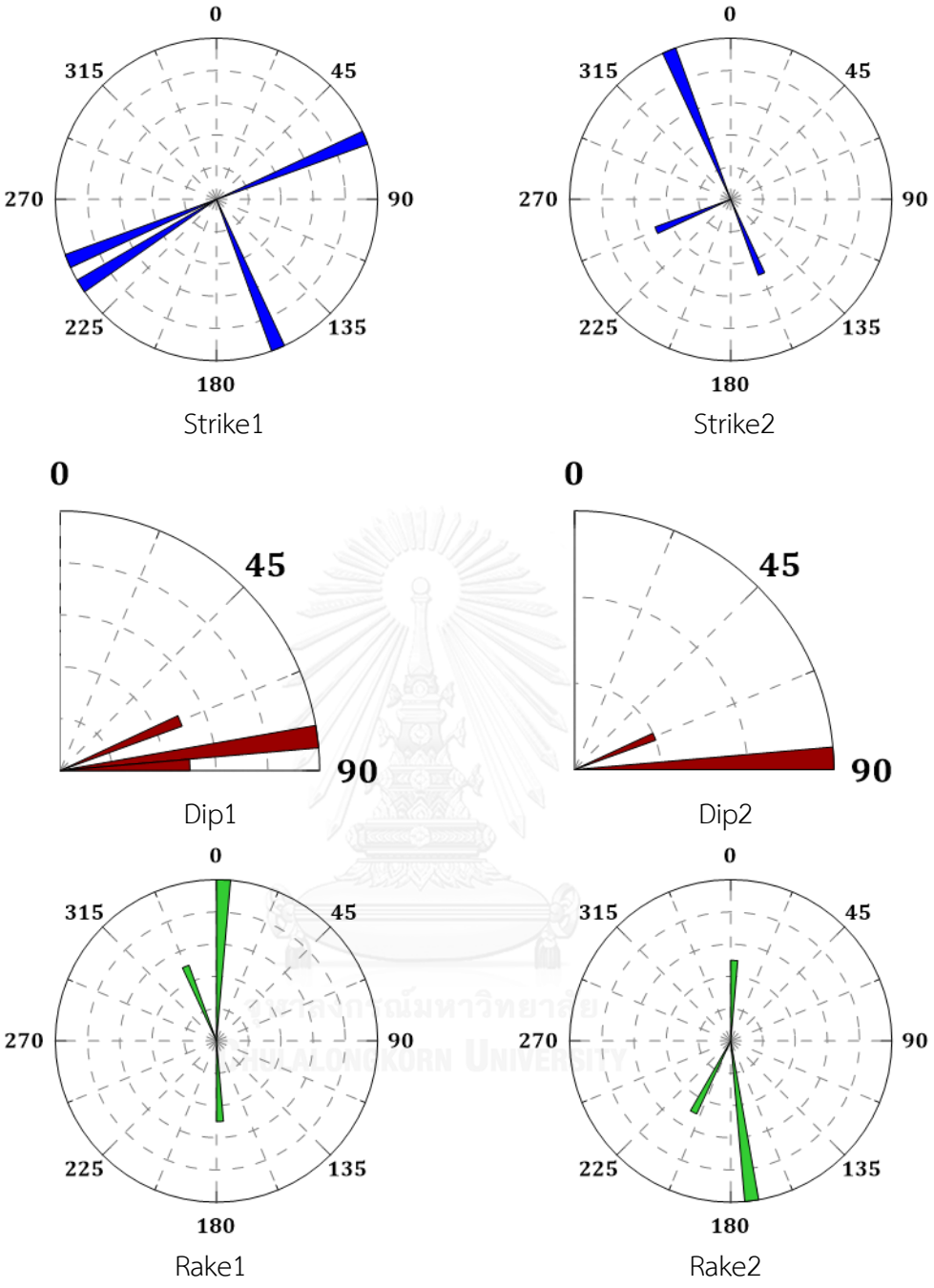

Figure 4. 15. The rose diagrams showing fault mechanism in Wang Nue fault zone.

CHAPTER V

FRACTAL DIMENSION

The data collection reported from 1965 to 2016 with magnitude 0.1-7.7 in TLMB region. We divided the data into 2 datasets as before and after declustering. In this study, the fractal dimension investigated in temporal and spatial term.

5.1. Temporal Investigation

The result of temporal term reported the magnitude of completeness (Mc), a value and b value that were analyzed at the epicenter of the Mae Lao and Tarlay earthquakes (Table 5.1.). The before-declustering data of Mae Lao has the highest b value on 2-time window as 1965-1980 and 1965-1985 and the b values are 1.2-1.6 and 1.1-1.3, respectively. After that, the b value had decreased. While, the after declustering process presents the b value as shown in Table 5.1a and b. Then, we considered the Dc values that have lower than 1 at the time window between 1965 and 1980. They give the lowest b value ranged from 0.64 to 0.66 for non-declustering dataset. The Dc value closes to 2 for the after declustering dataset (Table 5.1a and b). We plotted the graphs between years and b values, they show the Dc value significantly went down in 2015 for non-declustering dataset. In contrast, the dataset of after declustering do not vary.

The Tarlay earthquake shows the low b value of 1.08 ± 0.09, except for the b value between 1965 and 1985. The other areas provide the Dc value close to 2 for the before declustering data. According to the graph in Figure 4c, the dark line dramatically decreased to 0.65 in 1990, then, varied around 0.63 to 0.7. The gray line increased to 1.89 in 1990 and dropped at the end of graph. For the after declustering dataset, the b value is similar to before declustering data and the Dc value closes to 2. While, the graphs in Figure 4(d) that show as the black line and gray line were not fluctuated.

Table 5. 1. The result of temporal Mc, a, b, and Dc investigation analyzed at the epicenters of the Mae lao and Tarlay earthquakes busing the earthquake dataset that before and after declustering process.

(a) Mae lao before declustering

Year	EQ number	Mc	a	b	Dc
1965-1980	57	4.8	7.06	1.40 ± 0.20	0.65 ± 0.01
1965-1985	143	4.9	6.21	1.20 ± 0.10	1.45 ± NaN
1965-1990	326	4.6	4.73	0.87 ± 0.06	1.73 ± NaN
1965-1995	536	4.5	4.31	0.75 ± 0.04	1.38 ± NaN
1965-2000	682	4.0	3.68	0.62 ± 0.02	1.32 ± 0.03
1965-2005	858	4.2	4.23	0.74 ± 0.03	1.82 ± 0.03
1965-2010	1446	4.0	3.91	0.66 ± 0.02	1.75 ± 0.03
1965-2015	2516	4.0	3.92	0.65 ± 0.02	1.17 ± 0.02
1965-2016	2521	4.0	3.92	0.65 ± 0.02	1.55 ± 0.07

(b) Mae Lao earthquake after declustering

Year	EQ number	Mc	a	b	Dc
1965-2000	169	4.2	3.12	0.63 ± 0.05	2.01 ± 0.02
1965-2005	228	4.2	3.4	0.69 ± 0.05	2.00 ± 0.02
1965-2010	386	4.0	3.12	0.63 ± 0.04	1.98 ± NaN
1965-2015	490	4.0	3.12	0.63 ± 0.04	2.00 ± 0.01
1965-2016	492	4.0	3.13	0.63 ± 0.04	2.00 ± 0.01

(c) Tarlay earthquake before declustering

Year	EQ number	Mc	a	b	Dc
1965-1985	241	4.9	6.01	1.08 ± 0.09	1.12 ± 0.01
1965-1990	637	4.3	4.07	0.65 ± 0.02	1.89 ± 0.02
1965-1995	950	4.3	4.12	0.65 ± 0.02	1.87 ± 0.02
1965-2000	1168	4.3	4.21	0.67 ± 0.02	1.91 ± 0.01
1965-2005	1418	4.3	4.33	0.70 ± 0.02	1.92 ± 0.03

1965-2010	2262	4.3	4.35	0.70 ± 0.02	1.97 ± 0.02
1965-2015	3410	4.3	4.31	0.68 ± 0.02	1.35 ± 0.03
1965-2016	3420	4.3	4.33	0.68 ± 0.02	1.35 ± 0.03

(d) Tarlay earthquake after declustering

Year	EQ number	Mc	a	b	Dc
1965-1995	184	4.2	3.14	0.59 ± 0.04	1.91 ± 0.01
1965-2000	251	4.2	3.31	0.63 ± 0.04	2.10 ± 0.01
1965-2005	347	4.2	3.48	0.67 ± 0.04	1.99 ± 0.03
1965-2010	537	4.2	3.51	0.67 ± 0.04	2.05 ± NaN
1965-2015	640	4.0	3.23	0.62 ± 0.03	2.13 ± 0.01
1965-2016	643	4.0	3.23	0.62 ± 0.03	2.17 ± 0.01

5.2. b and Dc Relationship

The b-Dc relationship has been suggested as an effective indicator of seismic hazards (Bayrak and Bayrak, 2011; 2012). Empirically, the b-Dc relationship can be either a positive or a negative correlation. For example, a positive correlation was defined at the earthquake source zone in Northeast India (Bhattacharya et al., 2010). A negative correlation was revealed at some seismogenic source in Japan (Hirata, 1989) and the volcanic earthquake at Long Valley Caldera in California, USA (Barton et al., 1999).

In this study, we obtained the relations between b and Dc values of the Mae Lao and Tarlay earthquake sources (Figure 5.2a,b). The Mae Lao earthquake provided the positive relation. It got $Dc = 1.41b + 0.53$ and $Dc = 0.14b + 1.90$, fitted with the regression line (R^2) that are 0.24 and 0.16 for non-declustering and after declustering dataset, respectively.

Regarding to the epicenter of the Tarlay earthquake, the relationship of the before-declustering dataset is $Dc = 1.23b + 1.08$ with $R^2 = 0.72$. While, the after-declustering dataset reveals the b-Dc relationship as $Dc = 0.99b + 1.45$ with $R^2 = 0.09$.

In contrast to the Mae Lao earthquake, the b-Dc relationship of the Tarlay earthquakes expresses the negative linear correlation as shown in Figure 5.2c and d.

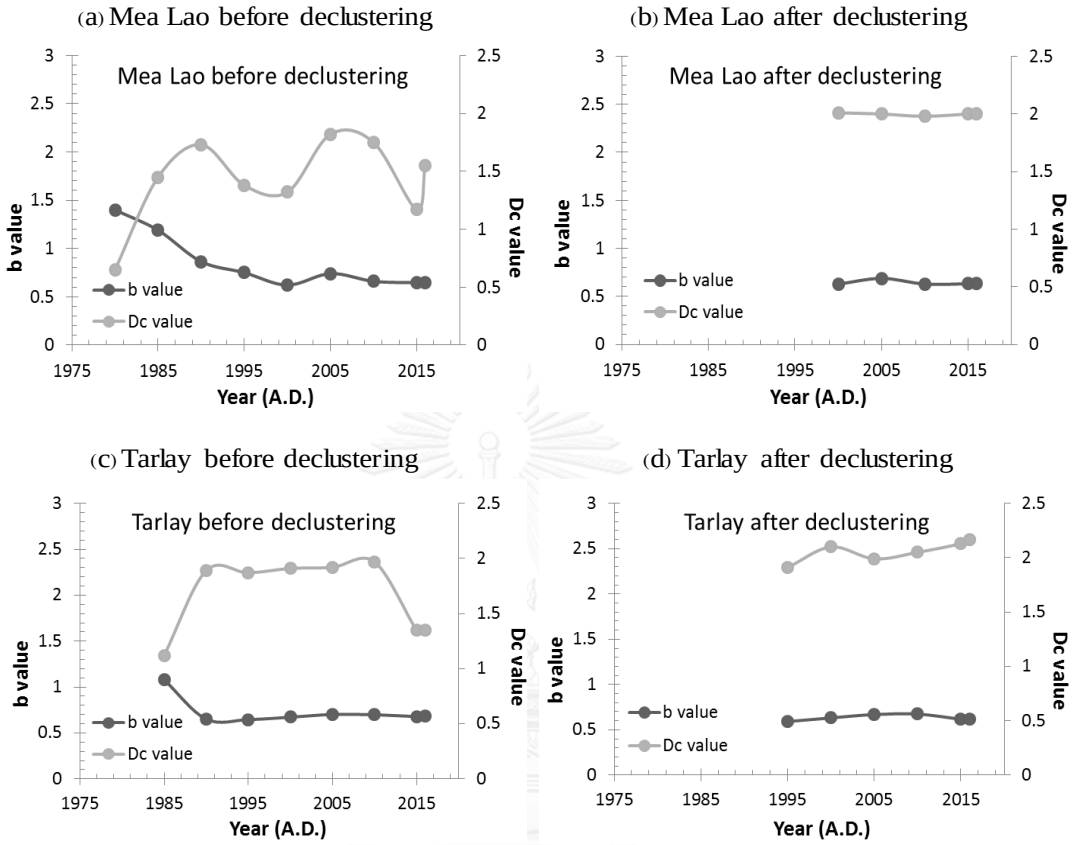

Figure 5. 1. Graphs showing the temporal variation of b (black line) and Dc (grey line) values from 4 case studies. The utilized datasets are comprised of a) Mae Lao before declustering, b) Mae Lao after declustering c) Tarlay before declustering and d) Tarlay after declustering.

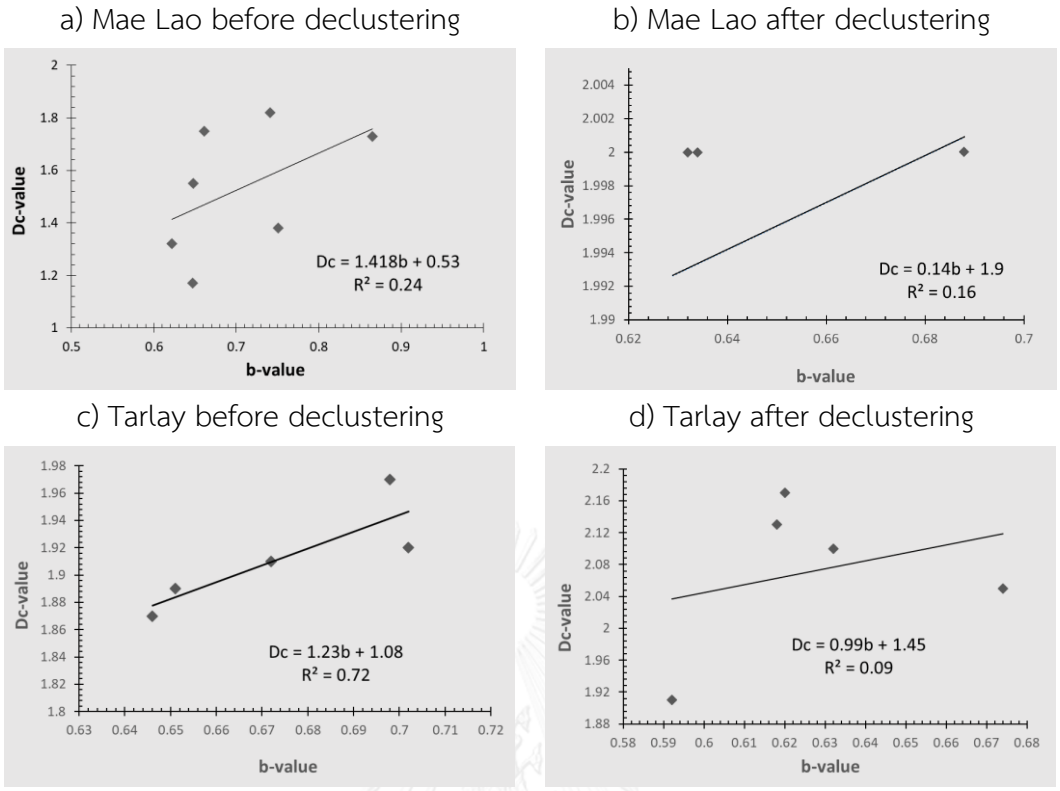

Figure 5. 2. Empirical relationships between the b and Dc values analyzed from a) Mae Lao before declustering, b) Mae Lao after declustering, c) Tarlay before declustering and d) Tarlay after declustering. The straight lines represent the linear regressions fitted with the observed data.

5.3. Spatial Investigation

Furthermore, we also investigated on the spatial term. In this study, we used the same datasets as the temporal term that are the before and after declustering data. The b value and Dc value were plotted on the spatial map to examined which area is the high-risk potential earthquake zone.

5.3.1. Before declustering dataset.

According Figure 5.4 that indicates the b value distribution, the result suggests that northern, center and southern Chiang Mai got the low b value varying from 0.3 to 0.75 as the green zone and 0.15 to 0.3 as the grey zone. The b value was more than

0.75 ranged from the yellow zone to orange zone at the northeast and southwest. For the Dc distribution map, the north of map in Figure 5.5 got the Dc ranged from 1.7 to 2.1.

The Northern Thailand has 3 zones of difference Dc value. The violet circle shows the low Dc value of 0.9 and the light blue and blue areas indicate the Dc values less than 1.5 to 1.1. The light green and green areas present the Dc value varying between 1.5 and 1.9. The center of map shows the yellow color which provides the Dc value of approximately 1.9 to 2.1. We divided the Dc values into 3 range as 0.5-1.5, 1.5-2.5 and 2.5-3.5 as shown in yellow, green and red, respectively in Figure 5.6. Chiang Mai and southern Chiang Mai present as yellow zone which the Dc value closes to 1. The other show as the green area meaning the Dc closes to 2.

Normally, when we compute the results that aim for values, the calculation of error allows us to determine the precision of estimated values. In this method, we used the distance to get the result of fractal dimension in each area. The errors of Dc from similar distance were calculated as shown in Figure 5.7. The low error is found in the white area, whereas the high error is shown in the dark brown area, the lowest and highest error are 0 and 0.004, respectively. The central of the study area got the error ranged from 0.02 to 0.04. Finally, the spatial investigation of before declustering dataset has been observed that the shortest distance is not over than 10 km. The longest distance is 10 to 160 km. However, some areas have the longer distance as nearly Chiang Mai that was using the longest distance around 280 km that found in fractal dimension relationship (Figure 5.8, 5.9).

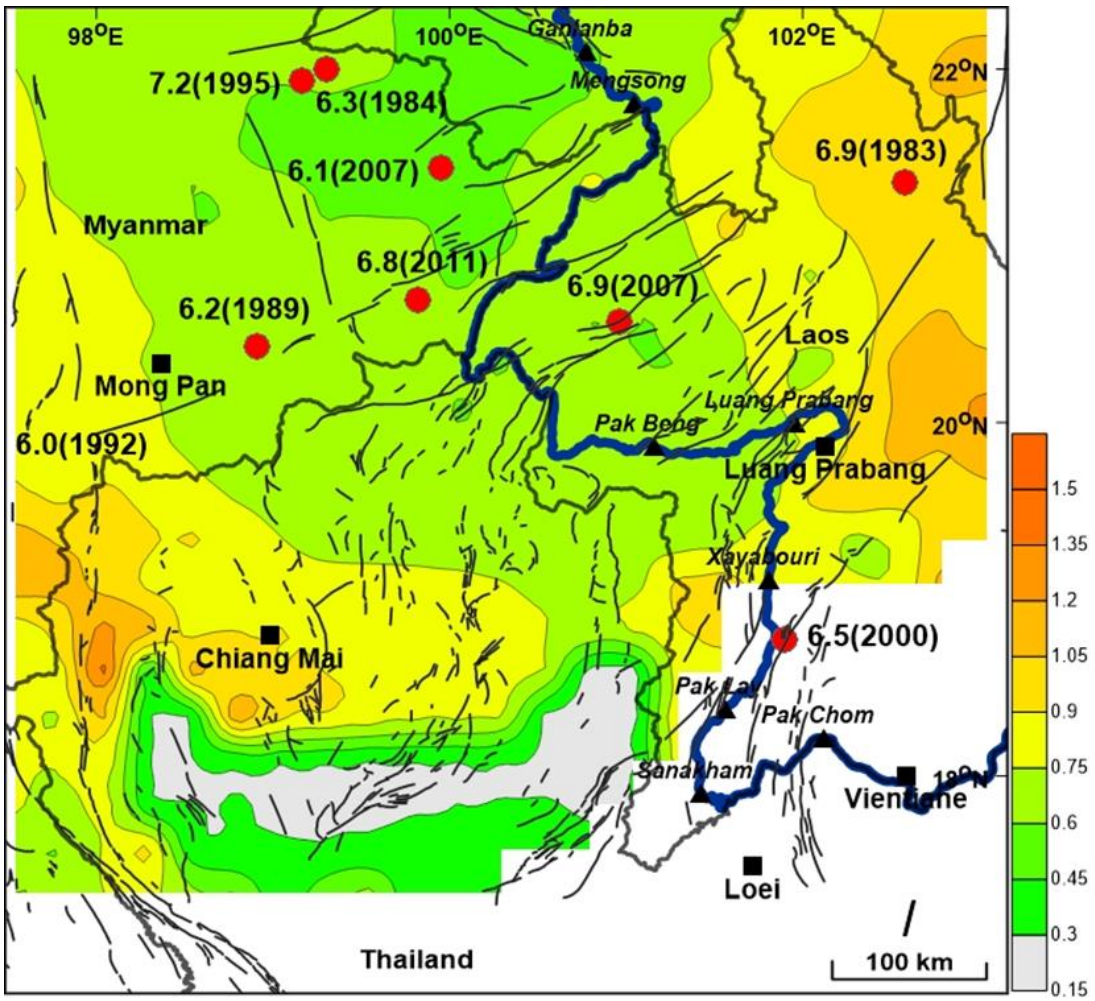

Figure 5. 3. Map of The TLMB region. This map shows the b-value distribution in the study area for the before declustering dataset. Earthquakes occurred with magnitude greater than 6 (red dots) and the fault lines, hydropower dam and major cities are shown with thin grey lines, black triangles and black squares, respectively.

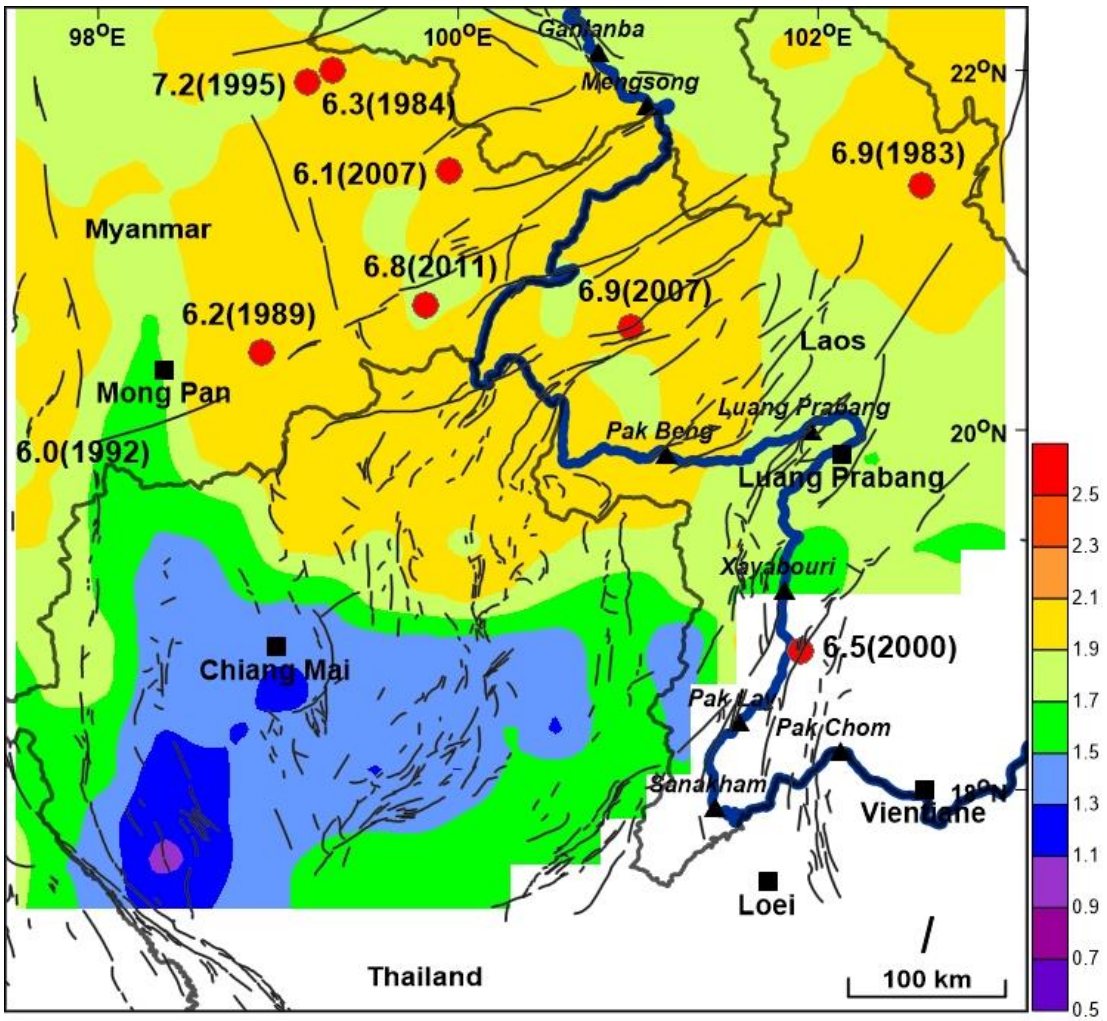

Figure 5. 4. Map of The TLMB region. This map shows the Dc distribution in the study area for the before declustering dataset. Earthquakes occurred with magnitude greater than 6 (red dots) and the fault lines, hydropower dam and major cities are shown as thin grey lines, black triangles and black squares, respectively.

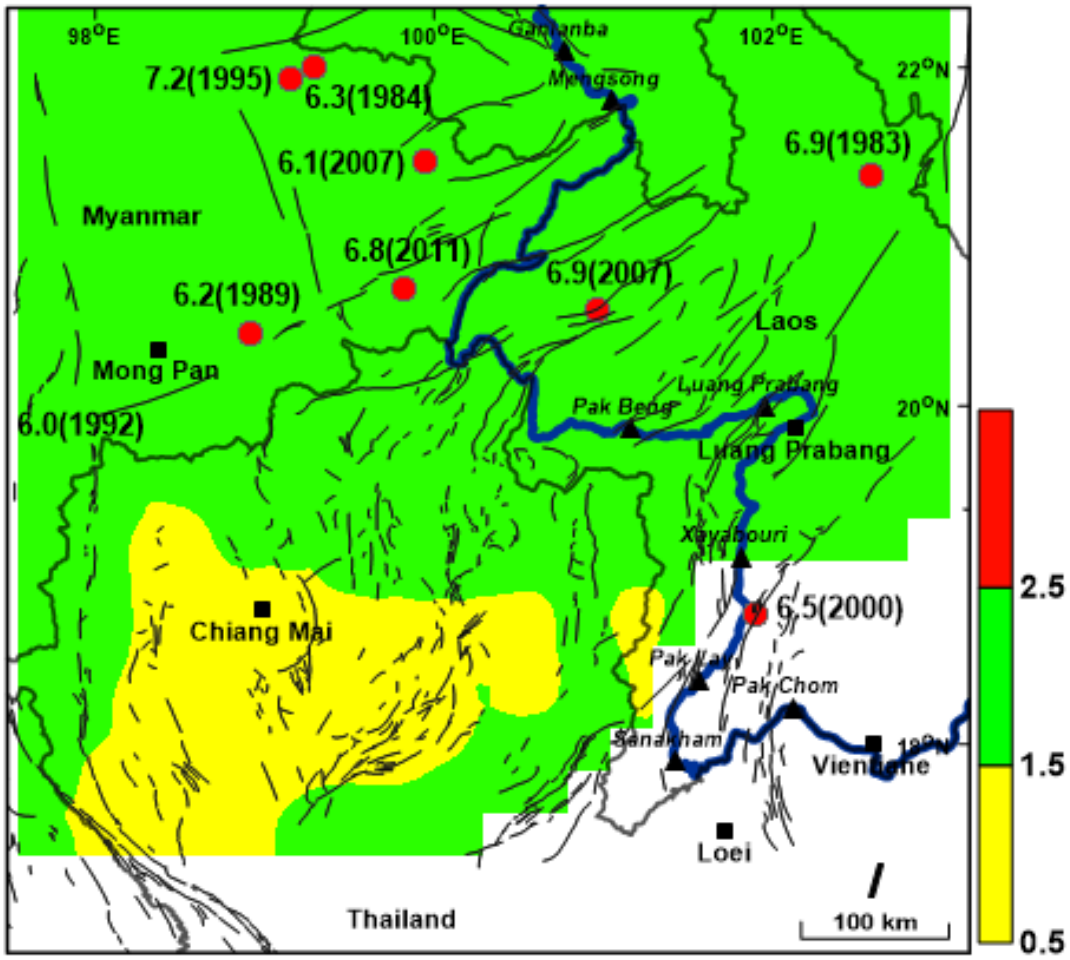

Figure 5. 5. Map showing the Dc values of before declustering process in 3 ranges. The Dc values are between 0.5-1.5 (yellow), 1.5-2.5 (green) and 2.5-3.5 (red) in the TLMB region.

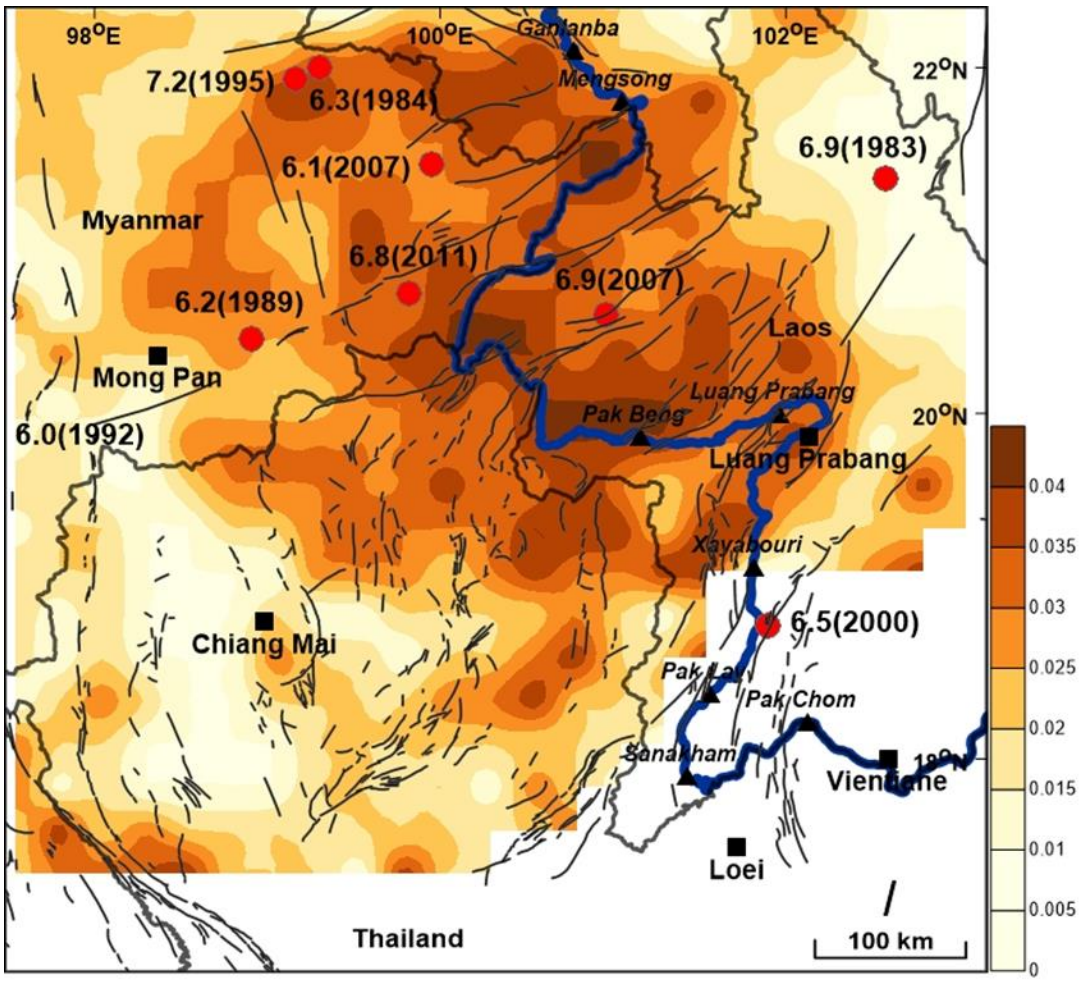

Figure 5. 6. Map of the TLMB region. This map shows the error of the Dc value distribution for the before declustering dataset. Earthquakes occurred with magnitude greater than 6 (red dots) and the fault lines, hydropower dam and major cities are shown as thin grey lines, black triangles and black squares, respectively.

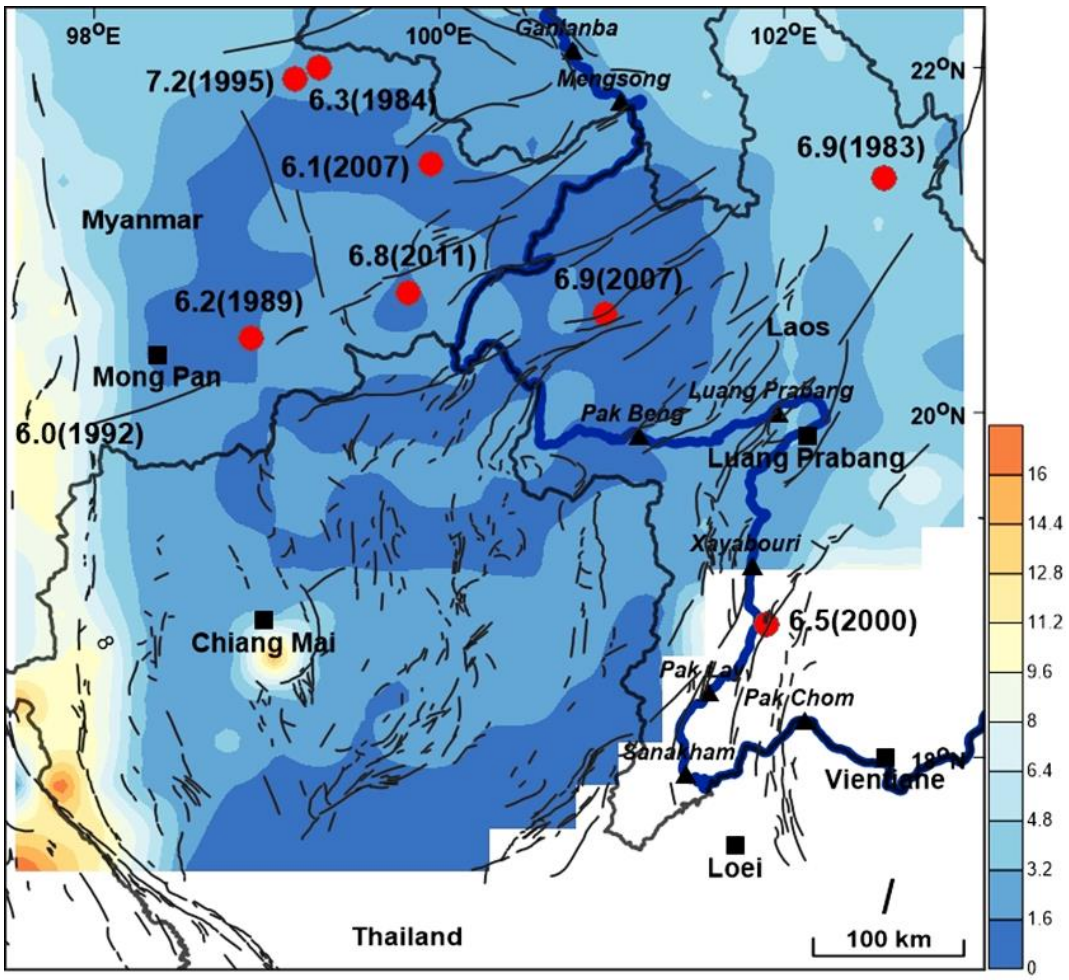

Figure 5. 7. Map of the TLMB region. This map shows the shortest distance between 2 earthquakes that was found in fractal dimension relationship for the before declustering dataset. Earthquakes occurred with magnitude greater than 6 (red dots) and the fault lines, hydropower dam and major cities are shown as thin grey lines, black triangles and black squares, respectively.

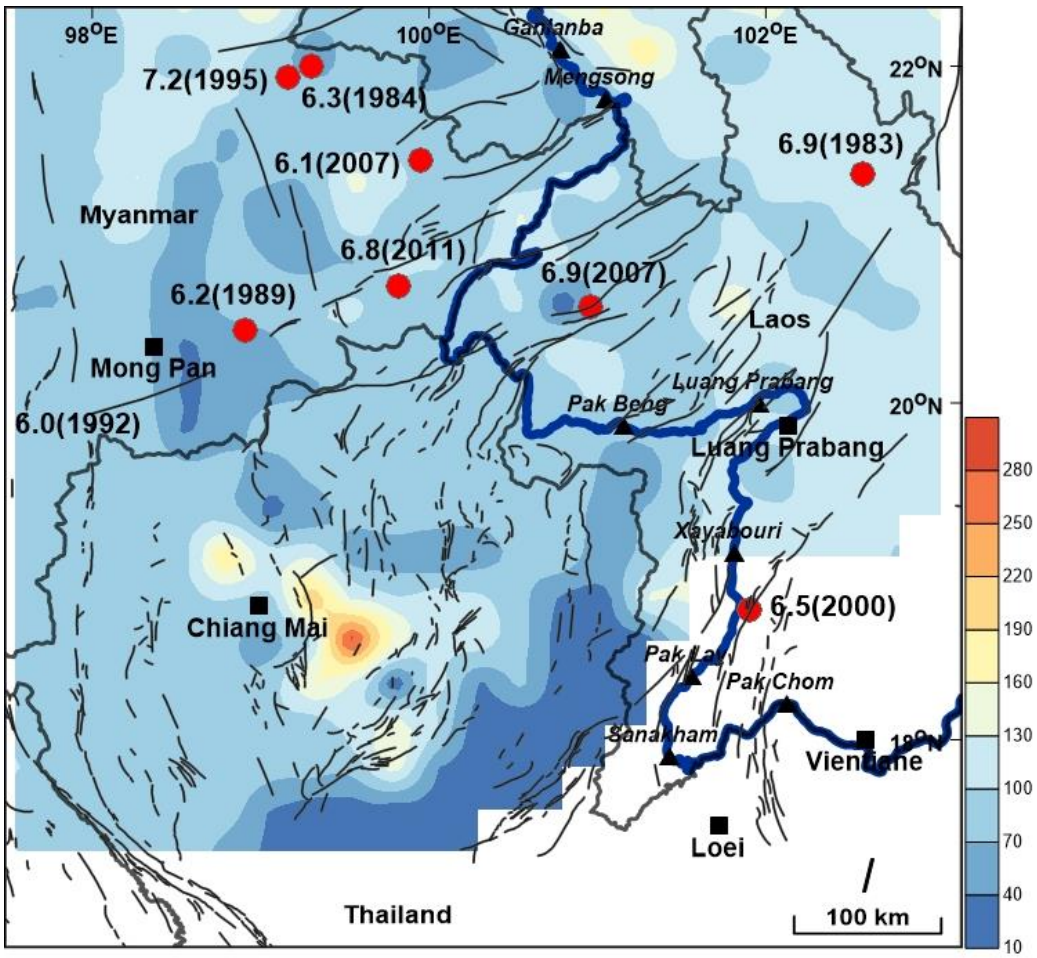

Figure 5. 8. Map of the TLMB region. This map shows the longest distance between 2 earthquakes that was found in fractal dimension relationship for the before declustering dataset. Earthquakes occurred with magnitude greater than 6 (red dots) and the fault lines, hydropower dam and major cities are shown as thin grey lines, black triangles and black squares, respectively.

5.3.2. After declustering dataset

The other result of spatial investigation was calculated from the after declustering dataset which was eliminated the foreshock and aftershocks. Thus, this result can be derived from the mere main shock data.

According to the map in Figure 5.10, there are the b value between 0.7 and 1.1 in northeast and southwest of Chiang Mai, covering Mong Pan of Myanmar that shows the b value between 0.7 and 0.9. The anomalous low b value is shown as the green area on northern and southern map. While, the Dc value implies the high value of more than 2 locating on Laos (northeast of map), that showing in Figure 5.11. The Dc values that are illustrated as the green and yellow areas close to 2. It has been observed in Figure 5.12 that most of the study area got the Dc value close to 2 as presented by green. The error of Dc from distance was computed by the fractal dimension method, the high error lies on northern Thailand. And the other areas present the low values. (Figure 5.13)

The shortest distance between 2 earthquakes that was found in fractal dimension relationship for the after declustering dataset is different in each area. For example, the northern map obtained the shortest similar distance ranged from 16 to 32 km, whereas the southern is more than 20 km. While, the northeast and southwest got the shortest distance varied between 0 and 20 km (Figure 5.14.). The longer distance was using for the fractal dimension investigation. We found that most of the study areas were using the long distance of more than 80 km. Except for some areas at the eastern map, they were using shortest 70 km for investigation. (Figure 5.15)

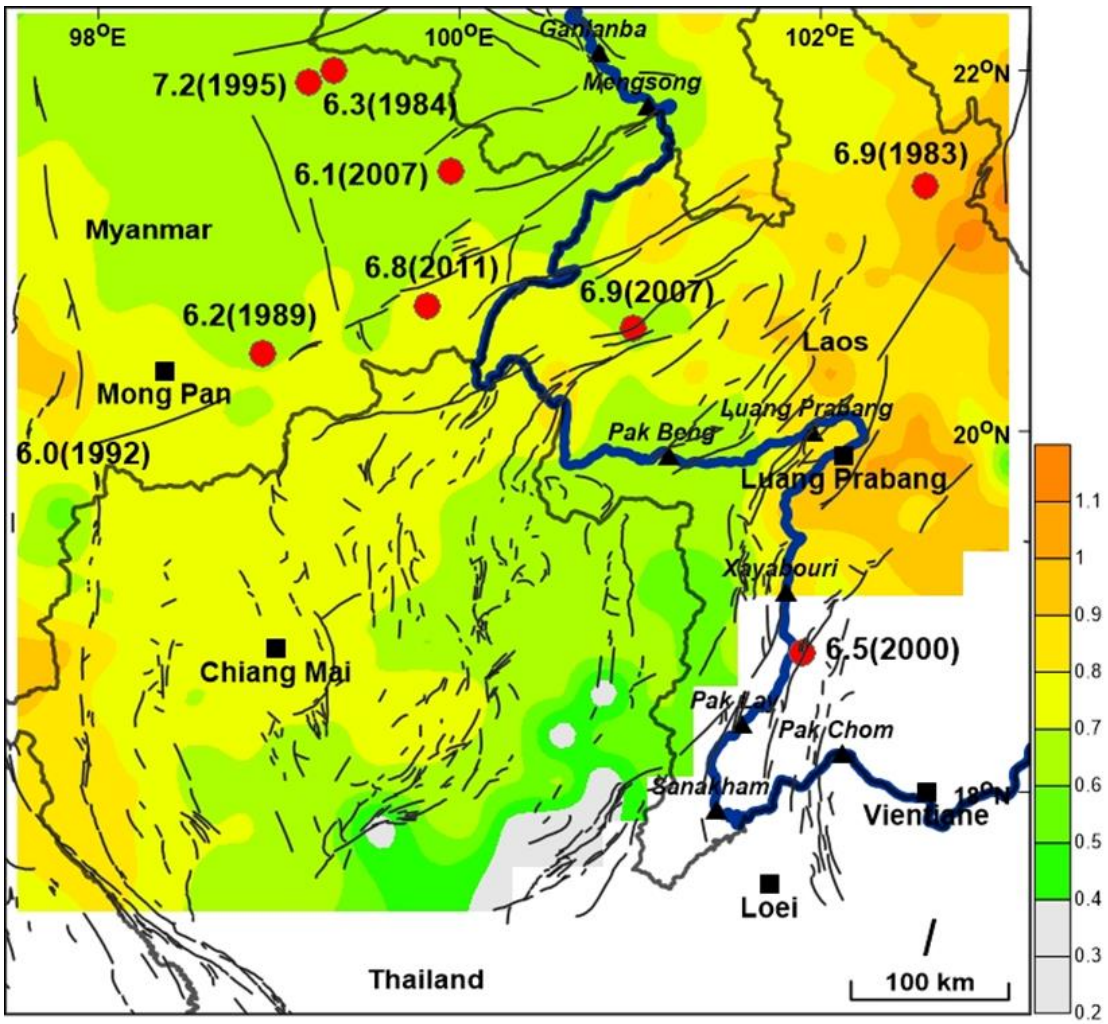

Figure 5. 9. Map of the TLMB region. This map shows the b value distribution in the study area for the after declustering dataset. Earthquakes occurred with magnitude greater than 6 (red dots) and the fault lines, hydropower dam and major cities are shown as thin grey lines, black triangles and black squares, respectively.

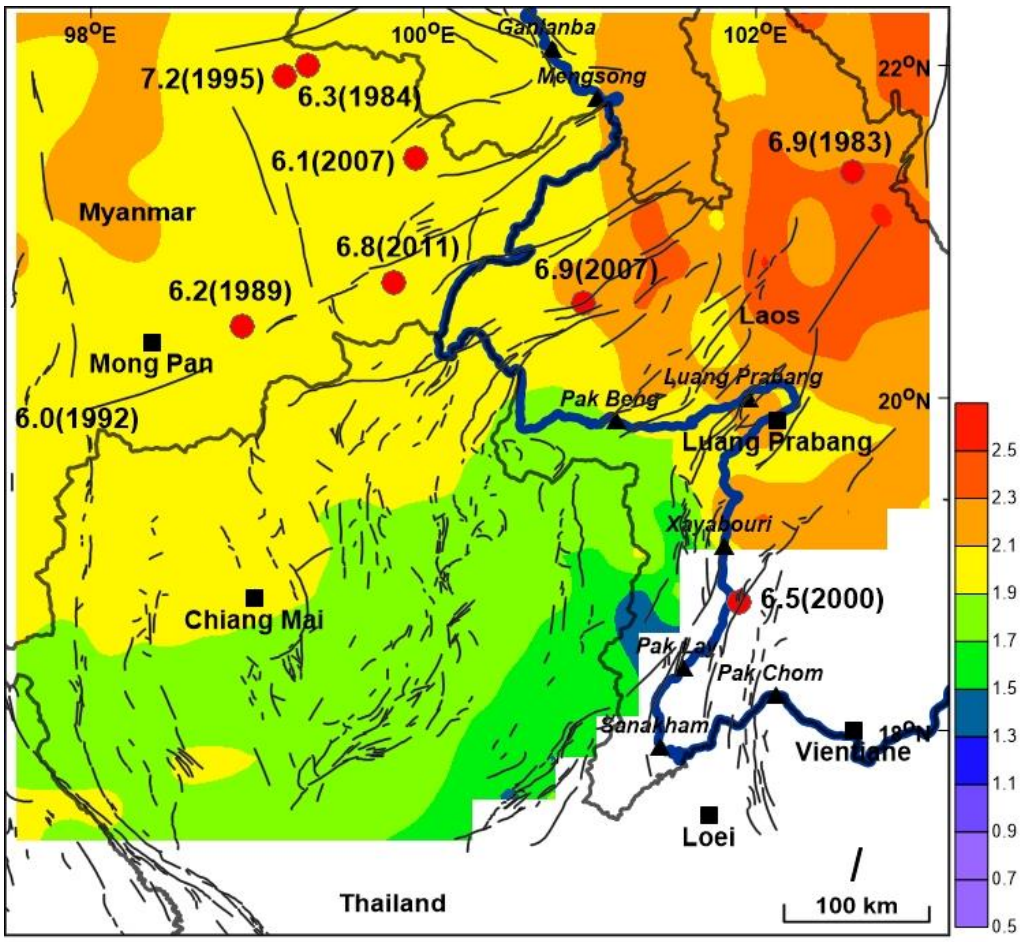

Figure 5. 10. Map of the TLMB region. This map shows the Dc distribution in the study area for the after declustering dataset. Earthquakes occurred with magnitude greater than 6 (red dots) and the fault lines, hydropower dam and major cities are shown as thin grey lines, black triangles and black squares, respectively.

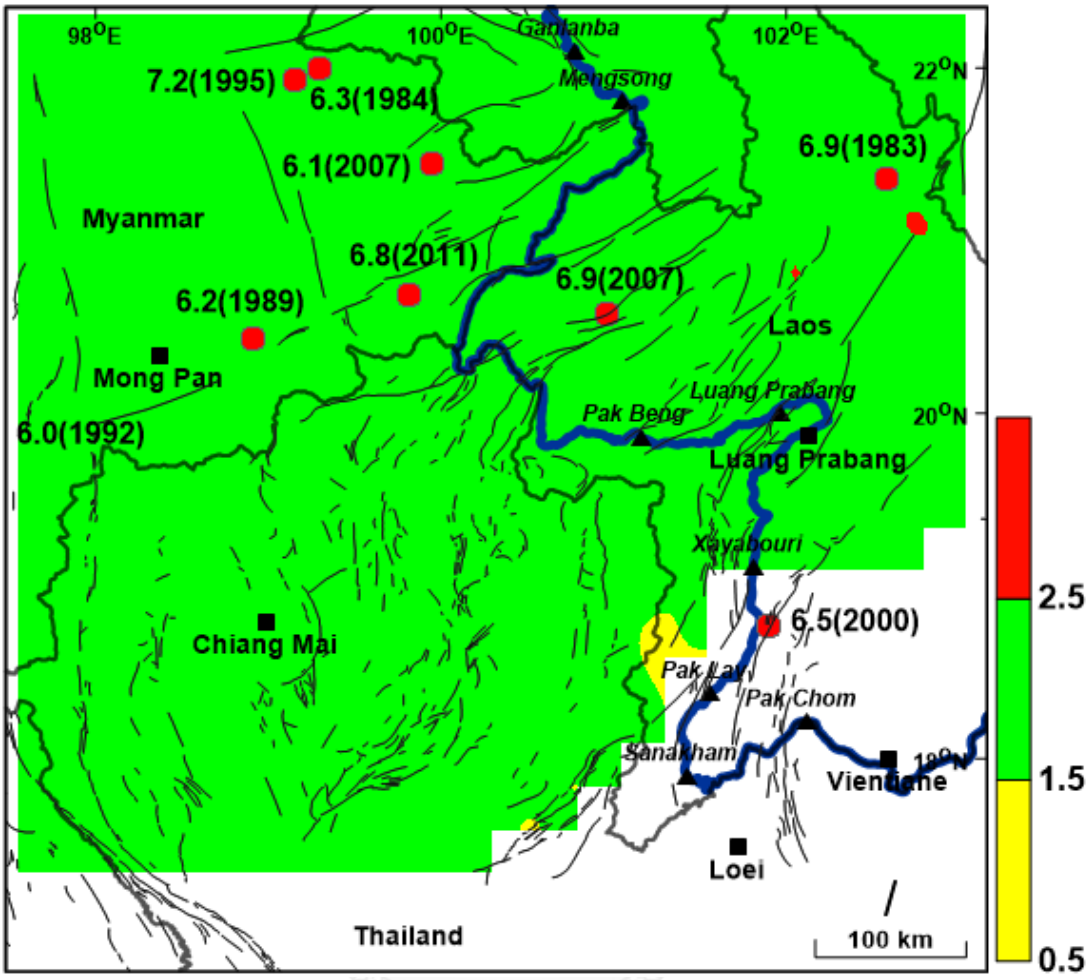

Figure 5. 11. Map showing the Dc values of the after declustering process in 3 ranges. The Dc values are between 0.5-1.5 (yellow), 1.5-2.5 (green) and 2.5-3.5 (red) in the TLMB region.

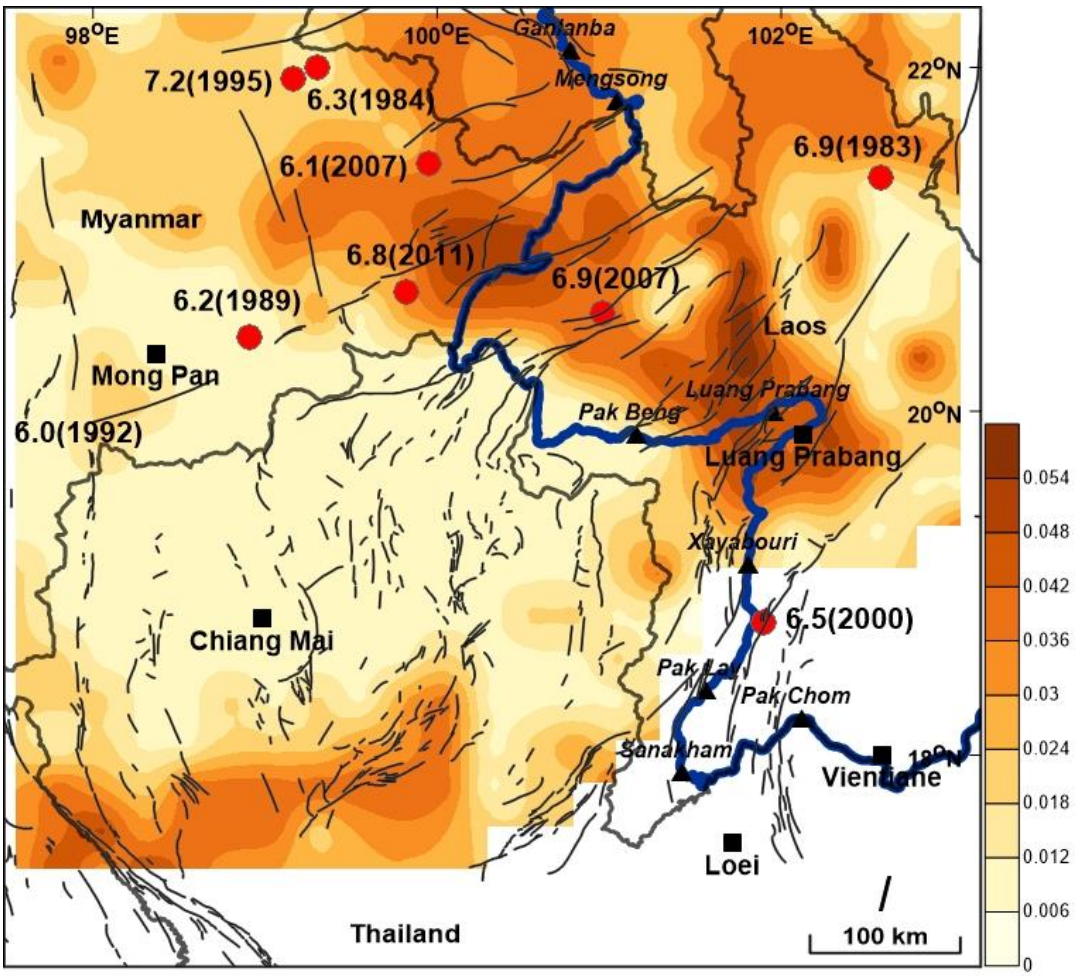

Figure 5. 12. Map of the TLMB region. This map shows the error of the Dc value distribution for the after declustering dataset. Earthquakes occurred with magnitude greater than 6 (red dots) and the fault lines, hydropower dam and major cities are shown as thin grey lines, black triangles and black squares, respectively.

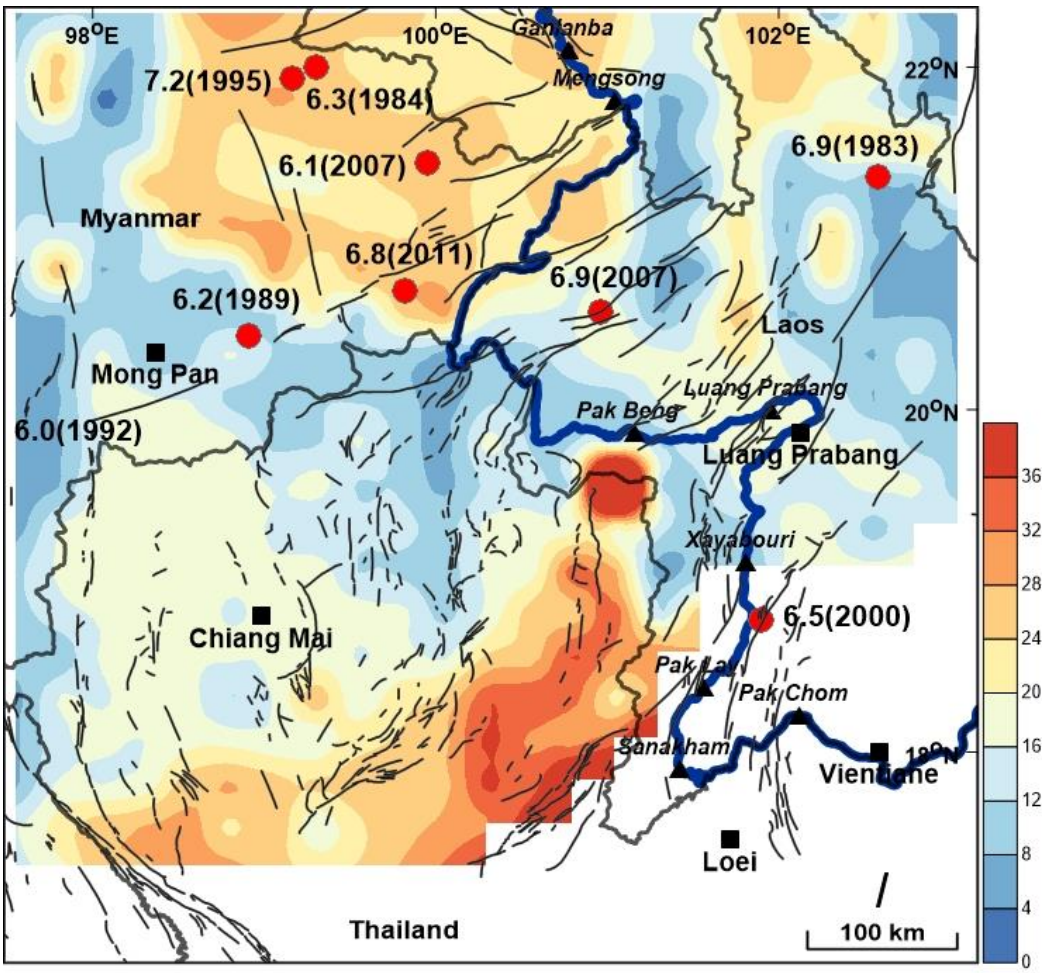

Figure 5. 13. Map of the TLMB region. This map shows the shortest distance between 2 earthquakes, that was found in fractal dimension relationship for the after declustering dataset. Earthquakes occurred with magnitude greater than 6 (red dots) and the fault lines, hydropower dam and major cities are shown as thin grey lines, black triangles and black squares, respectively.

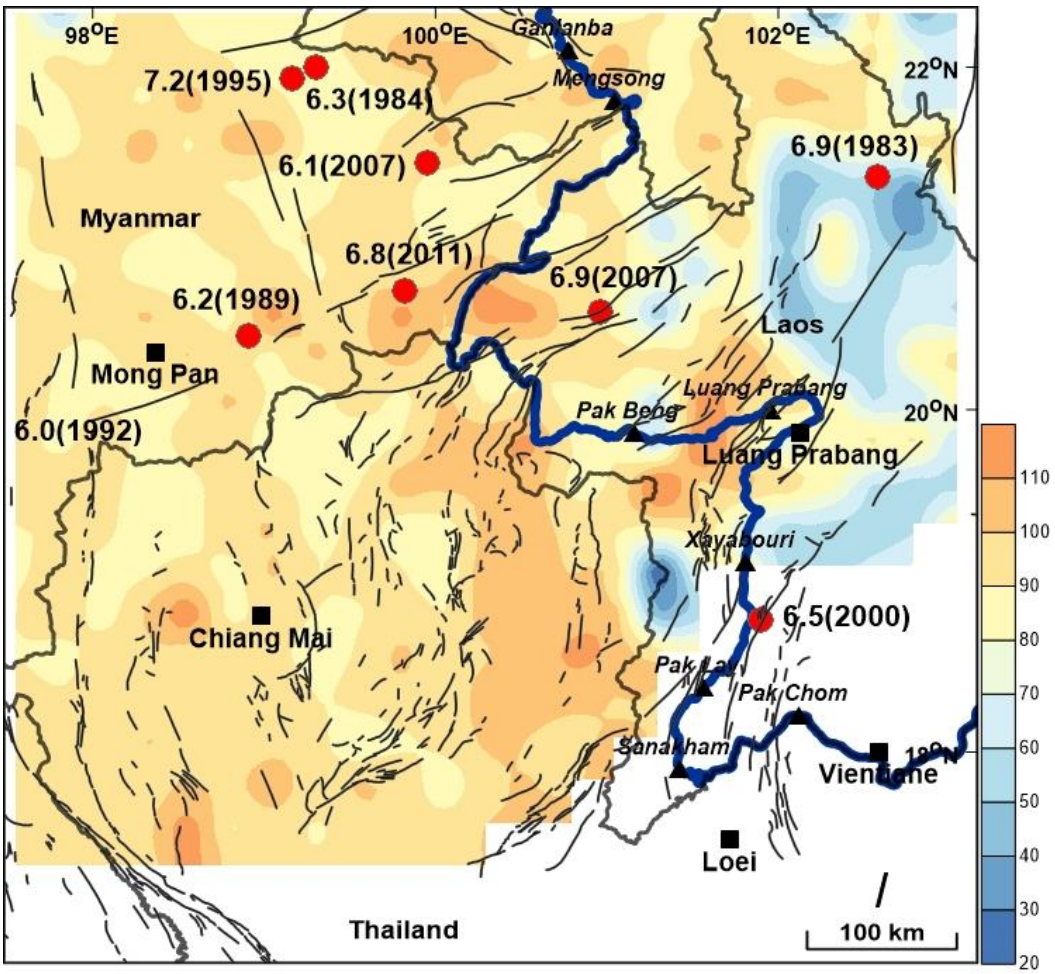

Figure 5. 14. Map of the TLMB region. This map shows the longest distance between 2 earthquakes, that was found in fractal dimension relationship for the after declustering dataset. Earthquakes occurred with magnitude greater than 6 (red dots) and the fault lines, hydropower dam and major cities are shown as thin grey lines, black triangles and black squares, respectively.

CHAPTER VI
DISCUSSION

6.1. Magnitude Conversion

From the chapter III, we got the database reported from the different data sources, such as International Seismogical Center, National Earthquake Information Center and The Global Centroid Moment Tensor. These data source reported the different magnitude scales as surface magnitude (Ms), body-wave magnitude (Mb), local magnitude (Ml) and moment magnitude (Mw). The statistical seismology should to use the seismic data that have homogeneous. Thus, we choose to convert the other magnitude scales to Mw. All the earthquakes reported in the Mb or Ms were converted directly to the Mw by using the relationships as $Mw = 0.16Mb^2 - 0.73Mb + 4.71$ and $Mw = 0.06Ms^2 - 0.03Ms + 3.72$, the coefficient of determination (R^2) are 0.786 and 0.941 respectively. (Figure 6.1a and b) Meanwhile, the Ml was converted to Mb according to the relationship of $Mw = 0.10Ml^2 - 0.26Ml + 3.42$ in Figure 6.1c with R^2 is 0.558. After that, the obtained Mb was reconverted to the MW by relationship as shown in Figure 6.1a.

By comparison with the report of Prayot (2015) who also studied in the TLMB, he found the different relationship. The relation between Mb-Mw, Ms-Mw and Ml-Mb are $Mw = -0.12Mb^2 + 2.11Mb - 2.61$, $Mw = -0.09Ms^2 + 2.42Ms - 5.22$ and $Mb = 0.22Ml^2 - 0.95Ml + 4.45$, with R^2 as 0.7336, 0.9421 and 0.7336 respectively. (Figure 6.2)

In addition, Pailoplee and Charusiri (2017) studied in Laos which overlaps some parts of our study area. They got the distinct relation as well. The magnitude conversion between Mb to MW have the equation as $Mb = 0.24Mb^2 - 1.38Mb + 6.16$ with 0.86 of R^2 (Figure 6.3a). While, the M_S and MW equation is $Mw = 0.59Ms + 2.22$ with 0.95 of R^2. The last is the relationship of ML and Mb which is $Mb = 0.05Ml^2 + 0.13Ml + 2.64$ and R^2 is 0.54.

As can be seen from the results and the previous studies, the magnitude conversion relationships and their coefficient of determination are almost the same. However, we choose our obtained relations because they are the most appropriate for this study.

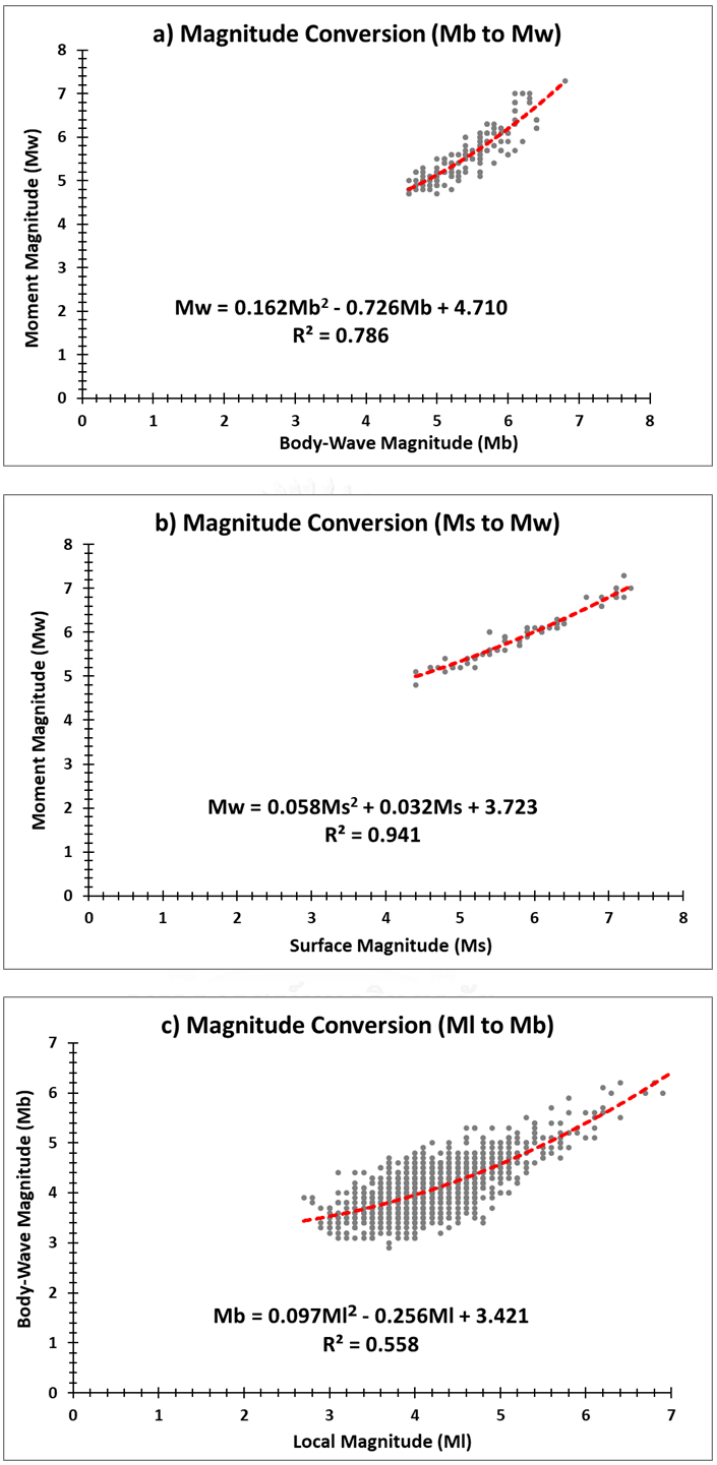

Figure 6. 1. Relationships of the magnitude scales between a) Mb-Mw, b) Ms-Mw and c) Ml-Mb of this study.

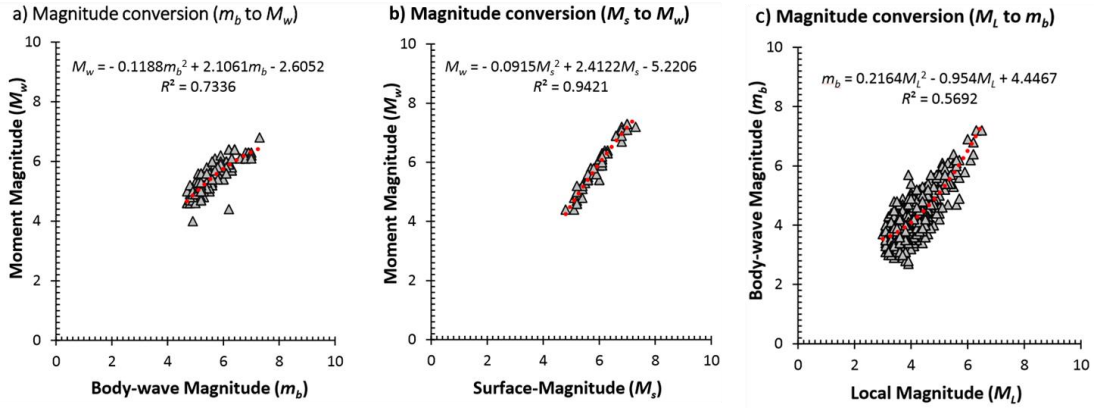

Figure 6. 2. Relationships of seismicity data a) between Mb and Mw, b) between Ms and Mw and c) between Ml and mb. The grey triangles indicate the earthquake events and the red dash lines indicate the polynomial trend lines. (Prayot., 2015)

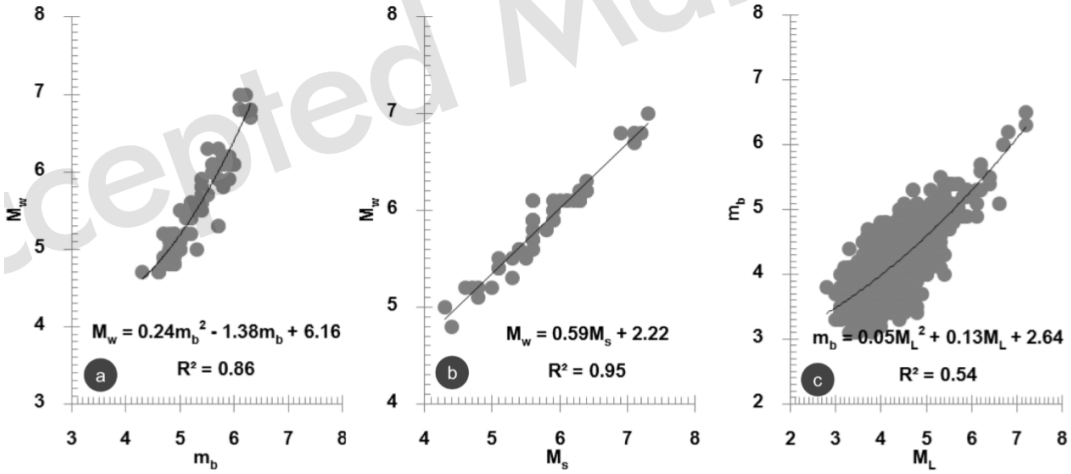

Figure 6. 3. Relationships of the magnitude scales between a) Mb-Mw, b) Ms-Mw and c) Ml-Mb. (Piloplee and Charusiri., 2017)

6.2. Cumulative Number

After magnitude conversion process, we obtained the homogeneous magnitude scales to analyze by statistical seismology. The statistical seismology should imply only the main shock which directly related to tectonic activities. In order to constrain the results of completeness of seismicity data, the several works were attempted to observe the relationships of the cumulative number of earthquakes and time. In this study, we observed the cumulative number of earthquakes against time, that curve of

the total seismicity data represents the flat trend line generated between 1965 and 1980. After that, although the cumulative curve raised gradually until 2010. The cumulative number curve of after declustering indicates the flat trend line during 1965 and 1980. Afterward, the cumulative curve developed gradually until the before 2010. We had 12,133 earthquakes before cutting off the foreshocks and aftershocks. After declustering the surplus data are 2,195 earthquakes (Figure 6.4). By comparison on both of the results, we found the cumulative number's graph of declustering data set got straightest. In addition, we compared this result with previous study referred to Pailoplee et al. (2013). That was flat trend line generated between 1965 and 1980 and after that the cumulative curve raised gradually until end of data. The linear is the straightest than our research because we did not cut the man-made seismicity off. (Figure 6.5)

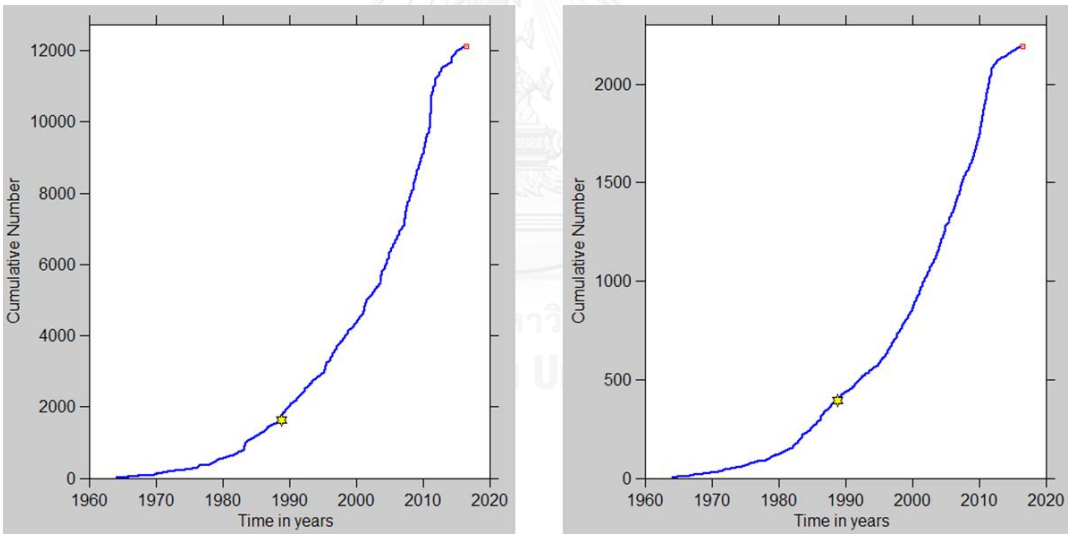

Figure 6. 4. Cumulative number of earthquakes showing the different rates of seismicity reported during the years 1964 - 2015.

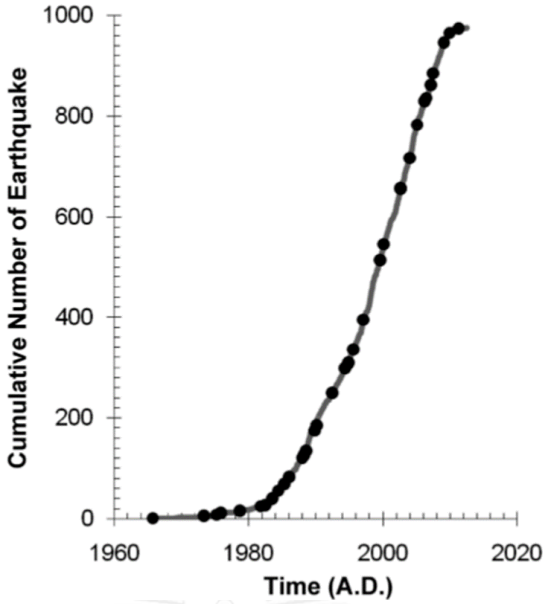

Figure 6. 5. Cumulative number of earthquakes with a Mb ≥ 2.8 (grey line) showing the different rates of seismicity reported during the years 1964 - 2012. The black circles are earthquakes with a Mb of ≥ 5.0.

6.3. Focal Mechanism

We got the focal mechanism information from Harvard moment centroid as 26 beach balls. Most of focal beach balls presented left - lateral strike slip covering almost all of the area. Nevertheless, there is a ball in Northern Thailand presented normal dip slip as shown in Figure 4.1. As reported by Uttamo et al. (2003), they said the Northern Thailand dominated by strike slip faults more than 70. The Northeastern Thailand got striking as left - lateral strike slip faults and north to northwest shown striking as normal to normal oblique faults (Fenton et al., 2003). Moreover, we referred the directions of the faults in the study area laying in NE-SW and NW-SE. The result accorded to the study by Pailoplee et al. (2009). They found the fault directions in Thailand-Laos-Myanmar border which are NE-SW and NW-SE by remote sensing.

We divided the beach balls into 8 zones following by the fault zones referred by Pailoplee et al. (2009), which are Menglian, Jinhong, Nam Ma, Mengxing, Mae Chan, Mae Ing, Dein Bien Phu and Wang Nue fault zones (as area 1 to area 8 respectively). We got the information of strike, dip and rake for each fault zones by these following:

6.3.1. Strike

These results were investigated by the Faultkin program, it reported information into 2 set of data. Each fault matches with the different each set of information, the suitable matching depends on the strike and fault line in each zone. We obtained the direction of faults in the study area laying on northeast and some southwest direction. It accorded to (Fenton et al., 2003) and (Uttamo et al., 2003) .

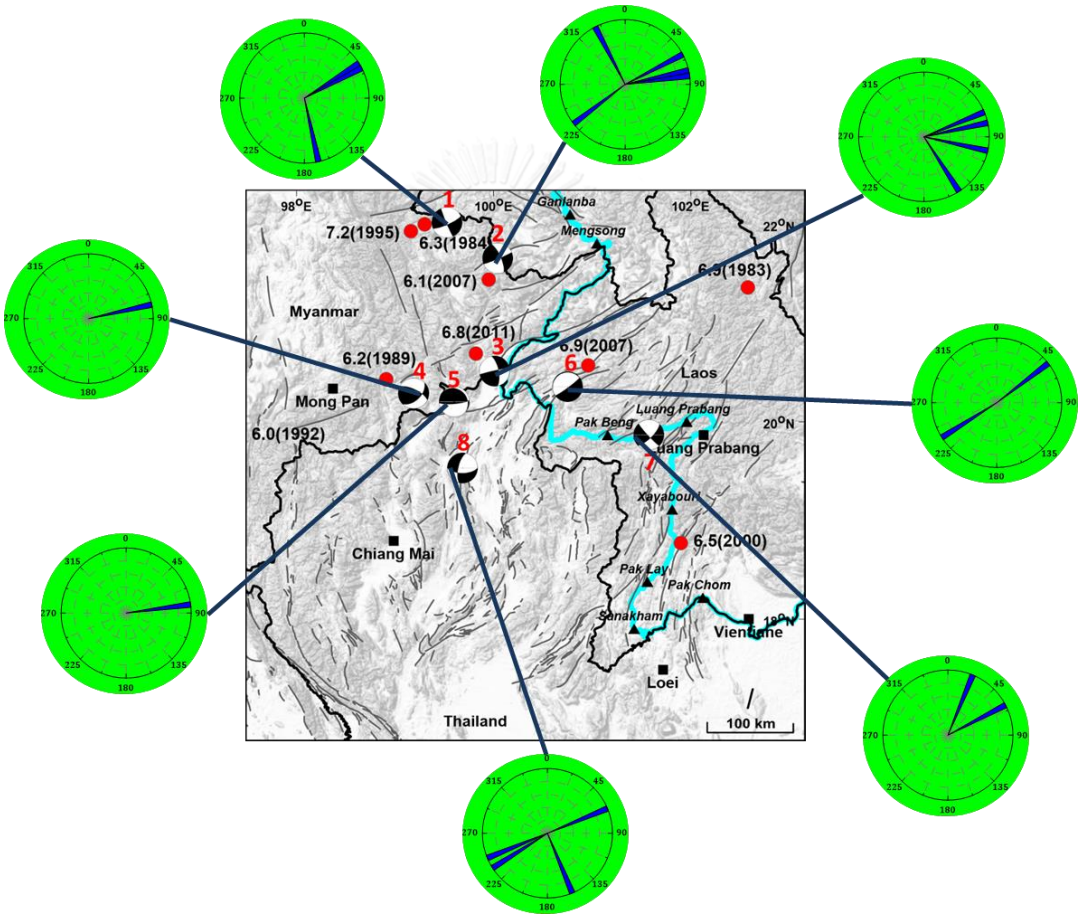

Figure 6. 6. The strike of each fault zones.

After selecting information set to paraphrase, we considered the dip and rake in the same set of strike.

6.3.2. Dip

Fenton et al. (2003) used dip of $60^{\circ} \pm 15^{\circ}$ in their study and Wood et al. (2014) estimated the dip of Mae Chan fault zone is between 50° to 70°. In the other way, this

result presented dip are over 65° till 85° for the faults cover the study area and Mae Lao is 80° for dip angle.

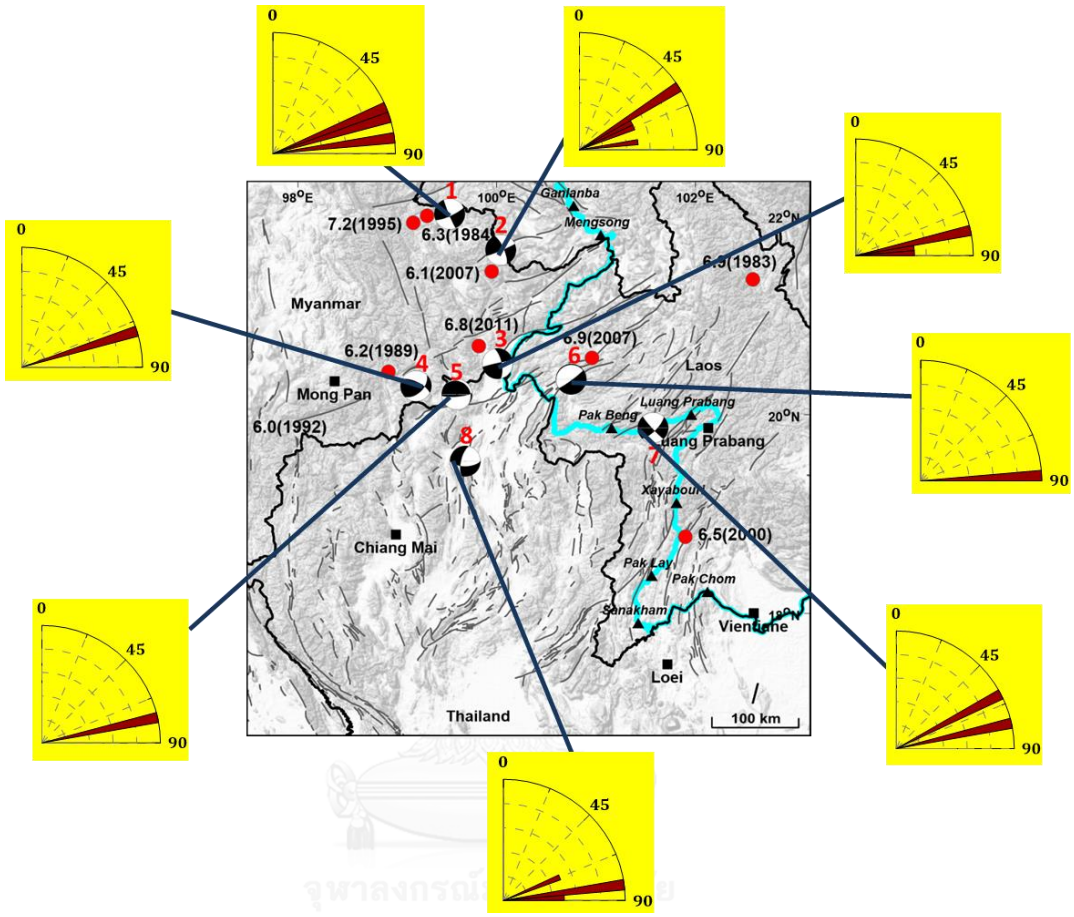

Figure 6. 7. The dip of each fault zones.

6.3.3. Rake

We obtained 7 fault zones are left – lateral strike slip fault and, but Mae Chan fault zone is right – lateral strike slip. It gives the adverse result with Fenton et al. (2003) which informed that the Mae Chan fault is left – lateral strike slip.

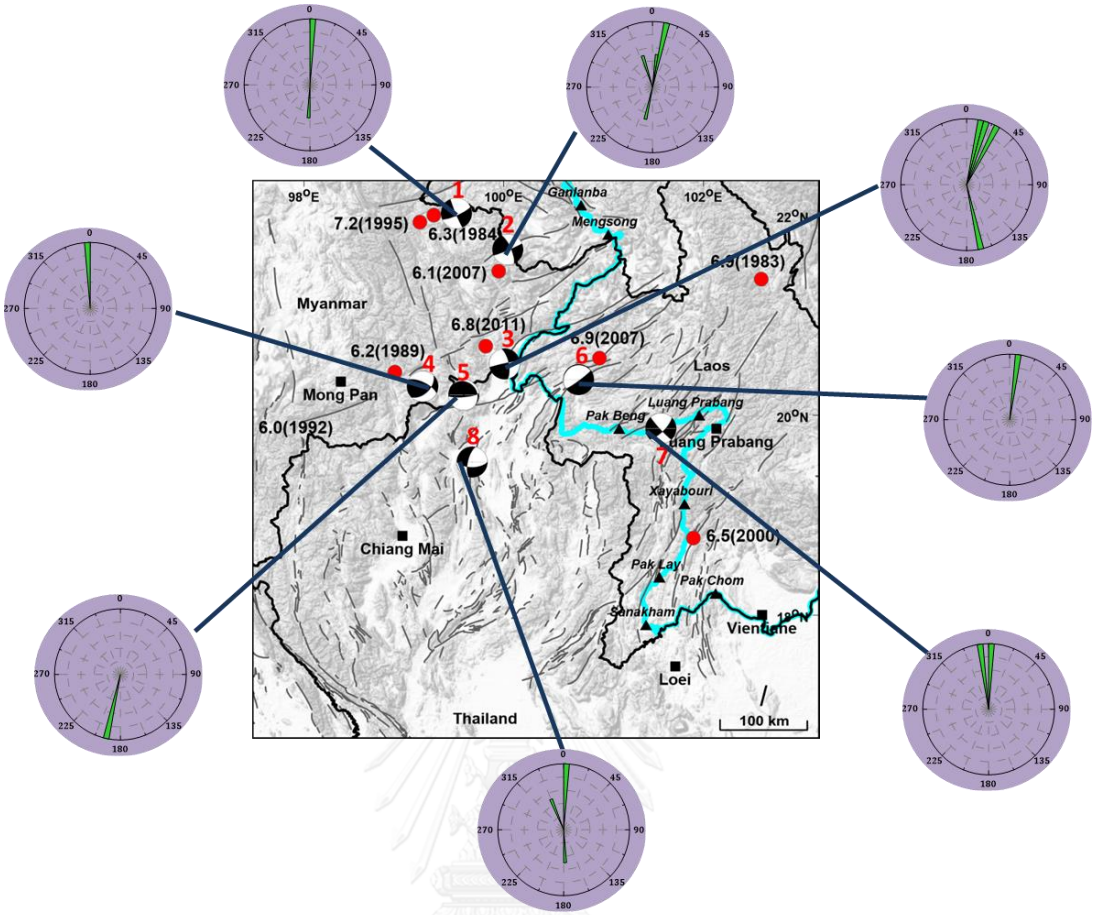

Figure 6. 8. The rake of each fault zones.

6.4 Fractal Dimension (Dc value) and B value

6.4.1 Temporal variation

From the result, we selected the results of before declustering data set to imply the variation of Dc and b values in different time because the before declustering data is better than after declustering data as it shows more variable than after declustering data.

The graphs between Dc and years of Mae Lao and Tarlay earthquake, the Dc values had clearly decreased before occurring Mae Lao earthquake in 2014 and Tarlay earthquake 2011. The result accords to the result of Kei Murase (2004), that presented the Dc had decreased in time before Tokachi-oki earthquake in Hokkaido, Japan in 2003 (Figure 2.13). Moreover, the b value was continuously decreasing before occurring the great earthquakes. That means the study area was gleaning the stress before the

great earthquake in 2011 and 2014 occurrences. So, the b value and Dc value can be the earthquake precursor.

6.4.2 Dc value and b value relationship of temporal term

From temporal variation of fractal dimension (Dc value) and b value, we focused on the result of before declustering data. This research, we analyzed the relationship between Dc value and b value of before declustering data of Mae Lao and Tarlay events. The results give the positive relationships for both case studies (Figure 5.3). There is not only the TLMB area are referred as the positive relationship, but also the other seismic source zones. For examples, Bhattacharya et al. (2010) studied the earthquake source zone in Northeastern India and the correlation of b and Dc was positive (Figure 6.7). Wyss et al. (2004) obtained positive relation for San Andres fault in California (Figure 6.8) and Chen et al. (2006) reported the relation of b and Dc value for Chi-Chi earthquake in Taiwan was positive as well (Figure 6.9). As can be observed, the areas represented positive relationship between b and Dc value are areas was generated earthquake in the land, known as the intraplate earthquake.

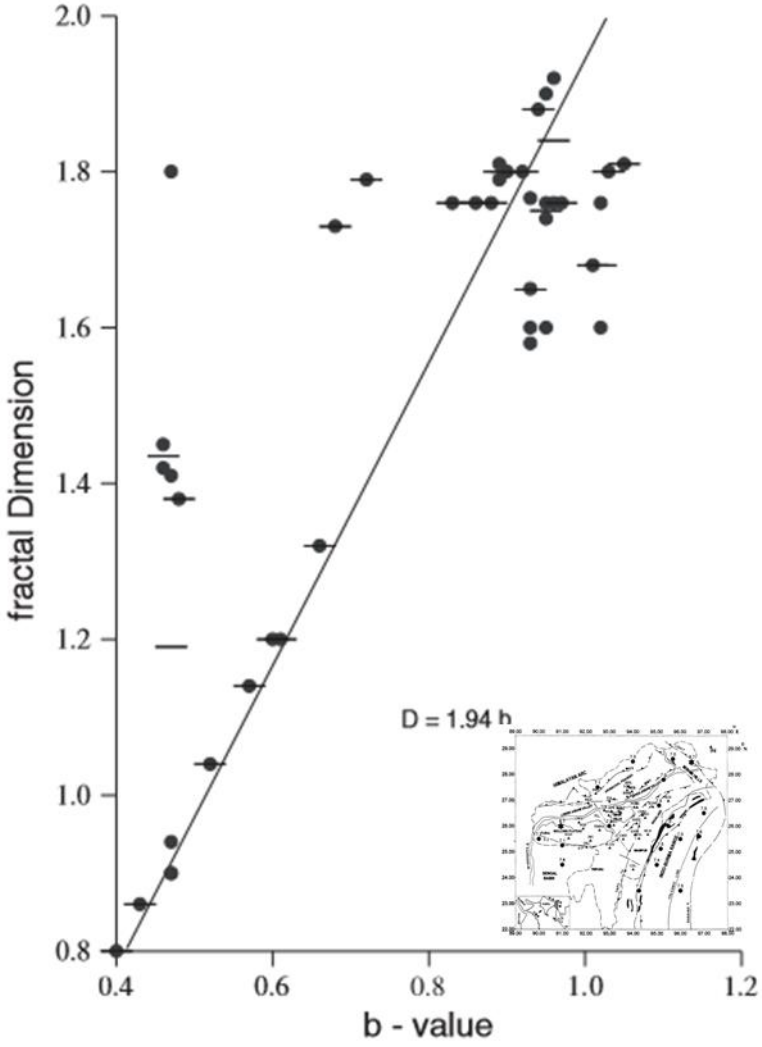

Figure 6. 9. Plot showing the relation between fractal dimension and b value in northern India. (Bhattacharya et al., 2010)

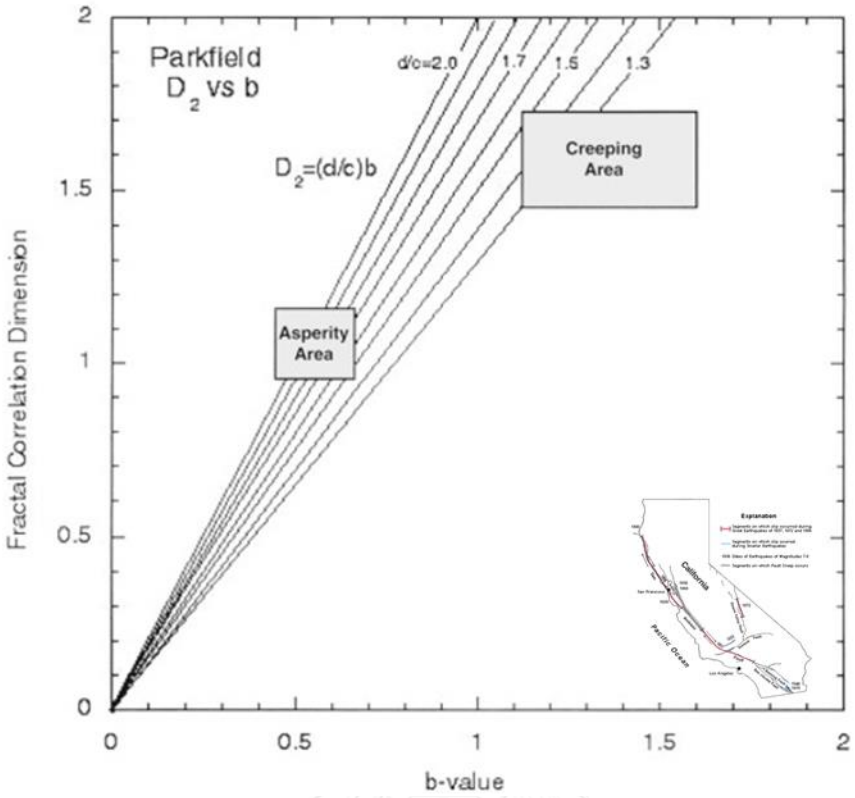

Figure 6. 10. Graph showing the relationship between b value and fractal dimension for intraplate earthquake of San Andres fault in California. (Wyss et al., 2004).

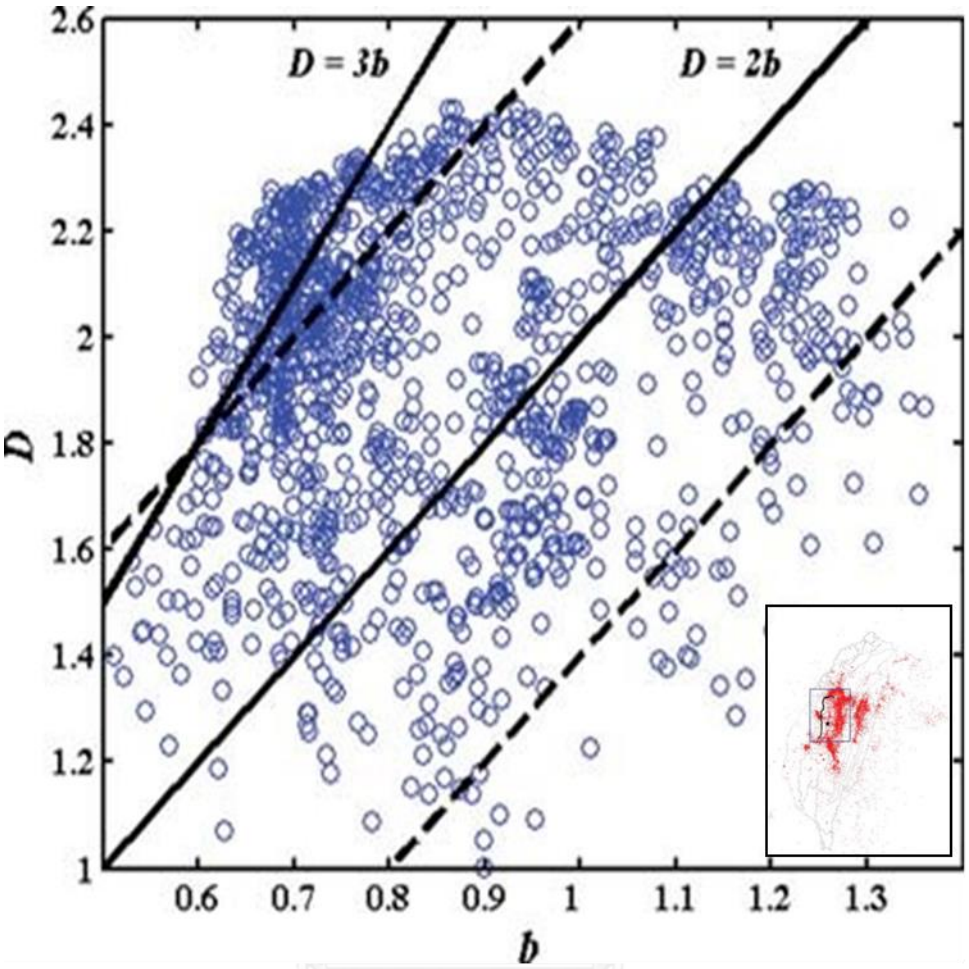

Figure 6. 11. The relationship between b value and fractal dimension for intraplate earthquake of Chi-Chi earthquake 1999 in Taiwan. (Chen et al., 2006).

6.4.3 Spatial variation

From the temporal term, we focused on the before declustering data to consider which provided the lowest b value on Southern study area. According to the study of Pailoplee et al. (2013), they showed the lowest b value on the center of study area. The b value varied 0.5-1.2 covering the area, same as Pailoplee et al. (2013) as shown in Figure 6.10. (Pailoplee et al., 2013)

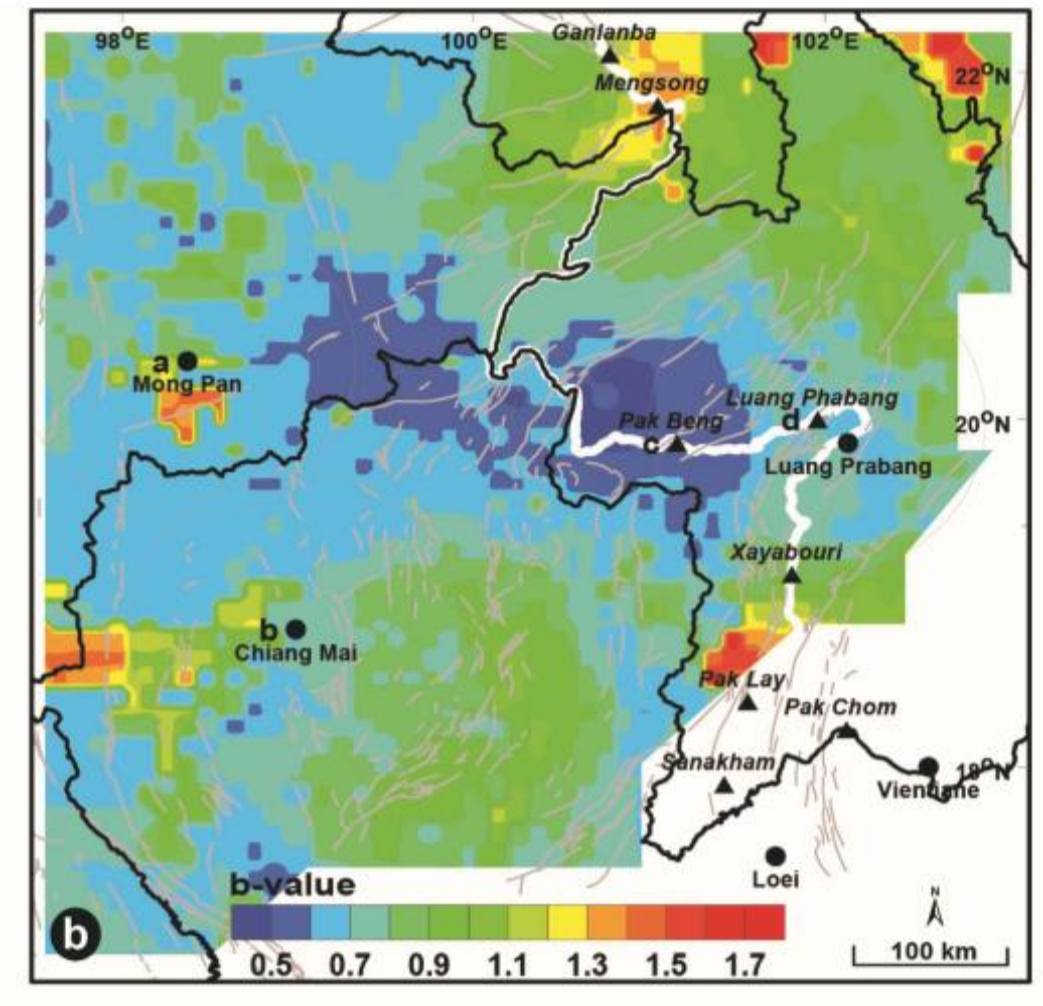

Figure 6. 12. The spatial distribution of b value for TLMB.

As considering Dc distribution in spatial term, most of the characteristics of fault system in this study area is a plane because the Dc value close to 2, presented by the Dc map in Figure 5.5. It accorded to Pailoplee and Choowong (2014) which yielded the Dc varied between 1.8-2.0. However, some areas, such as Chiang Mai, is a line source.

CHARPTER VII
CONCLUSION AND RECOMMENDATION

The study investigates focal mechanism and fractal dimension in TLMB to understand the mechanism of fault rupture and seismic pattern. The results conclusion as the following;

7.1 Earthquake Magnitude Conversion

The magnitude conversion is the first process to complete data for statistical seismology. We converted the other scales to Mw by using the appropriate relationships. Our relationship is conforming to data earthquake.

7.2 Cumulative Number of Earthquake

The relationship between time and cumulative number of after declustering process present graph is rather straighter than before declustering graph because of cutting off foreshocks and aftershocks. Anyway, it is not matter for declustering process because the fractal dimension method was analyzed the similarity distance between earthquake.

7.3 Focal Mechanism

The focal mechanism in TLMB provided the faults laying on NE-SW and NW-SE direction, dip angle varied over 60 degrees till 90 degrees and most of the faults movement is left- letter strike slip.

7.4. Fractal Dimension and B value

7.4.1 Temporal variation

The b value has decreasd continuously before occurring the great earthquake. Therefore, the b value can be precursor.

7.4.2 Dc value and b value relationship

The relationships between Dc value and b value of before declustering process are both positive for Mae Lao and Tarlay earthquake.

7.4.3 Spatial variation

Because of discussion of temporal term, before declustering data is better than after declustering data. Thus, we focused on the before declustering data. It indicates that the seismic patterns in the Thailand-Laos-Myanmar border are plane covering almost all of the study area.

7.5 Recommendation

From the focal mechanism results, this research referred strike, dip and rake. The information is useful parameter to build data to input in the program Coulomb3.3. This program is used to investigate the coulomb stress change to predict the risk area from aftershock in the TLMB region.

REFERENCES

Barton, D., Foulger, G., Henderson, J. and Julian, B., 1999. Frequency–magnitude statistics and spatial correlation dimensions of earthquakes at Long Valley caldera, California. Geophysical Journal International, 138(2): 563-570.

Båth, M., 1965. Lateral inhomogeneities of the upper mantle. Tectonophysics, 2(6): 483-514.

Bayrak, Y. and Bayrak, E., 2012. Regional variations and correlations of Gutenberg–Richter parameters and fractal dimension for the different seismogenic zones in Western Anatolia. Journal of Asian Earth Sciences, 58: 98-107.

Chen, C.-C., Wang, W.-C., Chang, Y.-F., Wu, Y.-M. and Lee, Y.-H., 2006. A correlation between the b-value and the fractal dimension from the aftershock sequence of the 1999 Chi-Chi, Taiwan, earthquake. Geophysical Journal International, 167(3): 1215-1219.

Fenton, C.H., Charusiri, P. and Wood, S., 2003. Recent paleoseismic investigations in Northern and Western Thailand. Annals of Geophysics, 46(5).

Gardner, J. and Knopoff, L., 1974. Is the sequence of earthquakes in Southern California, with aftershocks removed, Poissonian? Bulletin of the Seismological Society of America, 64(5): 1363-1367.

Gutenberg, B. and Richter, C.F., 1944. Frequency of earthquakes in California. Bulletin of the Seismological Society of America, 34(4): 185-188.

Hirata, T., 1989. A correlation between the b value and the fractal dimension of earthquakes. Journal of Geophysical Research: Solid Earth, 94(B6): 7507-7514.

Kagan, Y. and Knopoff, L., 1980. Spatial distribution of earthquakes: The two□point correlation function. Geophysical Journal International, 62(2): 303-320.

Mogi, K., 1967. Earthquakes and fractures. Tectonophysics, 5(1): 35-55.

Morewood, N.C. and Roberts, G.P., 2001. Comparison of surface slip and focal mechanism slip data along normal faults: an example from the eastern Gulf of Corinth, Greece. Journal of Structural Geology, 23(2): 473-487.

Murase, K., 2004. A characteristic change in fractal dimension prior to the 2003 Tokachi-oki Earthquake (MJ= 8.0), Hokkaido, Northern Japan. Earth, planets and space, 56(3): 401-405.

Nanjo, K., Rundle, J., Holliday, J. and Turcotte, D., 2006. Pattern informatics and its application for optimal forecasting of large earthquakes in Japan, Computational Earthquake Physics: Simulations, Analysis and Infrastructure, Part II. Springer, pp. 2417-2432.

Omori, F., 1894. On the after-shocks of earthquakes, 7. The University.

Pailoplee, S. and Choowong, M., 2014. Earthquake frequency-magnitude distribution and fractal dimension in mainland Southeast Asia. Earth, Planets and Space, 66(1): 8.

Pailoplee, S., Sugiyama, Y. and Charusiri, P., 2009. Deterministic and probabilistic seismic hazard analyses in Thailand and adjacent areas using active fault data. Earth, planets and space, 61(12): 1313-1325.

Pailoplee, S., Surakiatchai, P. and Charusiri, P., 2013. b-VALUE ANOMALIES ALONG THE NORTHERN SEGMENT OF THE SUMATRA–ANDAMAN SUBDUCTION ZONE: IMPLICATIONS FOR UPCOMING EARTHQUAKES. Journal of Earthquake and Tsunami, 7(04): 1350030.

Phodee, P., Trisirisatayawong, I. and Aobpaet, A., 2014. Coseismic and Postseismic Displacement of 2011 Mw 6.8 Tarlay Earthquake, Myanmar using InSAR Techniques and Inversion Analysis. ENGINEERING JOURNAL, 19(2).

Scholz, C., 1968. The frequency-magnitude relation of microfracturing in rock and its relation to earthquakes. Bulletin of the Seismological Society of America, 58(1): 399-415.

Shanker, D., Paudyal, H. and Singh, H., 2011. Discourse on seismotectonics of Nepal Himalaya and vicinity: appraisal to earthquake hazard. Geosciences, 1(1): 1-15.

Shebalin, P., Keilis-Borok, V., Gabrielov, A., Zaliapin, I. and Turcotte, D., 2006. Short-term earthquake prediction by reverse analysis of lithosphere dynamics. Tectonophysics, 413(1): 63-75.

Uttamo, W., Elders, C. and Nichols, G., 2003. Relationships between Cenozoic strike-slip faulting and basin opening in northern Thailand. Geological Society, London, Special Publications, 210(1): 89-108.

APPENDIX

VITA

Kanokkarn Vajchakom was born on Apirl 26, 1991 in Saraburi, Thailand. She studied in Princess Chulabhorn's College Lopburi. Then, she went to Bangkok to study in Department of Physics, Faculty of Science, King Mongkut's University of Technology Thonburi. She received her Bachelor of Science degree (B.SC.) in 2012. She began her master degree in in Earth Sciences Program, at the Department of Geology, Faculty of Sciences, Chulalongkorn University. During her studies, she focused in the field of Earthquake.